The Role of Nitrosohydroxylamine Secondary Metabolites in Microbial Antagonism and Cell-Cell Communication in *Burkholderia cenocepacia* H111

Dissertation

zur

Erlangung der naturwissenschaftlichen Doktorwürde

(Dr. sc. nat.)

vorgelegt der

Mathematisch-naturwissenschaftlichen Fakultät

der

Universität Zürich

von

Christian Wilfried Jenul

aus

Österreich

Promotionskomitee

Prof. Dr. Leo Eberl (Vorsitz)
Prof. Dr. Jakob Pernthaler
Prof. Dr. Aurelien Carlier
Dr. Gabriella Pessi

Zürich, 2016

To my family and Katrin

Table of contents

Summary

Burkholderia cenocepacia is a member of the *Burkholderia cepacia* complex (Bcc), a group of 20 closely related species, which are important opportunistic human pathogens but are also a rich source for bioactive secondary metabolites that show great potential for biotechnological applications. Nevertheless, safety concerns because of the potential virulence of many Bcc members have hampered the development of *Burkholderia* for biotechnological applications. Although bacteria are unicellular organisms they constantly interact with other bacteria in their vicinity by means of cell-cell communication systems which rely on small signalling molecules which accumulate in the environment as a function of their population densities. When a certain threshold concentration is reached, the so- called “quorum”, the signaling molecules bind to their cognate receptors, which in turn activate or repress target gene expression. These cell-cell communication systems are commonly referred to as quorum sensing systems.

Previous work has shown that in many *Burkholderia* strains the production of antibiotic secondary metabolites is regulated by *N*-acyl homoserine lactone (AHLs)-dependent quorum sensing systems. The CepIR quorum sensing system, which is present in all Bcc species, was shown to control the production of diverse antifungal compounds, including pyrrolnitrin in *Burkholderia lata*, *Burkholderia ambifaria* and *Burkholderia pyrrocinia*, enacyloxin in *B. ambifaria* and an occidiofungin-like cluster in *B. ambifaria*.

Many bioactive natural products are synthesized by polyketide synthases (PKS) or non-ribosomal peptide synthetases (NRPS). NRPS enzymes consist of a minimum of three domains. The adenylation (A) domain recognizes and activates the amino acid substrate which is then transferred and covalently bound to the thiolation (T) domain. Peptide bond formation between T domain bound amino acids from two adjacent modules is catalyzed by the condensation (C) domain. The growing peptide chain is normally released from the last module in the NRPS assembly line *via* a thioesterase (TE) or a reductase (R) domain.

In this thesis I characterized the genetic locus responsible for antifungal activity of *B. cenocepacia* H111 and elucidated the structure of the main antifungal agent

produced by this organism. Furthermore, the regulatory network which underlies antifungal activity has been analysed.

My work showed that antifungal activity of *B. cenocepacia* H111 is dependent on the CepIR quorum sensing system and the LuxR solo CepR2. Furthermore, I could demonstrate that an NRPS-like gene cluster, named the *ham* (H111 antifungal metabolite) gene cluster, produces fragin, the main antifungal metabolite of *B. cenocepacia* H111. Fragin belongs to the rare class of nitrosohydroxylamine natural products and is active against fungi, yeast and Gram-positive bacteria because of its metal chelating activity. During the course of the study it became apparent, that the *ham* cluster also produces valazole, another nitrosohydroxylamine which is structurally similar to fragin. Valazole is a novel signaling molecule that regulates its own production and the biosynthesis of fragin. It also controls expression of several genes involved in metal transport and homeostasis or which rely on metals for their enzymatic activity.

Zusammenfassung

Burkholderia cenocepacia ist ein Mtiglied des *Burkholderia cepacia* Komplexes (*Burkholderia cepacia* complex; Bcc), einer Gruppe von 20 eng verwandten bakteriellen Spezies, welche opportunistische Humanpathogene sind, aber auch eine reiche Quelle für bioaktive Sekundärmetabolite mit grossem Potential für biotechnologische Anwendungen. Die Entwicklung von *Burkholderien* für biotechnologische Anwendungen wurde aufgrund von Sicherheitsbedenken ob der potentiellen Virulenz vieler Mitglieder des Bcc erschwert. Obwohl Bakterien unizelluläre Organismen sind, interagieren sie ständing mit Bakterien in ihrer unmittelbaren Nähe. Dies geschieht mit Hilfe von Zell-Zell Kommunikationssystem welche Signalmoleküle verwenden, die in der Umgebung als Funktion der Populationsdichte akkumulieren. Wenn ein bestimmter Schwellenwert in der Konzentration erreicht wird, genannt “Quorum”, binden die Signalmoleküle and Rezeptoren, welche wiederum die Expression bestimmter Gene aktivieren oder reprimieren. Dies Zell-Zell Kommunikationssysteme warden gewöhnlich als Quorum Sensing Systeme bezeichnet.

Frühere Arbeiten haben gezeigt, dass in vielen *Burkholderia* Stämmen die Produktion von Antibiotika über *N*-acyl homoserine lactone (AHL)-abhängige Quorum Sensing Systeme gesteuert wird. Das CepIR Quorum Sensing system, welches von allen Spezies des Bcc verwendet wird, steuert die Produktion verschiedener antifungieller Naturstoffe. Darunter befinden sich Pyrrolnitrin, welches von *Burkholderia lata*, *Burkholderia ambifaria* und *Burkholderia pyrrocinia* produziert wird, Enacyloxin welches von *B. ambifaria* produziert wird und Occidiofungin-ähnliche Stoffe welche ebenfalls von *B. ambifaria* produziert werden.

Viele bioaktive Naturstoffe werden von Polyketidsynthasen (PKS) oder nichtribosomalen Peptidesynthetasen (non-ribosomal peptide synthetases; NRPS) synthetisiert. NRPS Enzyme bestehen aus wenigstens drei verschiedenen Proteindomänen. Die Adenylierungs(A)-Domäne erkennt und aktiviert eine Aminosäure welche dann an die Thiolierungs(T)-Domäne transferiert und kovalent gebunden wird. Die Peptidbindung zwischen zwei Aminosäuren, welche an zwei angrenzende T-Domänen gebunden sind, wird durch die Kondensations(C)-Domäne katalysiert. Die wachsende Peptidkette wird schließlich vom letzten Modul des

NRPS-Enzyms mit Hilfe einer Thioesterase(TE)-Domäne oder einer Reduktase(R)-Domäne entlassen.

In dieser Doktorarbeit habe ich den genetischen Lokus, der für die antifungielle Aktivität von *B. cenocepacia* H111 verantwortlich ist charakterisiert, sowie die Strukture des antifungiellen Stoffes aufgeklärt, welcher von diesem Bakterium produziert wird. Des Weiteren wurde das regulatorische Netzwerk, welches antifungiellen Aktivität zugrunde liegt, analysiert.

Meine Arbeit hat gezeigt, dass die antifungielle Aktivität von *B. cenocepacia* H111 sowohl vom CepIR Quorum Sensing System wie auch vom solo LuxR Regulator CepR2 abhängig ist. Des Weiteren konnte ich zeigen, dass ein NRPS-ähnlicher Gencluster, genannt *ham* (H111 antifungieller Metabolit) Gencluster, den antifungiellen Metaboliten Fragin produziert. Fragin gehört zur Klasse der Nitroso-Hydroxylamine, welche nur selten als Naturstoffe vorkommen. Fragin zeigt aufgrund seiner metalchelierenden Eigenschaften antibiotische Wirkung gegen Pilze, Hefe und grampositive Bakterien. Im Laufe dieser Studie wurde klar, dass der *ham* Cluster auch Valazole produziert. Dabei handelt es sich um ein weiters Nitrosohydroxylamine welches strukturell Fragin sehr ähnlich ist. Valazole ist ein bisher unbekanntes Signalmolekül welches seine eigene Produktion sowie die Biosynthese von Fragin reguliert. Es kontrolliert auch die Expression mehrerer Gene, die im Transport und der Homeostase von Metallen beteiligt sind oder welche Metalle für ihre enzymatische Aktivität benötigen.

Chapter I: Introduction

1 Introduction

1.1 The genus *Burkholderia*

The genus *Burkholderia* is a group of ecologically and metabolically highly diverse Gram-negative bacteria from the *Betaproteobacteria* class. Currently, the genus consists of 90 validly named free-living species, along with several currently uncultivable candidate species which exist in symbiosis with plants [1-3]. Based on ribosomal multilocus sequence typing (rMLST), the genus can be divided into two major clades (Figure 1) [3]. The first clade contains the members of the *Burkholderia cepacia* complex (Bcc), the *Burkholderia pseudomallei* group and the two rice pathogens *Burkholderia glumae* and *Burkholderia gladioli*. The second clade consists of members of the *Burkholderia xenovorans* group, including members of the *Burkholderia glathei* group, which form a distinct branch in 16s rRNA-sequence based phylogeny trees. Burkholderia symbiotica, *Burkholderia rhizoxinica* and *Burkholderia andropogonis* represent unique lineages which do not closely associate with the two main *Burkholderia* clades [3].

.

Figure 1: Phylogeny tree of the genus *Burkholderia* based on ribosomal multilocus sequence typing (rMLST). Type strains are shown in bold letters. Figure is taken from Depoorter and colleagues [3].

Members of the genus *Burkholderia* inhabit various ecological niches including the plant rhizosphere, soil, invertebrates and the human respiratory tract [1, 4, 5]. In recent years, several fungal and plant symbionts have also been identified as *Burkholderia* species [6-9]. Some species of the genus *Burkholderia* are important human, animal and plant pathogens. *B. pseudomallei* is the causative agent of melioidosis [10], a potentially fatal human disease and its close relative *B. mallei* causes glanders in animals [11]. Together with *Burkholderia thailandensis*, they form the *B. pseudomallei* group [3]. The two most important plant pathogens of the genus *Burkholderia* are *Burkholderia glumae* and *Burkholderia gladioli* [5]. Both species are rice pathogens which have spread around the globe. *B. gladioli* is able to grow at elevated temperatures (30 °C to 35 °C) and is therefore thought to become an increasingly serious threat worldwide, as global warming progresses [12]. Aside from these for the most part pathogenic species, approximately 40 *Burkholderia* species are known to be mainly plant associated and beneficial, and have therefore been referred to as the plant-associated beneficial and environmental (PBE) group [5]. Probably the best studied group of *Burkholderia* is the *Burkholderia cepacia* complex, which is described below in more detail.

1.1.1 The *Burkholderia cepacia* complex (Bcc)

The *Burkholderia cepacia* complex (Bcc) is a group of 20 closely related species [13], which are important opportunistic human pathogens but also promising biocontrol agents and have great potential for the biodegradation of various pollutants [14]. In terms of pathogenicity, several members of the Bcc are closely associated with infections in cystic fibrosis patients [15-17] and two prominent members of the Bcc, *B. cepacia and Burkholderia multivorans*, are known for their ability to cause a fatal pneumonia referred to as “cepacia syndrome” [18, 19]. One of the most important regulatory systems of the Bcc members is the quorum sensing (QS) system, which regulates virulence factor expression, biofilm formation and secondary metabolite production [20-23].

1.2 Quorum sensing

Bacteria are unicellular organisms, but they constantly interact with their environments, including other bacterial cells in their vicinity. Gram-positive as well as Gram-negative bacteria have evolved cell-cell communication systems to coordinate their behavior in a cell-density dependent manner, a mechanism called quorum sensing (QS). Bacteria capable of QS produce signaling molecules which accumulate in the environment as a function of the bacterial population density. When a certain threshold is reached, the so called “quorum”, the signaling molecules bind to specific receptors, which in turn activate or repress target gene expression [24].

Gram-positive bacteria mainly employ circular peptides as signaling molecules, also referred to as autoinducing peptides (AIPs) [25, 26]. Various metabolic pathways, transporters and most notably secreted virulence factors are regulated by such QS systems [25, 26]. Gram-negative bacteria, like *Burkholderia* sp. use Lux-type QS systems, with acyl-homoserine lactones (AHLs) as signaling molecules [27-29].

QS was first observed in the squid symbiont *Vibrio fischeri*, a marine bacterium that inhabits the light organs of squids and controls bioluminescence by means of QS [30]. More than a decade later, Eberhard and colleagues identified the signaling molecule which was responsible for the induction of luminescence of *V. fischeri* as *N*-(3-oxohexanoyl)homoserine lactone (3-oxo-C6-HSL) [31]. The term quorum sensing to describe bacterial cell-cell communication was coined in 1994 by Fuqua and colleagues, although at that time, it was only used for AHL-dependent QS systems [32].

1.2.1 Acyl-homoserine lactone quorum sensing

Among the different QS signaling molecules, AHLs are at present the most thoroughly investigated and have been shown to regulate a spectrum of bacterial processes, including biofilm formation, virulence, bioluminescence, motility, conjugation and symbiosis [28, 33-35]. A typical AHL-based QS system consists of an AHL synthase (LuxI) and a cytoplasmic receptor/transcription factor (LuxR) that can bind the AHL signaling molecule [36-39]. AHLs are synthesized by LuxI from

acyl-acyl carrier proteins (acyl-ACP) and S-adenosyl methionine (SAM) [28, 40]. Transcription of LuxI is often positively regulated by LuxR, creating a positive feedback loop resulting in increased AHL production [35].

All members of the Bcc have at least one QS system, the CepIR system [41-43]. The main product of the LuxI homologue CepI is *N*-octanoyl-homoserine lactone (C8-HSL) while *N*-hexanoyl-homoserine lactone (C6-HSL) is produced in lower amounts [43, 44]. Besides the CepIR QS system, several Bcc members also harbor additional QS systems, like the CciIR system found in *B. cenocepacia* ET12 lineage strains [22].

1.2.2 LuxR-solos

LuxR-type receptors that lack a cognate LuxI protein are present in many proteobacteria, and have been termed LuxR solos or orphans [45-48]. These LuxR solos can either be present in bacteria that also have a distinct LuxI/LuxR pair, or in bacteria that do not have a LuxI-type protein encoded in their genome [45, 47]. So far, LuxR solos have been shown to respond to either 1) exogenously produced AHLs ,for example SdiA, which has lost its cognate LuxI protein in several bacteria, but still responds to AHLs [49], 2) endogenously produced AHLs from a LuxI homolog produced by the same bacterial cell, as seen for the *P. aeruginosa* LuxR solo QscR [50] or 3) signaling molecules other than AHLs. In the latter case, the normally very well conserved AHL binding box shows clear deviation from the consensus sequence [51]. The most recent examples of LuxR solos interacting with non-AHL molecules are LuxR solos from plant-associated bacteria which specifically respond to yet unidentified plant-derived molecules [51], and PluR and PauR from *Photorhabdus sp*. which respond to α-pyrones and dialkylresorcinols, respectively [52, 53]and. As PluR and PauR were shown to respond to endogenously produced signals other than AHLs, the term LuxR solo or orphan might not be suitable for these regulators. All *B. Cenocepacia* strains encode one LuxR solo, designated CepR2, which showed negative autoregulation, as well as negative regulation by the CciIR QS system in *B. cenocepacia* strain K56-2 [54]. Furthermore, CepR2 regulates the expression of a subset of known QS regulated genes, including a zinc-dependent metalloprotease, the biosynthesis genes of the siderophore pyochelin and an uncharacterized NRPS-

like gene cluster adjacent to *cepR2* [54, 55]. Although the AHL binding domain of CepR2 shows very good conservation of the known consensus sequence, Malott and colleagues showed that CepR2 is not able to bind AHLs [54], while the study of Ryan and Winans showed binding of AHLs by CepR2 [55].

1.2.3 Fatty acid based quorum sensing

Besides the AHL QS system, several Gram-negative bacteria use QS systems employing fatty acid based signaling molecules. This was first reported for the plant pathogen *Xanthomonas campestris* pv *campestris*, which uses cis-11-methyl-2-dodecenoic acid (diffusible signal factor; DSF) as a quorum sensing molecule [56, 57]. A similar QS system was recently shown to exist in *B. cenocepacia* and the QS molecule, cis-2-dodecenoic acid was subsequently termed *Burkohlderia* diffusible signal factor (BDSF) [58]. BDSF accumulates in a cell density-dependent matter but unlike in AHL QS, BDSF QS does not involve a positive-feedback loop [59]. BDSF has been shown to regulate several important bacterial processes, including motility, EPS and protease production, biofilm formation and virulence [60-62]. The AHL- and BDSF QS systems control specific and overlapping sets of genes in *B. Cenocepacia* [63].

1.2.4 Quinolone based quorum sensing

Several *Pseudomonas* strains, and also some *Burkholderia* strains, have a quorum sensing system which uses alkyl quinolones (AQs) as signaling molecules [64]. The primary signaling molecule of the AQ quorum sensing system is 2-heptyl-3-hydroxy-4-quinolone, also known as *Pseudomonas* quinolone signal (PQS), which regulates its own biosynthesis as well as several virulence factors such as elastase, rhamnolipids and pyocyanin [65-68]. In addition to PQS, its immediate biosynthetic precursor 2-heptyl-4-quinolone (HHQ) has been shown to act as a signal molecule. HHQ also modulates interspecies and interkingdom behavior and was shown to repress biofilm formation in *Bacillus subtilis* and *Candida albicans* and exhibited bacteriostatic activities against Gram-negative bacteria [69]. The biosynthesis of

HHQ is dependent on the *pqsABCDE* operon, whereas the biosynthesis of PQS from its precursor HHQ is dependent on the quorum sensing regulated FAD-monooxygenase PqsH [65, 70]. PQS production is enhanced under iron limiting conditions and was shown to chelate iron, leading to higher siderophore production. PQS is thought to associate with the bacterial cell membrane and function as an iron trap, which can transfer ferric iron to either pyochelin or pyoverdin [71-74].

1.3 Microbe-derived secondary metabolites

Microbe-derived secondary metabolites are the basis for most drugs currently used in clinics, including antibiotics [75]. The success story of antibiotics started with the discovery of penicillin from the fungus *Penicillium notatum* by Alexander Fleming in 1929 [76]. The subsequent realization that this antibiotic could be used to battle multiple microbial infections during the 1940s resulted in the so called “golden age of antibiotics “, which lasted for two decades [77]. Nevertheless, it soon became clear that bacteria were able to evolve resistance against antibiotics [78]. While this is an inevitable evolutionary mechanism, the misuse and widespread introduction of antibiotics has certainly accelerated the development and spread of resistance among microbes [77]. Antibiotic resistance normally emerges within several months to years [79]. For example, the first penicillin resistant bacteria arose in clinics only two years of the introduction of penicillin on the market [78].

1.3.1 Secondary metabolite biosynthesis in the genus *Burkholderia*

Burkholderia sp. have proven to be a rich source of natural products with important and interesting biological activities, ranging from antibacterial and antifungal compounds, to herbicidal and insecticidal agents and metal chelators [3, 80]. The analysis of 15 genomes from strains representing the diversity of the genus *Burkholderia* showed that *Burkholderia* species dedicate up to 14% of their genome, equating to 22 gene clusters, to the biosynthesis of secondary metabolites [3]. This makes *Burkholderia* a valuable genus for the discovery of novel antibiotics, with great potential for biotechnological applications. Nevertheless, safety concerns regarding

the virulence of many *Burkholderia* species have hampered the development of *Burkholderia* as a biocontrol agent and its biotechnological exploitation [2, 3].

1.3.1.1 Secondary metabolite biosynthesis in non-Bcc members

One of the most prolific non-Bcc members in terms of secondary metabolite biosynthesis is *Burkholderia thailandensis*, a non-pathogenic member of the *Burkholderia pseudomallei* group. This bacterial species is known to synthesize a range of bioactive secondary metabolites. Capistruin for example is a ribosomally synthesized lasso peptide which exhibits antibacterial activity against *Burkholderia* and *Pseudomonas* strains [81]. A series of polar compounds (bactobolin A – D) derived from an NRPS/PKS hybrid gene cluster [82], which has antibacterial activity against several Gram-positive bacteria, has also been isolated from *B. thailandensis* [83]. A molecule representing a third class of secondary metabolites synthesized by *B. thailandensis* is the polyketide thailandamide A, which has cytotoxic and anticancer activities [84]. In addition, *B. Thailandensis* and *B. pseudomallei* produce several benzoquinones with activity against *Bacillus subtilis* and *Saccharomyces cerevisae* and the ability to inhibit eukaryotic phosphodiesterase [85]. Another natural product derived from a cryptic NRPS-PKS hybrid gene cluster is produced by several members of the *B. pseudomallei* group, and was described in 2012 by two independent research groups. This molecule was named malleilactone by Biggins and colleagues [85] and burkholderic acid by Franke and colleagues [86]. It possesses iron chelating properties and was found to be toxic in several non-mammalian model systems [85].

In addition to members of the *B. pseudomallei* group, several plant-associated *Burkholderia* species have been shown to produce secondary metabolites. The plant pathogens *Burkholderia glumae* and *Burkholderia gladioli* produce the phytotoxin toxoflavin, a yellow pigment which causes rice seedling rot and grain rot [87, 88]. *Burkholderia gladioli* pv. *cocovenenans* produces the polyketide bongkrekic acid [89] as well as an antifungal polyketide from the enacyloxin family [90].

1.3.1.2 Secondary metabolites from symbiotic *Burkholderia* species

Bacterial symbionts have emerged as a rich source of secondary metabolites and it has become evident that many metabolites originally associated with a eukaryotic host are in fact derived from bacterial symbionts.

The endofungal symbiont *Burkholderia rhizoxinica,* for example, produces two toxins, the macrocylic polyketide rhizoxin [6, 91] and the cyclopeptide rhizonin [92], both of which were originally thought to be produced by the fungal host.

A recent example of a natural product derived from a symbiotic *Burkholderia* species is kirkamide, a metabolite of the C_7N aminocyclitol family [93]. Kirkamide was isolated from leaves of the plant *Psychotria kirkii* and was found to be toxic to aquatic arthropods and insects. Kirkamide is thought to be encoded by a set of genes in the obligate leaf symbiont Candidatus *Burkholderia kirkii*, which show high similarity to biosynthetic genes encoding other aminocyclitol compounds [8].

Another obligate leaf nodule symbiont, Candidatus *Burkholderia crenata*, synthesizes a cyclic depsipeptide showing biomedical properties, similar to those associated with its plant host, *Ardisia crenata* [9].

1.3.1.3 Secondary metabolite biosynthesis in members of the Bcc

Members of the Bcc are a rich source of antifungal metabolites but have also been shown to produce a wealth of other secondary metabolites with different properties, such as siderophores and molecules with antibacterial activities against multi drug resistant strains [3, 80].

1.3.1.3.1 Pyrrolnitrin

One of the best studied antifungal compounds from members of the Bcc is pyrrolnitrin, also known as 3-chloro-4-(2`-nitro-3`-chlorophenyl)-pyrrole. Pyrrolnitrinis derived from tryptophan by the enzymatic activity of the *prnABCD* operon [94-96] and was shown to be produced by *Burkholderia lata* [23]. Although its biosynthetic gene cluster is also found in other Bcc members, including *Burkholderia ambifari*a and *Burkholderia pyrrocinia*, members of the *B. pseudomallei* group and several *Pseudomonas* and *Serratia* species. It is an important antimicrobial compound which shows activity against several Gram-positive bacteria and *Candida albicans* [97] as

well as phytopathogenic fungi, including the potato dry rot fungus *Fusarium sambucinum* and *Rhizoctonia solani* [23, 98], a soil-borne fungal pathogen that causes several different plant disease, among them tobacco leaf spot and root rot [99].

1.3.1.3.2 Xylocandins

Xylocandins [100] are a group of NRPS-derived cyclic lipopetides produced by different Bcc members. Cepacidine A is synthesized by *B. Pyrrocinia* [100] and *B. cepacia* AF2001 and was found to exhibit antifungal activity [101]. In addition, cepacidine A was shown to have immunosuppressive activity [102]. Burkholdines 1097 and 1229 were isolated from *Burkholderia ambifaria*. Both molecules are cyclic octapeptides comprised of nonproteinogenic amino acids and were shown to be potent antifungal agents [103]. Additional members of the xylocandin complex are occidiofungins, antifungal glycopeptides which were isolated from *B. Pyrrocinia* [104] and *Burkholderia contaminans* cultures and have potent antifungal activity against several important pathogenic fungi [105, 106], including *Aspergillus fumigatus* and *Aspergillus niger*, which are common causes of invasive pulmonary aspergillosis [107]. *Burkholderia vietnamensis* has a biosynthetic gene cluster homologous to the occidiofungin/burkholdine gene clusters. Mutation of genes within this NRPS cluster resulted in reduced hemolytic activity and reduced killing of the wax moth larva *Galleria mellonella* [108].

1.3.1.3.3 AFC-BC11

Burkholderia pyrrocinia, formerly known as *Burkholderia cepacia* BC11, synthesizes a lipopeptide with potent antifungal activity against *Rhizoctonia solani*. Although its structure has not yet been fully elucidated, AFC-BC11 reportedly consists of four amino acids, an aromatic component and a fatty acyl substituent. Furthermore, the lipopeptide was mainly associated with the membrane of *B. pyrrocinia* and only small amounts could be found in the culture supernatant [109]. The biosynthesis of AFC-BC11 has not been investigated, but the production of the molecule is associated with the *afc* cluster, which is located on megaplasmid pC3 of *B. pyrrocinia* and *B. cenocepacia* [109, 110]. The *afc* cluster was shown to be regulated by ShvR, a LysR-

type regulator encoded adjacent to the *afc* genes [111]. Furthermore, mutations of two genes from the *afc* cluster, *afcE* and *afcF*, resulted in the loss of antifungal activity in *B. cenocepacia* K56-2 [112].

1.3.1.4 Siderophores

Iron is one of the most important trace elements necessary for bacterial survival. Although it is one of the most abundant elements on Earth, iron is not readily available to bacteria, as it is rapidly oxidised from Fe^{2+} to insoluble Fe^{3+} in the presence of oxygen and at neutral pH. One of the most important bacterial strategies to solubilize iron is the production of siderophores, low molecular weight molecules which chelate iron outside the cell and are subsequently taken up via specific transporters [113, 114]. Members of the genus *Burkholderia* are able to produce and secrete a range of structurally different siderophores, mainly from the hydroxamate, catecholate and phenolate classes of molecules [115, 116].

1.3.1.4.1 Pyochelin

The phenolate siderophorepyochelin is synthesized by *B. cepacia* and *B. cenocepacia* and occurs in two stereoisomeric forms, pyochelin I and pyochelin II [117-119]. Two pyochelin molecules are necessary to bind one ferric ion [120] but the siderophore was also shown to bind other metals including zinc, copper, cobalt, vanadium and molybdenum [121-123]. Pyochelin is induced in the presence of aluminum under low iron and iron-replete conditions [124]. Pyochelin is synthesized from two L-cysteine residues and one salicylate residue by two NRPS enzymes, PchE and PchF [117, 125]. Although the pyochelin biosynthesis cluster is present in most *B. cepacia* and *B. cenocepacia* strains, about 50% of clinical Bcc isolates testedwere found either to produce no pyochelin, or negligible amounts [126, 127], which might be explained by the fact that the NRPS gene *pchF* has a frameshift mutation in several strains, including *B. cenocepacia* J2315.

1.3.1.4.2 Ornibactin

The linear tetrapeptide ornibactin possesses two hydroxamate and α-hydroxy carboxylate metal chelation groups and is the most prevalent siderophore among

Burkholderia species [115, 127], being produced by Bcc species including *B. cepacia*, *B. cenocepacia*, *B. ambifaria* and *B. vietnamiensis* [127-129]. Ornibactin biosynthesis is directed by the *orb* gene cluster, with *orbI* and *orbJ* coding for the two NRPS enzymes responsible for the biosynthesis of the peptide chain [130]. Mutations in the ornibactin biosynthesis genes and receptor in *B. cenocepacia* K56-2 resulted in attenuated virulence in the two invertebrate model organisms *Caenorhabditis elegans* and *Galleria mellonella* [131]. Ornibactin biosynthesis is upregulated under low iron conditions and is part of the Fur regulon. Fur regulates transcription of the OrbS sigma factor, which directs transcription of the ornibactin biosynthetic and transport genes [130]. Recently, it was shown that ornibactin expression is increased in the presence of zinc, copper and aluminum. In addition, ornibactin allowed *Burkholderia* to grow in the presence of aluminum, zinc, lead and copper, while growth of the respective ornibactin mutant strains was inhibited by these metals. This indicates that ornibactin can protect the cells from the toxic effects of these metals [124].

1.3.1.4.3 Additional siderophores

Members of the *B. pseudomallei* group synthesize the siderophore malleobactin [132], which is structurally very similar to ornibactin. The two molecules differ in the presence of a 2-amino-5-nitropentanoic acid in malleobactin, which replaces the *N*-hydroxy-*N*-acylornithine moiety present in ornibactin [133]. Furthermore, a siderophore was reported to be produced by *Burkholderia xenovorans*, which was proposed to be structurally related to malleobactin, but a complete structural elucidation is still pending [134].

The cyclic hydroxamate siderophore cepabactin was shown to be produced under iron-limited conditions by *B. cepacia* [135] and the catecholate siderophore cepaciachelin is produced by *Burkholderia ambifaria* isolated from the plant rhizosphere [136].

1.4 Regulation of secondary metabolite biosynthesis

It has become clear that in the genus *Burkholderia*, many secondary metabolites are regulated by quorum sensing as well as solo LuxR-type regulators, which can either be responsive to AHLs or not.

1.4.1 Regulation by quorum sensing

In the *B. pseudomallei* group, bactobolins, polar antibiotics derived from *B. thailandiensis* E264, were shown to be regulated by the BtaR2/BtaI2 quorum sensing system [83].

One of the most prominent secondary metabolites demonstrated to be quorum sensing regulated is pyrrolnitrin, which has been described above. Schmidt and colleagues showed that pyrrolnitrin production is dependent on the CepIR QS system in *B. lata* strain 383 and enzymatic inactivation of QS in *B. ambifaria* LMG19467 and *B. pyrrocinia* LMG21823 abolished or greatly reduced pyrrolnitrin production in these two strains [23].

B. ambifaria produces the polyketide metabolites enacyloxin IIa and its isomer cis-enacyloxin IIA which are highly active against the multi-drug resistant Gram-negative bacteria *Burkholderia multivorans*, *Burkholderia dolosa* and *Acinetobacter baumannii* [137]. Enacyloxin production was highest when the bacteria were grown with glycerol as sole carbon source and after they had reached stationary phase. Furthermore, enacyloxin production was dependent on the AHL synthase CepI as well as the presence of a solo LuxR-type regulator which is part of the enacyloxin biosynthesis cluster [137].

Occidiofungins, antifungal glycopeptides from several Bcc members, were shown to be regulated by two solo LuxR-type regulators, designated AmbR1 and AmbR2, which are encoded in close vicinity to the occidiofungin biosynthesis genes [138, 139]. Furthermore, a solo LuxR-type regulator which is part of an NRPS gene cluster in *B. vietnamiensis* DBO1 was essential for hemolytic activity and *G. mellonella* mortality; which was also shown for several mutants in the NRPS gene cluster [108].

A transposon mutagenesis study in *B. ambifaria* by Chapalain and colleagues confirmed the regulation of pyrrolnitrin by QS and also showed reduced expression of

genes from the enacyloxin and occidiofungin clusters in a *cepI* mutant background [140].

The two siderophores pyochelin and ornibactin are also quorum sensing regulated in *B. cenocepacia*. While ornibactin was demonstrated to be negatively regulated by the CepIR QS system [131, 141], pyochelin is not directly regulated by CepIR but is positively regulated by the solo LuxR-type regulator CepR2 [54].

1.5 The biosynthesis of secondary metabolites

Most antibiotics used to date derive from two distinct molecule classes, polyketides (PK) and non-ribosomal peptides (NRP) [75, 142-146]. In addition to their antibiotic activities, molecules of these classes can also possess potent antitumor or antiviral activity while some are used as immunosuppressives or can act as toxins. PKS and NRP are synthesized by multi domain enzymes known as non-ribosomal peptide synthetases (NRPS), with each domain serving a specific function, e.g. substrate recognition or chain elongation in the biosynthetic assembly line [147-152].

1.5.1 Non-ribosomal peptides (NRP)

NRPS-derived secondary metabolites have very high structural diversity. This is owed to the fact that not only the 20 proteinogenic amino acids can be incorporated into NRPS molecules, but also D-amino acids, carboxylic acids and α-hydroxy acids. Besides that, NRPS-derived molecules can also undergo extensive modifications, including methylation, acylation, glycosylation and ring formation. Finally, the release of the assembled molecule from the NRPS enzyme can yield a linear, cyclic or macrocyclic peptide. While the majority of known NRPS-derived molecules are assembled in a linear fashion, meaning that the single building blocks are incorporated in the growing peptide chain in the same order as the modules present in the assembly line, several NRPS-derived molecules have been identified which are synthesized in an iterative fashion [153]. Linear NRPS assembly lines start with an initiation module, followed by one or several elongation modules and end with a termination module. A detailed description of these three module types is given

below. Modules of iterative NRPS assembly lines are used more than once, which results in the incorporation of the same subunit into the final molecule multiple times. Enterobactin [154] and gramicidin S [155], for example, are synthesized by iterative NRPS assembly lines.

1.5.1.1 NRPS modules

Three different types of modules can be distinguished for NRPS enzymes. The NRPS assembly line starts with an initiation module, which is followed by one or more elongation modules and ends with the termination module. The initiation module normally starts with an adenylation (A) domain, followed by a thiolation (T) domain, which is also called peptidyl carrier protein (PCP) domain. In certain cases, starter condensation (starter C) domain can preceed the first domain of the initiation module. Elongation modules consist of three domains, the condensation (C) domain, an A domain and a T domain [147, 156]. The last module in the NRPS assembly line is the termination module which either ends with a thioesterase (TE) or a reductase (R) domain and is responsible for the release of the assembled molecule [157]. The molecular function of the different NRPS modules are discussed below and an overview of an NRPS assembly line is shown in Figure 2.

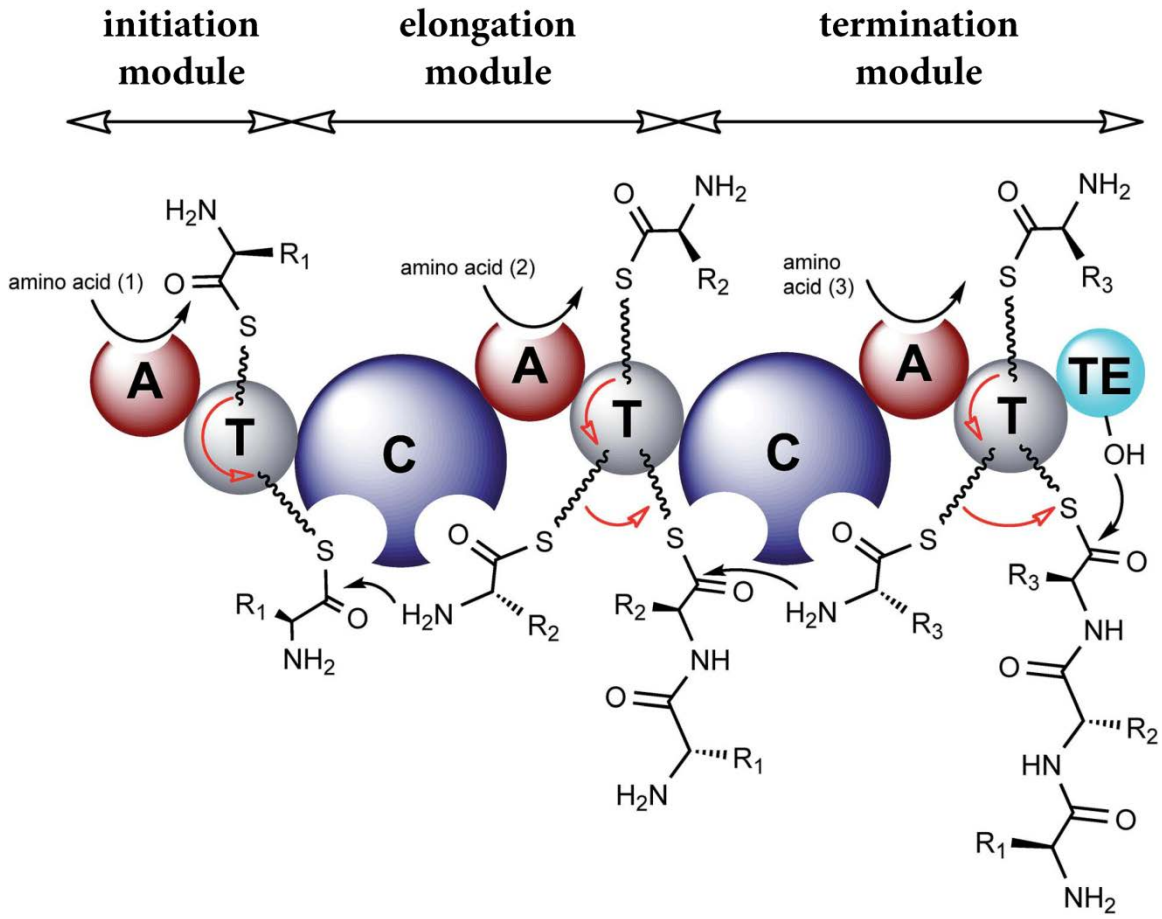

Figure 2 : Model of an NRPS assembly line. The amino acid is activated by the adenylation (A) domain and tethered to the thiolation (T) domain. The condensation (C) domain catalyses the peptide bond formation of amino acids of tethered to two adjacent T domains. The assembled peptide is release by the thioesterase (TE) domain via hydrolysis or cyclisaton. Modified from Winn and colleagues [158].

1.5.1.1.1 Initiation of peptide biosynthesis

Canonical NRPS enzymes start with an A domain at their N-terminus, which is responsible for initiating peptide formation. In special cases, NRPS enzymes start with a starter C domain. These domains connect the amino acid of the first A domain with a *β*-hydroxy-carboxylic acid [159]. The lipopeptides surfactin [160], lichenysin [161], fengycin [162] and arthrofactin [163] all derive from NRPS enzymes that have a starter C as the very first domain in their assembly line.

1.5.1.1.2 Peptide elongation cycle

The A domain of each module is responsible for the recognition and activation of the substrate amino acid. The amino acid is activated in an ATP-dependent adenylation step and the resulting aminoacyl adenylate intermediate is then tethered to the free thiol group of the 4`-phosphopantetheine (ppant) arm present on the T domain. The ppant arm is located on a conserved serine residue and derived from coenzyme A [164-167]. Subsequently, the C domain is responsible for the formation of a peptide bond between the T domain-bound amino acids of two adjacent modules [168]. C domains contain a conserved motif in their active site, with the consensus sequence HHxxxDG. The second histidine in the motif has been shown to be essential for the catalytic function of the C domain [169]. In addition to the already described starter C domain, three other subtypes of C domains exist. The most common one is the $^{L}C_{L}$ domain, which catalyses peptide bond formation between two L-amino acids. $^{D}C_{L}$ domains catalyse peptide bond formation between a D- and an L-amino acid. They are normally located immediately downstream of an epimerase (E) domain and are enantiospecific for D-amino acids from the donor site and L-amino acids from the acceptor site [170, 171]. The third C domain subtype is the dual E/C domain, which catalyses the epimerization of one amino acid and subsequent peptide bond formation with the second amino acid [172].

1.5.1.1.3 Peptide release

The growing peptide chain is covalently tethered to the NRPS enzyme during the whole elongation process. Only when the peptide reaches the termination module, is it released from the NRPS. In most cases, the peptide is released via the action of a TE domain. This is achieved by transferring the peptide to the hydroxyl of a serine residue located in the active site of the TE domain, and a peptidyl-acyl-*O*-serine intermediate is formed. The intermediate is then attacked by either an external nucleophile and the linear peptide is released by hydrolysis. Alternatively, an internal nucleophile attack from the peptide intermediate itself can lead to release by macrocyclization [157]. Linear peptide release by hydrolysis was demonstrated for yersiniabactin and vancomycin [173, 174], while release by macrocyclization was shown for daptomycin and erythromycin [175, 176].

In addition to TE domain catalysed peptide release, several NRPS systems have a R domain in their termination module. The peptide can be released from the NRPs either by a two-electron or a four-electron reduction. Release by a two-electron reduction was first described for the Lys2 protein from the lysine biosynthetic pathway [177]. In gramicidin A biosynthesis, the R domain also catalyses a two-electron reduction, but the aldehyde intermediate is then further reduced to an ethanolamine by an NADPH-dependent aldoreductase [178, 179].

Release by a four-electron reduction has been demonstrated for the biosynthesis of myxochelin A and B [180] as well as lyngbyatoxin [181]. During the release of the NRPS-bound myxochelin intermediate, the aminoacyl-S-T thioester is first reduced to an aldehyde in a two-electron reduction step, followed by a second two-electron reduction step to an alcohol, which yields myxochelin A. Interestingly, the second two-electron reduction step can be prevented by competitive transamination of the aldehyde to yield myxochelin B [180].

1.5.1.2 Tailoring reactions

The vast diversity of NRPS-derived secondary metabolites is partially owed to the introduction of structural diversity by tailoring reactions. Such tailoring reactions can be accomplished by enzymatic domains directly encoded by the NRPS enzyme or by separately encoded enzymes [158, 182, 183]. Most NRPS-derived molecules are modified by tailoring enzymes after release of the assembled peptide (post-assembly tailoring), but there are reports on a growing number of secondary metabolites which undergo structural modification while the intermediates are still bound to the NRPS enzyme. These tailoring reactions are referred to as on-line tailoring [182].

1.5.1.2.1 Epimerization reactions

A prominent tailoring reaction is the epimerization of L-amino acids to D-amino acids during the biosynthesis of the growing peptide chain. As discussed above, these reactions are carried out by E domains or by dual E/C domains as well as racemases [183]. Rather than a full conversion of L- to D-amino acids, E domains produce a racemic mix of D- and L- amino acids and the incorporation of the D-amino acid in

the growing peptide chain is dependent on the enantio specificity of the following $^{D}C_{L}$ domain, as seen in gramicidin S synthesis [184]. In contrast, in cyclosporin and HC-toxin biosynthesis, D-alanine, which is the first residue in both molecules, is provided by an alanine racemase [185, 186].

1.5.1.2.2 Glycosylation reactions

Glycosylations are an important modification of NRPS derived molecules, such as the clinically important glycopeptide antibiotics vancomycin, teicoplanin and chloroermomycin [187]. The glycosylation reactions are post-assembly tailoring steps which are carried out by glycosyltransferases encoded in the respective biosynthesis clusters [188-192]. Frequently, the sugars added to the NRPS backbone are not D-isomers, but rather nucleoside diphosphoesters of deoxy- and aminodeoxyhexoses [193, 194]. The enzymes which convert the abundant metabolites UPD-glucose and TDP-glucose to the necessary NDP-hexoses are often also encoded within the NRPS biosynthesis clusters [195].

1.5.1.2.3 Oxidative tailoring

One of the best studied and most important examples of oxidative tailoring is the production of β-lactam antibiotics. After release from the NRPS assembly line, the biosynthesis intermediate aminoadipoyl-cysteinyl-valine (ACV) is first oxidized by the Fe^{II}-*α*-ketoglutarate dependent oxygenase isopenicillin N synthase to yield isopenicillin N. After epimerization to penicillin N, a second oxygenase deacetoxycephalosporin C synthase oxidizes the molecule to deacetoxycephalosporin C [196-198]. Besides post-assembly oxidation, vancomycin and teicoplanin also undergo on-line oxidative tailoring by several hemeproteins from thecytochrome P450 family [174]. These reactions take place while the peptide is still bound to the last T domain of the assembly line. The conversion from the acyclic heptapeptide to the cup-shaped final structure of vancomycin and teicoplanin is thought to trigger the TE domain-catalysed release of molecules from the assembly line [199-201].

1.5.1.2.4 Methylation reactions

N-methylation of NRPS molecules is carried out by N-methyltransferases, which are encoded between the A and the T domain. Accordingly, methylation is carried out while the amino acid is incorporated into the growing peptide chain [169]. The methyl group is derived from S-adenosylmethionine and in most cases it is transferred to the amino group of the T domain-tethered amino acid [202]. In the case of enniatin and the cyclooctadepsipeptide PF1022A, *N*-methylation takes place on the amino acid monomer before incorporation into the peptide chain [203, 204].

C-methylation is found in the PKS/NRPS hybrid molecule yersiniabactin, where the first methylation domain (MT1) acts on the PKS part of the molecule and the second methylation domain (MT2) acts on the NRPS part of the molecule [205].

O-methylation has been reported for the NRPS-derived molecule saframycin Mx1. A standalone *O*-methyltransferase encoded in the saframycin biosynthetic cluster is proposed to carry out the methylation reaction. Nevertheless, there are three distinct methylations found in the saframycin Mx1 structure and it is not known which of these is carried out by the o-methyltransferase [206].

1.5.1.2.5 Hydroxylation reactions

Important antibiotics like vancomycin, bleomycin and novobiocin contain β-hydroxy amino acids. It was shown that during novobiocin biosynthesis, the cytochrome P450 monooxygenase NovI introduces one atom from O_2 at the C_3 position of a T domain tethered tyrosine, which yields T domain tethered *β*-hydroxyamino acid (*3R*)-3-OH-tyrosine [207].

Aims of the thesis

Antifungal activity of *B. cenocepacia* was thought to depend on the presence of the *afc* gene cluster located on megaplasmid pC3. This work was initiated by the observation that deletion of megaplasmid pC3 resulted in complete loss of antifungal activity in *B. cenocepacia* K56-2 while strain H111 still showed antifungal activity. This indicated that another antifungal compound is encoded by one of the two chromosomes in *B. cenocepacia* H111.

The aim of this thesis was to identify the genetic locus responsible for the antifungal activity of *Burkholderia cenocepacia* H111 and to entangle the regulation of antifungal activity. Furthermore, this thesis aimed to elucidate the chemical nature of the antifungal metabolite(s) produced by B. cenocepacia H111. In the course of this study it became apparent, that the same genetic locus which is responsible for the biosynthesis of the antifungal metabolite, also produces a novel signalling molecule. Thefore we also persued to chemically characterize this novel signalling molecule and determine its regulon.

Chapter II: Results

2 Results I: Microbial Antagonism

2.1 Identification of genetic clusters involved in antifungal activity

Many antifungal compounds are either polyketides (PK), non-ribosomal peptides (NRP) or hybrids thereof. Genome-wide identification of secondary metabolite biosynthesis gene clusters with the antiSMASH 3.0 software [208] identified a total of 15 secondary metabolite clusters, of which three are non-ribosomal peptide synthetase (NRPS) clusters and one is a type 1 polyketide synthase (PKS) cluster (Table 1). The predicted PKS cluster is part of the capsular polysaccharide I locus, while the identified NRPS like clusters are the well characterized ornibactin and pyochelin biosynthesis gene clusters and a so far uncharacterized NRPS-like gene cluster (Table 1).

Table 1: Secondary metabolite clusters of *B. cenocepacia* H111 predicted with the AntiSMASH 3.0 software

Replicon	Type	Location (nt start – stop)	Function
Chromosome 1	T1PKS	682853 – 730463	Capsular polysaccharide locus
Chromosome 1	NRPS	1712441 – 1767140	Ornibaction biosyntehsis
Chromosome 1	Terpen	2083072 – 2103905	unknown
Chromosome 1	Arylpolyene	3045402 – 3086625	unknown
Chromosome 2	Bacteriocin	28172 – 41229	unknown
Chromosome 2	NRPS	203774 – 251199	Uncharacterized NRPS-like
Chromosome 2	Phosphonate	1215171 – 1256859	unknown
Chromosome 2	Terpene	1409532 – 1430599	unknown
Chromosome 2	Homoserinelactone	1959336 – 1979944	unknown
Chromosome 2	Terpene	2141000 – 2162079	unknown
Chromosome 2	Terpene	2221517 – 2242587	unknown
Chromosome 2	NRPS	2384780 – 2437568	Pyochelin biosynthesis
Chromosome 2	Terpene	3081510 – 3102677	unknown
pC3	Terpene	188420 – 210300	unknown
pC3	Bacteriocin	717851 - 728666	unknown

It was previously established that enzymatic inactivation of the AHL-dependent QS system with the *Bacillus sp*. derived AiiA lactonase reduced antifungal activity in different *Burkholderia* strains, among them *B. cenocepacia* H111 [23]. This suggests that antifungal activity of *B. cenocepacia* H111 is under QS control. In addition, antifungal activity of *B. cenocepacia* K56-2 is dependent on the *afc* gene cluster [112], which is located on megaplasmid pC3 in several *B. cenocepacia* strains [110]. Interestingly, when *B. cenocepacia* H111 is cured of megaplasmid pC3, antifungal activity is reduced, but not entirely lost [110]. This indicates that pC3 might have a regulatory effect on antifungal activity of *B. cenocepacia* H111, rather than directly encode the antifungal determinant. To explore this possibility and identify candidate NRPS or PKS clusters for the biosynthesis of the unknown antifungal agent produced by strain H111, the published transcriptomes of the QS mutant *B. cenocepacia* H111 Δ*cepR* and a ΔpC3 derivative strain were compared with the transcriptomes of the H111 parental strain [110, 209]. The uncharacterized NRPS-like gene cluster

(I35_4188 – I35_4195) identified by antiSMASH 3.0 was downregulated in both the Δ*cepR* and the ΔpC3 mutant compared to the wild type strain (Table 2). The gene cluster consists of two operons, which are transcribed in opposite directions, one comprising five and the other two genes, which were named *hamABCDE* (H111 antifungal metabolite, see below) (I35_4191 – 4195) and *hamFG* (I35_4189 and I35_4188) (Figure 3A).

Table 2: Deregulation of the *ham* genes in the published transcriptomes of a pC3-null mutant (ΔpC3) and a CepR quorum sensing mutant (Δ*cepR*) compared to the wild type strain (wt). Data derived from [110, 209].

Gene	Name	ΔpC3 vs wt*	ΔcepR vs wt	J2315 ortholog
I35_4188	*hamG*	-5,0	-22,1	bcam0190
I35_4189	*hamF*	-4,9	-12,8	bcam0191
I35_4191	*hamA*	-12,0	-46,8	bcam0192
I35_4192	*hamB*	-12,2	-47,7	bcam0193
I35_4193	*hamC*	-14,5	-52,2	bcam0194
I35_4194	*hamD*	-9,3	-34,0	bcam0195
I35_4195	*hamE*	-10,4	-37,7	bcam0196

Often the expression and transport of secondary metabolites is governed by regulators and transporters encoded within the respective PKS and NRPS gene clusters [148]. Located upstream of the *hamFG* operon are genes encoding the AraC-type regulator CepS (I35_4187) and the solo LuxR-type regulator CepR2 (I35_4186), which were both shown to be involved in the regulation of the *ham* cluster in *B. cenocepacia* K56-2 [54, 55]. Located immediately downstream of the *hamAE* operon are genes encoding an uncharacterized AraC-type (I35_4197) and a LysR-type regulator (I35_4196). In addition, a tripartite multidrug resistance system (*mdr*1-*mdr*3; I35_4198 – I35_41200) is located near the *ham* cluster (Figure 3A).

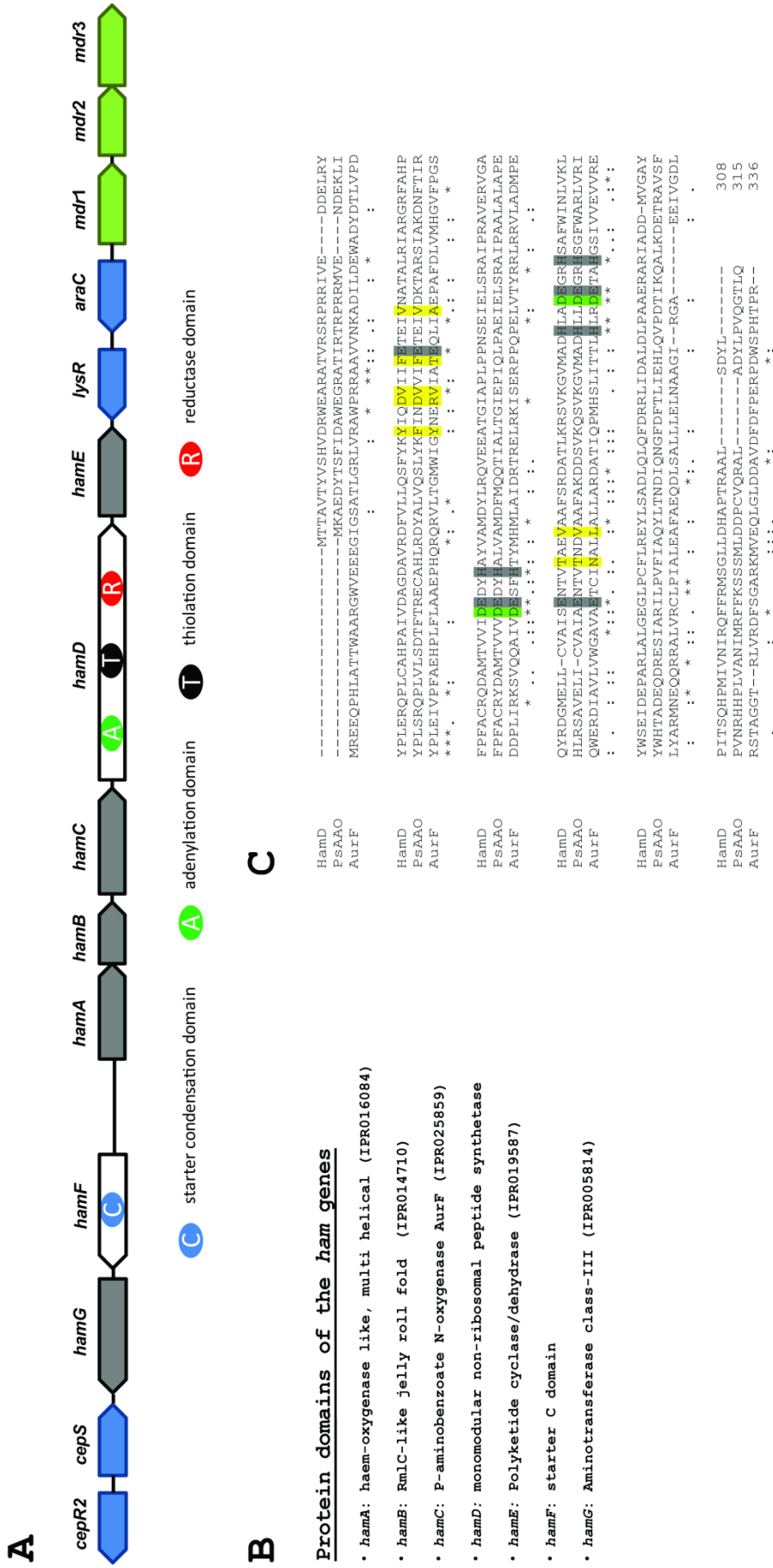

Figure 3: Genetic organization and domain predictions of the *ham* cluster and surrounding genes. A) The *ham* cluster is organized into two operons and surrounded by genes encoding four regulators and an uncharacterized multi-drug resistance system. Domains typical for NRPS-like enzymes were found in *hamD* and *hamF*. B) Predictions of protein domains and enzyme functions for all seven *ham* genes. Predictions were made with the Interproscan online tool. C) Amino acid alignment of HamC with its characterized homologues AurF and PsAAO. Metal coordinating residues are highlighted in dark grey, residues of the active site pocket are highlighted in yellow and residues from the second coordination sphere are highlighted in green.

2.2 Bioinformatic predictions of the ham gene cluster

The NRPS-like protein HamD encodes for an adenylation (A) domain, a thiolation (T) domain and a reductase (R) domain (NRPS/PKS analysis tool) [210] (Figure3A). Further analysis of the *hamD*-encoded A domain predicted phenylalanine (NRPSsp online tool) [211] and leucine (NRPSpredictor2 online tool) [212] as the most likely amino acid substrates (Table 3). HamF is a free-standing starter C domain (InterProScan 5; NaPDoS; Natural Product Domain Seeker) [213] (Figure 3A). In contrast to conventional C domains, starter C domains acylate amino acids bound to the T domain with a β-hydroxy-carboxylic acid [159]. Thus, the main building blocks of the predicted biosynthetic product of the *ham* cluster are an amino acid and a fatty acid. Analysis of the remaining five genes in the *ham* cluster with the InterProScan 5 online tool suggested that they are tailoring enzymes (Figure 3B).

Table 3: Substrate specificity of the HamD, PvfC and MgoA A domains

Enzyme	Residues binding pocket*	Amino acid substrate NRPSpredictor2	Amino acid substrate NRPSsp
HamD	DALFVGIV	Leucine	Phenylalanine
PvfC	DALFVGIV	Leucine	Phenylalanine
MgoA	DSIFMGLV	Leucine	Phenylalanine

The putative tailoring enzyme HamC, is an arylamine *N*-oxygenase. Alignments of HamC with its characterized homologs from *Streptomyces thioluteus* (AurF) and *Pseudomonas syringae pv. phaseolicola* (PsAAO) show conservation of the iron-coordinating ligands and residues for establishing the second coordination sphere (Figure 3C), as has been shown previously [214]. The residues responsible for substrate specificity are highly conserved between HamC and PsAAO (Figure 3C) suggesting a similar substrate range. Both enzymes, AurF and PsAAO, have aromatic amine substrates and catalyze the oxidation of the amino group to a nitro group [214, 215].

An architecture search of the *ham* cluster with the multi gene blast software showed that homologs of the *ham* cluster are present in most sequenced *B. cenocepacia* strains (Figure 4). Furthermore, the *hamABCDE* operon is fully conserved in *Burkholderia glumae* PG1, *Pseudomonas aeruginosa* PA7 and *Pseudomonas fluorescens* strain X. A homologous operon that lacks *hamB* is also present in various *Pseudomonas* and *Pandoraea* species (Figure 4). Two of these operons, *pvf* and *mgo* from *Pseudomonas entomophila* and *Pseudomonas syringae pv*. *syringae* UMAF0158, respectively, were previously shown to synthesize an unknown signal molecule which regulates virulence and the production of secondary metabolites [216, 217]. In this context it was of interest to know if PvfC and MgoA might have the same amino acid substrate as HamD. Prediction and comparison of the residues present in the A domain substrate binding box of the three proteins with the PKS/NRPS analysis software [210] could not identify a possible amino acid substrate, but showed full conservation of the residues in the substrate binding box between HamD and PvfC, while MgoA differed in four out of eight amino acids (Table 3). Additional analysis with the NRPSpredictor2 and NRPSsp software predicted leucine and phenylalanine as substrates for all three enzymes (Table 3). Based on these predictions, the amino acid incorporated into the final biosynthesis product of the *ham*, *pvf* and *mgo* cluster is likely to be the same.

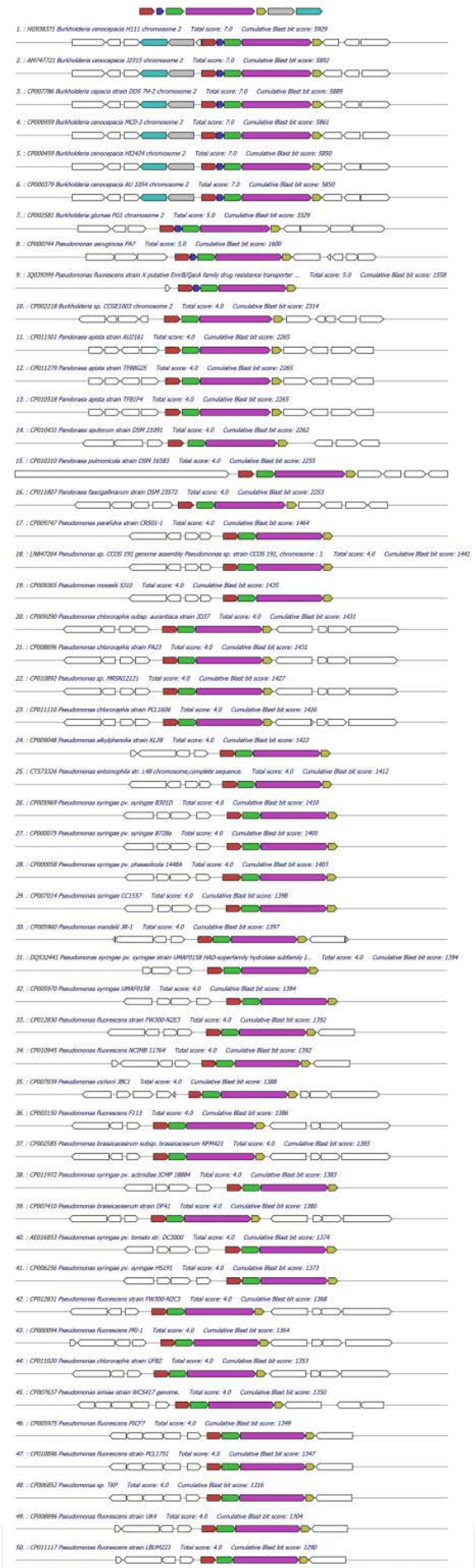

Figure 4 : Distribution of the *ham* gene cluster in the domain bacteria. Shown are the top 50 hits derived from a multigene blast of all seven *ham* genes identified in *B. cenocepacia* H111, against the complete bacterial genomic database at NCBI. Red = HamA; blue = HamB; green = HamC; pink = HamD; yellow = HamE; grey = HamF and cyan = HamG.

2.3 Antifungal activity is quorum sensing controlled, but not dependent on the *afc* gene cluster

Antifungal activity of *B. cenocepacia* H111 is reduced by enzymatic inactivation of the quorum sensing signaling cascade [23], but direct proof of the dependency of antifungal activity on QS is not available. To unequivocally prove that antifungal activity is regulated by QS and that the observed reduction of antifungal activity by enzymatic inactivation of the QS system is not due to a pleiotropic effect of lactonase overexpression, we tested a strain in which the AHL synthase gene *cepI,* together with the QS regulator gene *cepR,* were deleted, for antifungal activity against *Fusarium solani* and *Rhizoctonia solani*. In agreement with the QS quenching approach, the H111 Δ*cepIR* mutant showed an approximately 50 % reduction in antifungal activity against both fungi (Figure 5).

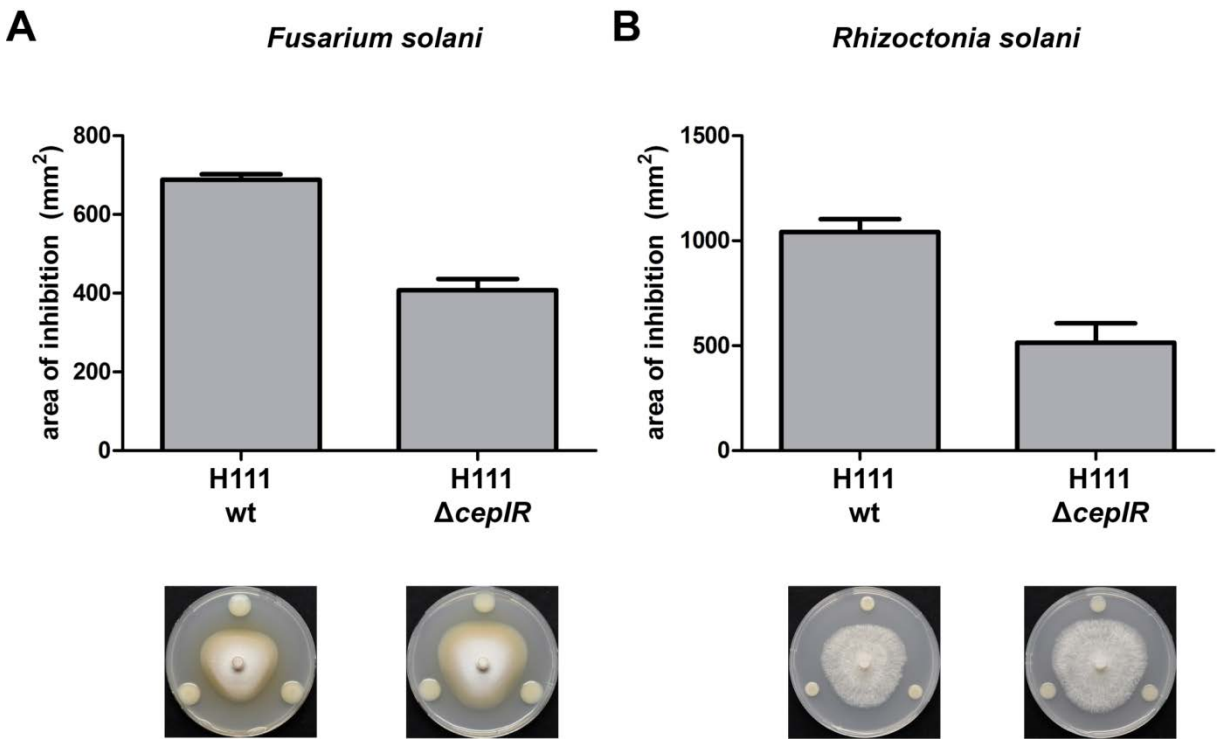

Figure 5: Regulation of antifungal activity by the quorum sensing system. Reduction of antifungal activity in a *cepIR* mutant (H111 Δ*cepIR*) compared to the wild type strain (H111 wt) against the fungus A) *Fusarium solani* and B) *Rhizoctonia solani*. Area of inhibition refers to the difference in plate surface covered with the fungus in the presence and absence of bacteria. Results are represented as means ± SD derived from at least 3 independent experiments. Representative pictures of the antifungal assays are shown below the respective bars.

To determine if the reduction of antifungal activity in the pC3-negative derivative of strain H111 is due to the loss of the *afc* cluster, an *afcA* mutant was tested for antifungal activity in dual culture plate assays as well as by fungal spray assay. Deletion of *afcA* did not alter the capability of strain H111 to inhibit the growth of *F. solani* and *R. solani* (Figure 6A and 6B), while the pC3-negative strain showed reduced antifungal activity (Figure 6C) against *F. solani*, as reported before [110]. This is compelling evidence that antifungal activity of *B. cenocepacia* H111 is not dependent on the *afc* cluster but is probably dependent on the *ham* cluster.

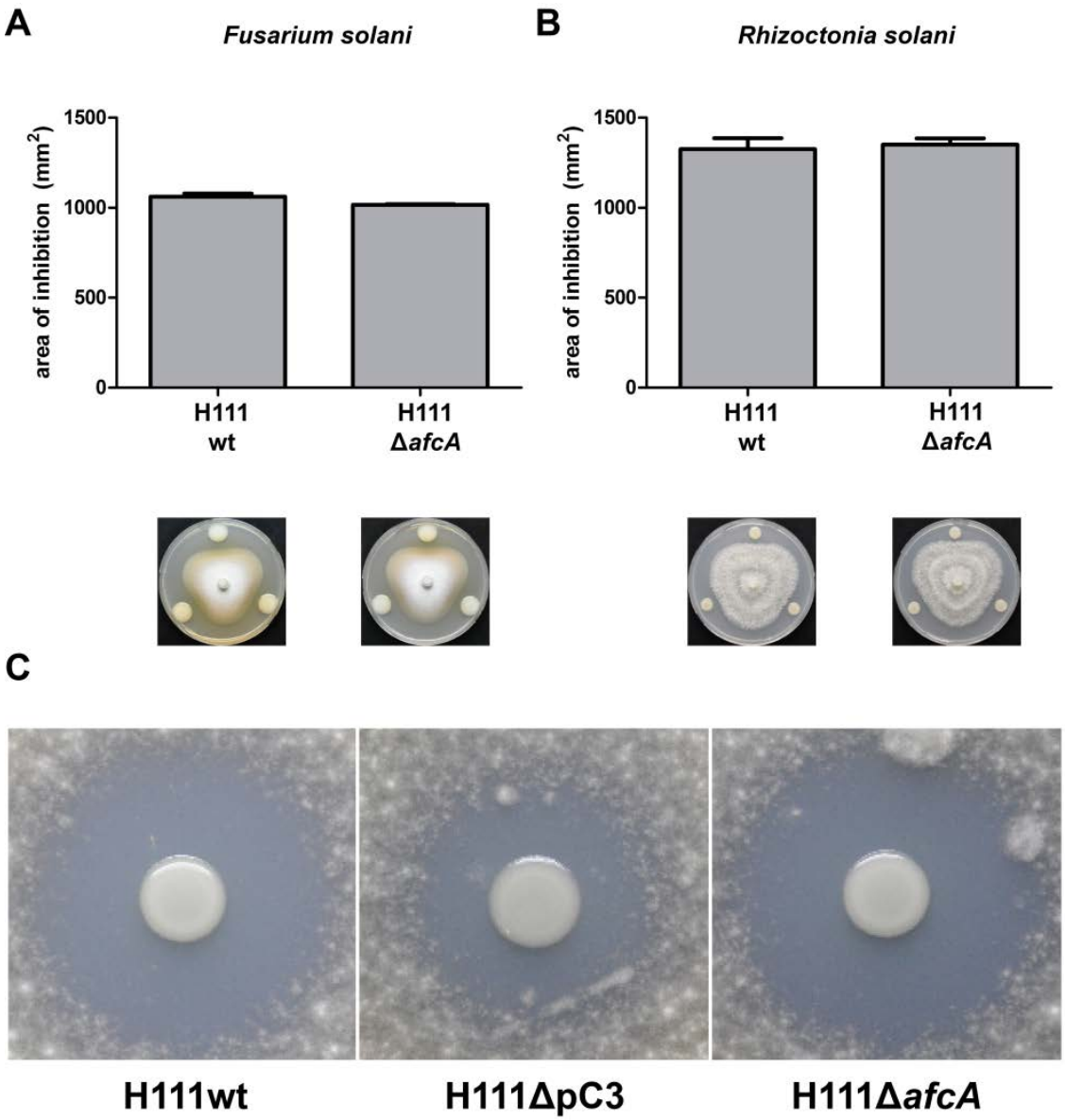

Figure 6: Impact of AfcA on antifungal activity of *B. cenocepacia* H111. Antifungal activity in an *afcA* mutant (H111 Δ*afcA*) compared to the wild type strain (H111 wt) against the fungus A) *Fusarium solani* and B) *Rhizoctonia solani*. Area of inhibition refers to the difference in plate surface covered with the fungus in the presence and absence of bacteria. Results are represented as means ± SD derived from at least 3 independent experiments. Representative pictures of the antifungal assays are shown below the respective bars. C) Antifungal activity is reduced in the pC3 negative derivative (H111 ΔpC3) of strain H111, compared to the wildtype strain (H111 wt) and the *afcA* mutant (H111 Δ*afcA*)..Antifungal activity is seen as a zone of fungal growth inhibition around the bacterial colony. Representative pictures of antifungal spray assays against the fungus *F. solani* are shown.

2.4 Antifungal activity is inversely regulated by CepR2 in strain H111 and K56-2

In a recent publication, the *ham* cluster was shown to be regulated by the two adjacently encoded regulators CepR2 and CepS in *B. cenocepacia* K56-2 [55]. In the proposed regulation model, the binding sites of CepR2 and CepS are located in the intergenic promoter regions of the *ham* cluster. CepR2 is thought to be a negative regulator that upon binding to its operator site blocks binding of the positive regulator CepS to the promoter region. To test if CepR2 negatively regulates *B. cenocepacia* antifungal activity, a *cepR2* mutant of *B. cenocepacia* H111 and K56-2 along with their respective wildtype strains were tested for antifungal activity against *F. solani*. The *B. cenocepacia* K56-2 wild-type strain exhibited less antifungal activity against *F. solani* than the *B. cenocepacia* H111 wild-type strain (Figure 7A). The *B. cenocepacia* H111 *cepR2* mutant was devoid of antifungal activity. In contrast, the K56-2 *cepR2* mutant strain showed increased fungal inhibition, which was comparable to that of the H111 wild-type strain (Figure 7A). This observation is in agreement with the proposed model of Ryan et al [55], that CepR2 is a negative regulator of the *ham* cluster in K56-2. In stark contrast, a *cepR2* mutant in strain H111 resulted in complete abbrogation of antifungal activity. To understand if this apparent discrepancy could be explained by a difference in the CepR2 structure or the CepR2 DNA binding site in the *ham* promoter region, the amino acid sequences of the K56-2 and H111 CepR2 protein were compared. An alignment of the amino acid sequences of the two proteins showed that they only differ by a single aminoacid. Importantly, the six amino acids responsible for AHL binding are fully conserved between the two proteins (Figure 7B). Inspection of the *ham* promoter region, especially of the CepR2 DNA binding site (as proposed in [55]), showed that the two CepR2 binding boxes only differ by one nucleotide (Figure 7C).

Figure 7: Regulation of antifungal activity by CepR2. A) Antifungal activity of the H111 wild type (H111 wt) is absent in the *cepR2* mutant (H111 Δ*cepR2*). In strain K56-2, antifungal activity is lower in the K56-2 wild type (K56-2 wt) strain than in the *cepR2* mutant (K56-2 Δ*cepR2*) derivative. B) The AHL binding domain of CepR2 is fully conserved between strains H111 and K56-2. Amino acid residues involved in AHL binding are highlighted in red. C) Nucleotide sequence of the CepR2 binding box of strains K56-2 and H111, according to Ryan and colleagues [55]. The difference between the nucleotide sequences of the two strains is highlighted in red.

2.5 The *ham* cluster is essential for antifungal activity of *B. cenocepacia* H111

After identification of the *ham* cluster as the possible source of the main antifungal compound of *B. cenocepacia* H111, the importance of the *ham* cluster for antifungal activity against the two fungal pathogens *F.solani* and *R.solani* was examined. Non-polar mutants in *hamD* and *hamF* were constructed as described in the material and methods section and, together with their respective *in trans* complemented derivatives, tested for activity against *F. solani* and *R. solani*. Deletion of *hamD* resulted in a strong decrease in antifungal activity. Deletion of the gene encoding the starter condensation domain protein HamF resulted in severely lowered antifungal activity against *F. solani,* but only a slight reduction of antifungal activity was observed against *R. solani* (Figures 8A and 8B). *In trans* complementation of H111 Δ*hamF* and H111 Δ*hamD* resulted in antifungal activity comparable to the wildtype strain against both fungi (Figures 8A and 8B), Therefore both operons of the *ham*

cluster seem to be essential for full antifungal activity and are likely to be involved in the biosynthesis of the main antifungal compound produced by strain H111. To ascertain the importance of individual *ham* genes for antifungal activity, non-polar mutants of the remaining five *ham* genes (*hamA*, *hamB*, *hamC*, *hamE* and *hamG*) were constructed. The wild-type strain and all seven *ham* mutant strains along with their *in trans* complemented derivatives were tested for antifungal activity against *F. solani* by antifungal spray assay. All seven *ham* mutants showed a complete loss of antifungal activity while the activities of their respective *in trans* complemented derivatives were comparable to that of the wild type (Figure 8C). This proves that the *ham* cluster is essential for antifungal activity and that the two *ham* operons most likely constitute a single biosynthetic unit which synthesizes the major antifungal compound of strain H111.

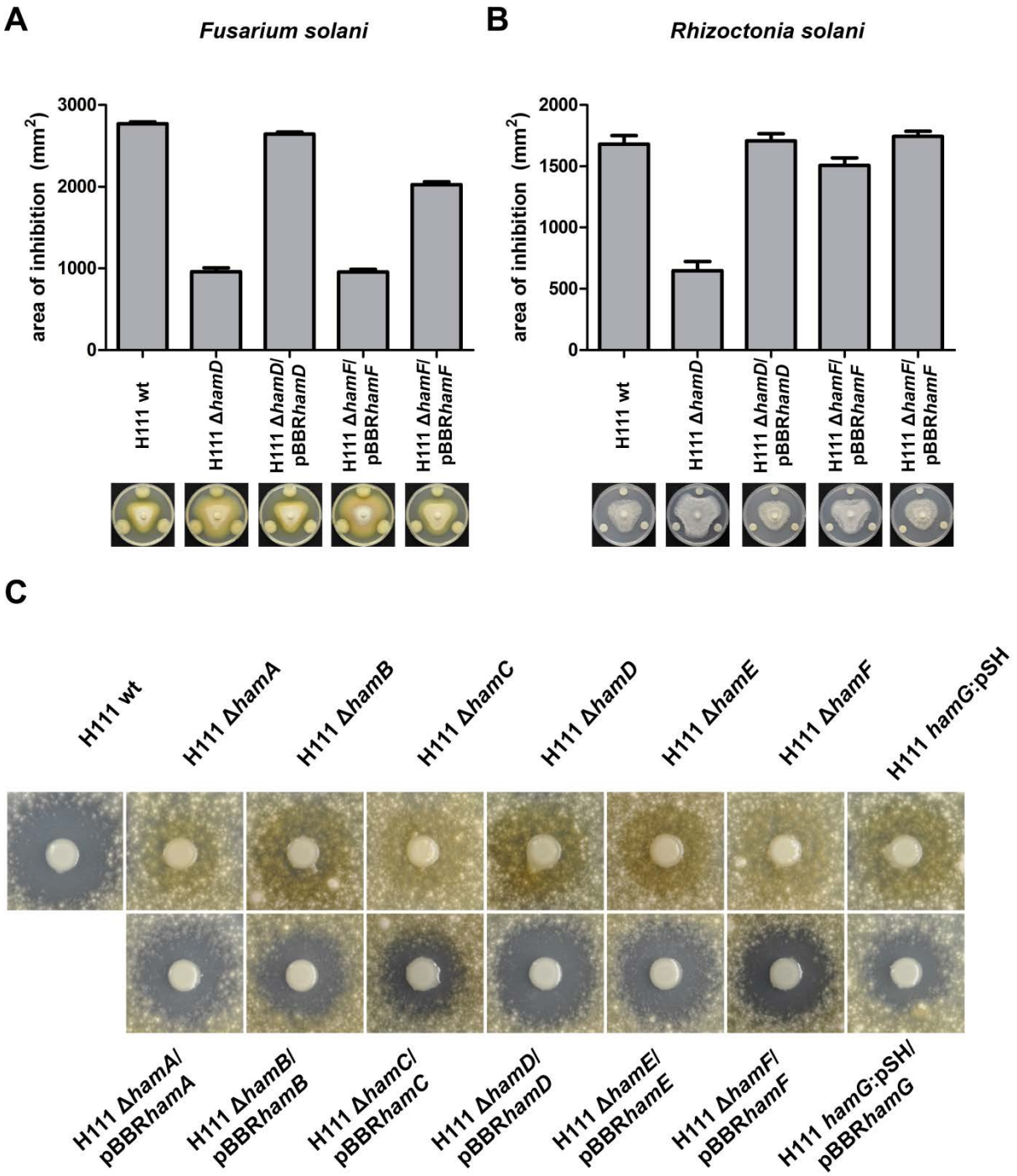

Figure 8: Antifungal activity is dependent on the *ham* gene cluster. Antifungal activity of the wild type (H111 wt), the *hamD* mutant (H111 Δ*hamD*), the *hamF* mutant (H111 Δ*hamF*) and the trans-complemented mutants (H111 Δ*hamD* pBBR*hamD* and H111 Δ*hamF* pBBR*hamF*) against A) *Fusarium solani* and B) *Rhizoctonia solani*. Area of inhibition refers to the difference in the plate surface covered with the fungus in the presence and absence of bacteria. Results are represented as means ± SD derived from at least 3 independent experiments. Representative pictures of the antifungal assays are shown below the respective bars. C) Antifungal activity is lost in single *ham* deletion mutants and restored by expression of the respective gene from a plasmid. Representative pictures of antifungal spray assays against the fungus *F. solani* are shown.

2.6 Fragin is the biosynthetic product of the *ham* cluster and the main antifungal compound of strain H111

After establishing that the *ham* cluster is essential for antifungal activity of *B. cenocepacia* H111, I attempted to identify the chemical nature of the antifungal molecule synthesized by the *ham* cluster. As described above, the genes of the *ham* cluster encode for an NRPS-like assembly line. Protein domain predictions for the *ham* genes suggest that the synthesized molecule is most likely a leucine or phenylalanine condensed with a fatty acid. Furthermore, the presence of the AurF-like protein encoded by *hamC* suggests that the structure might also contain a nitrogen group. To elucidate the structure of the biosynthetic product of the *ham* genes, the putative antifungal molecule was extracted from agar plates and ABG minimal broth cultures and the extracts were tested for antifungal activity. Extracts from the wildtype strain showed a clear inhibition of fungal rowth on MEA plates, while extracts from a *hamD* mutant did not inhibit fungal growth (Figure 9A).

To lower the complexity of the organic solvent extracts, a bioassay guided fractionation was carried out. Chloroform extracts of H111 wt and H111 Δ*hamD* were separated by TLC and the plate was divided into 14 sections. The stationary phase of the TLC plate was scraped off and re-extracted with methanol. All 14 fractions where then tested for their antifungal activity and the fraction with the highest antifungal activity (fraction 9) in the wildtype strain (Figure 9B) was used for high-performance liquid chromatography mass spectrometry (HPLC-MS) analysis. The corresponding fraction from H111 Δ*hamD* was also subjected to HPLC-MS analysis. The HPLC-MS spectra of fractions from the H111 wild type and the H111Δ*hamD* mutant were compared and a compound eluting with a retention time of 20.4 min was exclusively found in the wild type extract (Figure 9C). The compound was isolated by RP-HPLC using a Gemini-NX column, concentrated 200-fold and tested for its antifungal activity in a fungal spray assay as described above. As seen in Figure 9D, the isolated compound showed strong antifungal activity against the fungal model strain *F. solani*. The bioactive compound was further analysed by HPLC-MS and showed an *m/z* of 274.2 Da in positive mode and an *m/z* of 272.2 Da in negative mode, which suggested a molecular mass of 273.2 Da for the isolated compound.

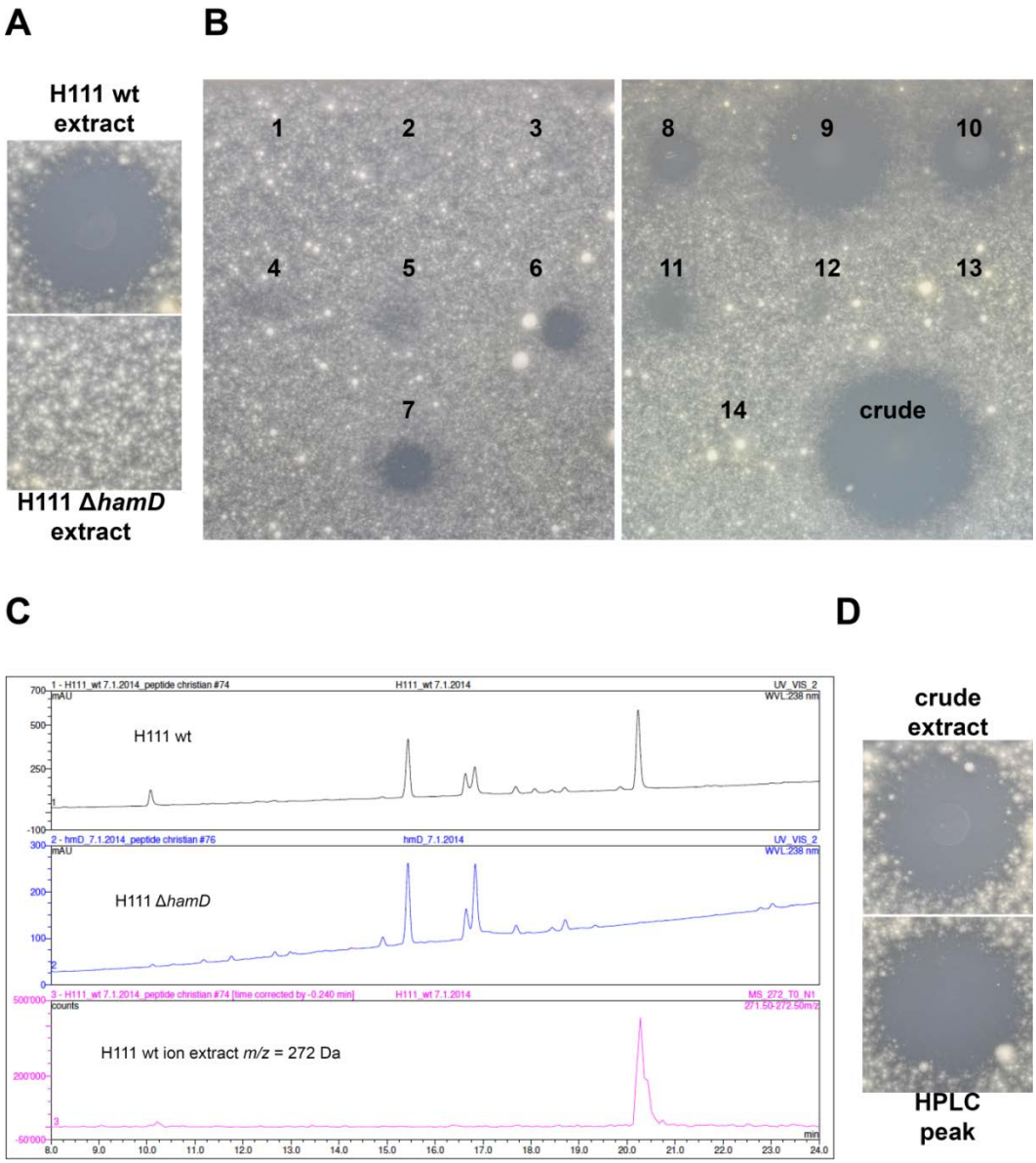

Figure 9 : Extraction and purification of the main antifungal metabolite from *B. cenocepacia* H111. A) Antifungal activity of concentrated chloroform extracts from wild type (H111 wt) and *hamD* mutant (H111 Δ*hamD*) cultures. B) Test for antifungal activity of the extracted antifungal compound after fractionation. Fractionation was carried out by TLC. The TLC plate was divided into 14 sections and antifungal compound(s) were recovered by methanol extraction. Fractions are labeled with numbers 1 to 14 and activities compared to that of the crude extract (crude). C) HPLC chromatograms of fraction 9 from the wild type strain (H111 wt) and the *hamD* mutant (H111 Δ*hamD*) show a distinct peak present in the wild type extract. The HPLC-MS chromatogram of the isolated peak from the wild type extract shows an *m/z* of 272 Da. D) Bioassay to confirm the antifungal activity of the HPLC-purified compound from fraction 9 of the wild type extract (HPLC peak). The isolated compound showed strong antifungal activity, comparable to the crude extract of the wild type culture. Representative pictures of an antifungal spray assay against the fungus *F. solani* are shown.

The structure of the compound was further determined by ^{1}H-NMR spectroscopy and together with the HPLC-MS measurements, the data are in agreement with the structure shown in Figure 10A, which resembles fragin, an antifungal compound which was first isolated from *Pseudomonas fragi* in 1967 [218]. The proposed structure of fragin was confirmed with a single crystal X-ray analysis of the isolated natural product. The obtained crystal structure of fragin was confirmed with chemically synthesized fragin. In addition, an enantioselective total synthesis was developed and single crystal X-ray analysis showed that the naturally produced fragin from *B. cenocepacia* H111 is in the D-configuration.

To confirm the antifungal activity of fragin, disc diffusion assays of chemically synthesized L- and D-fragin against the fungus *F. solani* and several Gram-positive and Gram-negative bacteria were performed. Both enantiomers showed antifungal activity against *F. solani*, but the activity of the naturally occurring D-fragin was higher than that of L-fragin (Figure 10B). Furthermore, both fragin enantiomers showed growth inhibition of Gram-positive bacteria, while none of the tested Gram-negative bacteria were inhibited (Figure 10C and 10D).

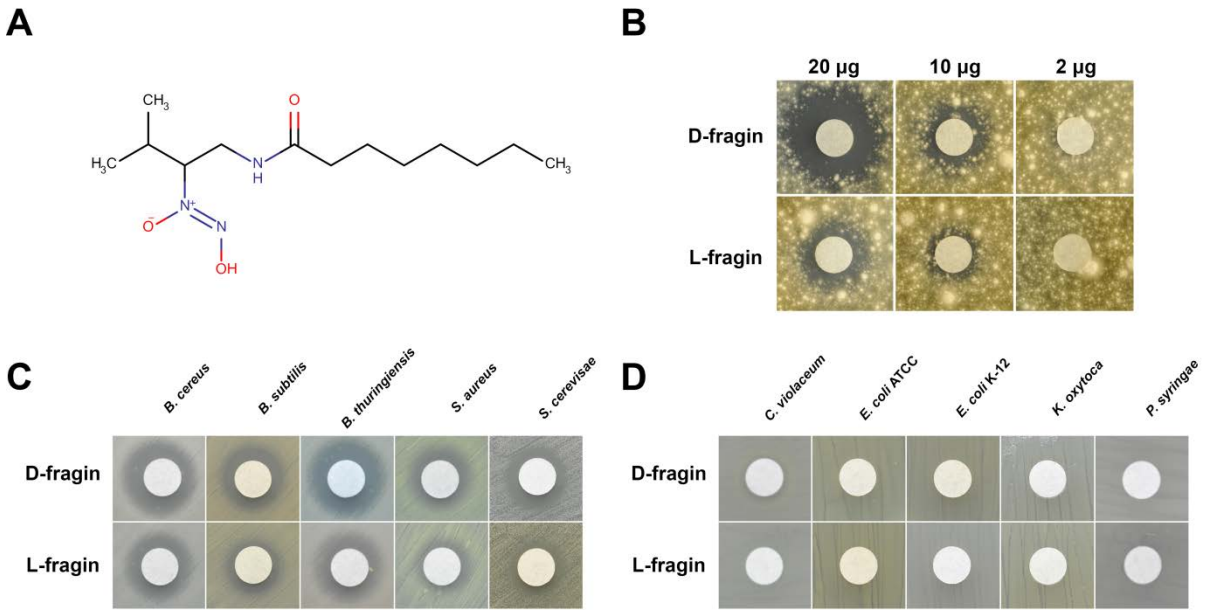

Figure 10 : Structure and bioactivity of the secondary metabolite synthesized by the *ham* cluster. A) Structure of fragin, the antifungal metabolite produced by the *ham* cluster. The molecule structure was drawn with the Marvin Sketch software from ChemAxon. B) Disc diffusion assays of synthetic D- and L-fragin to determine the antifungal activity. Representative pictures of an antifungal spray assay against the fungus *F. solani* are shown. C) Disc diffusion assay of 20 µg synthetic D- and L-fragin to determine activity against the Gram-positive bacteria *Bacillus cereus*, *Bacillus subtilis*, *Bacillus thuringiensis*, *Staphylococcus aureus* and the yeast *Saccharomyces cerevisiae*. D) Disc diffusion assay of 20 µg synthetic D- and L-fragin to determine activity against the Gram-negative bacteria *Chromobacterium violaceum*, *Eschericia coli ATCC*, *E. coli K-12*, *Klebsiella oxytoca* and *Pseudomonas syringae*. Representative pictures are shown for all disc diffusion assays

Several bioinformatic tools had predicted that the A domain of HamD was most likely to incorporate phenylalanine or leucine into the antifungal compound. Based on the structure of fragin, phenylalanine is a very unlikely substrate. To clarify whether leucine or possibly valine is the precursor of fragin, feeding studies with C^{13}- and N^{15}-labeled L-valine and L-leucine were carried out. Labeled L-valine or L-leucine was fed to H111 wild-type cultures over a period of 72 hours and fragin was subsequently extracted from the cultures and analysed by ESI-MS. This analysis revealed that approximately 4 % of the C^{13}- and N^{15}-labeled L-leucine, 5.5 % of the N^{15}-labeled L-valine, and nearly 10 % of the C^{13}-labeled L-valine were incorporated into fragin (Table 4). Feeding with N^{15} labeled L-leucine and L-valine also showed incorporation into the siderophore pyochelin, suggesting that the N^{15} enters the nitrogen cycle of the cell.

Table 4: Incorporation rate of isotopically labeled amino acids into fragin.

	mass	relative intensity	% labeled fragin
L-valine ^{15}N			
recorded value			
$C_{13}.H_{27}.O_3.N_3.Na$	296.19405	100	
$C_{13}.H_{27}.O_3.N_2.^{15}N.Na$	297.19114	7.02	
calculated value			
$C_{13}.H_{27}.O_3.N_3.Na$	296.19446	100	
$C_{13}.H_{27}.O_3.N_2.^{15}N.Na$	297.1915	1.11	
			5.58
L-leucine ^{15}N			
recorded value			
$C_{13}.H_{27}.O_3.N_3.Na$	296.19398	100	
$C_{13}.H_{27}.O_3.N_2.^{15}N.Na$	297.1911	5.55	
calculated value			
$C_{13}.H_{27}.O_3.N_3.Na$	296.19446	100	
$C_{13}.H_{27}.O_3.N_2.^{15}N.Na$	297.1915	1.11	
			4.25
L-valine $^{13}C5$			
recorded value			
$C_{13}.H_{27}.O_3.N_3.Na$	296.19408	100	
$C_8.^{13}C_5.H_{27}.O_3.N_3.Na$	301.21081	10.77	
calculated value			
$C_{13}.H_{27}.O_3.N_3.Na$	296.19446	100	
$C_8.^{13}C_5.H_{27}.O_3.N_3.Na$	301.21081	0	
			9.72
L-leucine ^{13}C			
recorded value			
$C_{13}.H_{27}.O_3.N_3.Na$	296.19411	100	
$C_{12}.^{13}C.H_{27}.O_3.N_3.Na$	297.1974	19.07	
calculated value			
$C_{13}.H_{27}.O_3.N_3.Na$	296.19411	100	
$C_{12}.^{13}C.H_{27}.O_3.N_3.Na$	297.1974	14.49	
			4.38

The experiments in this section were performed in collaboration with the Group of Prof. Karl Gademann, University of Zurich and University of Basel. HPLC-MS and ^{1}H-NMR spectroscopy were performed by Simon Sieber. Chemical synthesis of fragin was developed and performed by Christophe Daeppen. Incorporation of isotopically labeled amino acids was determined by the mass spectrometry service at the University of Zurich.

2.7 The *ham* cluster is essential for yellow colony phenotype under high iron concentrations

While trying to optimize the growth conditions for antifungal activity and production of the antifungal compound, we noticed that addition of excess iron to the medium resulted in the formation of yellow colonies on agar plates. *B. cenocepacia* is known to produce two different siderophores, pyochelin and ornibactin. To see if the yellow colony phenotype was dependent on the presence of either of the two siderophores, a pyochelin mutant (H111 Δ*pchAB*), an ornibactin mutant (H111 Δ*orbJ*) and a double mutant (H111 Δ*pchAB* Δ*orbJ*) were screened for the appearance of the yellow colony phenotype in the presence of different amounts of iron. While no change in colony color was observed in the H111 wild-type strain or the siderophore mutants in the presence of 10 µM iron, all four strains exhibited the yellow colony phenotype when incubated on MEA plates supplemented with 100 µM iron (Figure 11A). To see if the yellow colony phenotype was under the control of a regulatory system known to influence the expression of the *ham* cluster, strains H111 ΔpC3, H111 Δ*cepIR* and H111 Δ*cepR2* were tested for the yellow colony phenotype in presence of iron. As shown in Figure 11B, all three mutants lost their ability to form yellow colonies in the presence of 100 µM iron. As all three mutants are either defective in the expression of the *ham* cluster (H111 ΔpC3, H111 Δ*cepIR*) or have lowered antifungal activity (H111ΔpC3, H111 Δ*cepIR* and H111 Δ*cepR2*), the *ham* cluster probably plays an important role in the development of the yellow colony phenotype. Therefore a *hamD* mutant (H111 Δ*hamD*) along with a genetically complemented derivative (H111 Δ*hamD*/pBBRhamD) and the respective empty vector control (H111 Δ*hamD*/pBBR) were also tested for their ability to form yellow colonies in the presence of high amounts of iron. Indeed, mutation of *hamD* led to the loss of the yellow colony phenotype in the presence of 100 µM iron and was restored when *hamD* was

expressed *in trans* from a plasmid (Figure 11C). As expected, the yellow colony phenotype was not restored in the empty vector control strain (Figure 11C). These experiments established a clear connection between the iron-dependent yellow colony phenotype and the *ham* cluster.

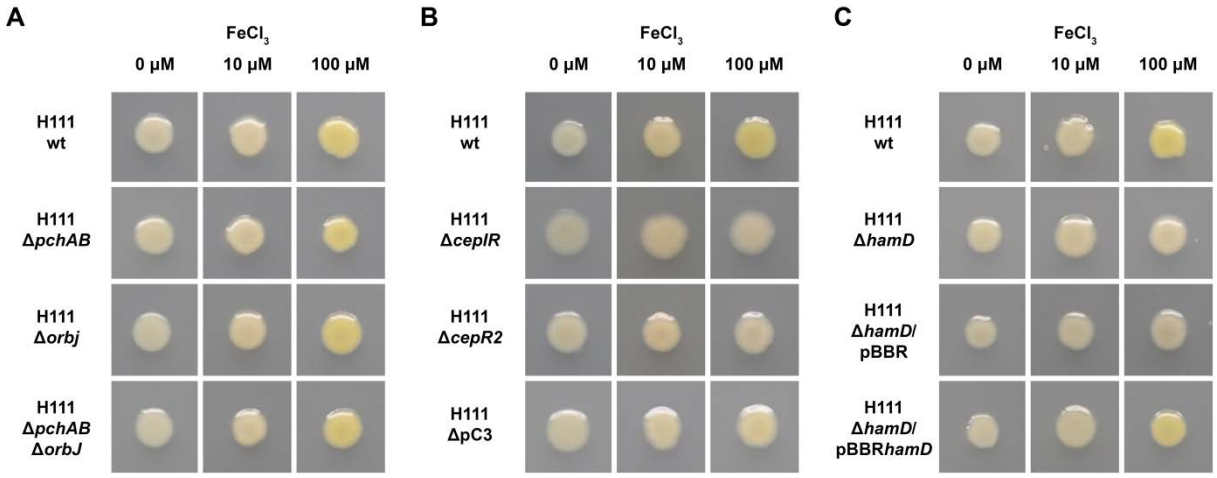

Figure 11 : Development of the yellow colony phenotype of *B. cenocepacia* H111 on agar plates supplemented with excess iron. A) The pyochelin (H111 Δ*pchAB*), ornibactin (H111 Δ*orbJ*) and double (H111 Δ*pchAB* Δ*orbJ*) mutants develop a yellow colony phenotype in the presence of 100 µM $FeCl_3$ on malt extract agar (MEA) plates. B) Mutation of *cepIR* (H111 Δ*cepIR*) and the solo LuxR regulator gene *cepR2* (H111 Δ*cepR2*), prevent the development of the yellow colony phenotype. Loss of megaplasmid pC3 (H111 ΔpC3) leads to a less pronounced yellow color formation. C) Mutation of *hamD* (H111 Δ*hamD*) results in the loss of yellow colony formation, which is restored by expression of *hamD* from a plasmid (H111 Δ*hamD* pBBR*hamD*). No restoration of yellow colony formation was observed in the empty vector control (H111 Δ*hamD* pBBR). Representative pictures are shown for all bacteria grown on MEA plates with and without $FeCl_3$.

2.8 High iron concentrations diminish antifungal activity *of B. cenocepacia*

As antifungal activity as well as the development of the iron-dependent yellow colony phenotype, were both dependent on the *ham* cluster, it was of interest to know if iron influences the antifungal activity of *B. cenocepacia* H111. The H111 wild type strain along with several mutants impaired in antifungal activity and yellow colony formation (H111 Δ*cepIR*, H111 Δ*cepR2*, H111 ΔpC3 and H111 Δ*hamD*) were tested for their antifungal activity under different iron concentrations. As controls, the *in trans*

complemented *hamD* mutant (H111 Δ*hamD*/pBBR*hamD*) and the empty vector strain (H111 Δ*hamD*/pBBR) were also tested for their antifungal activities under the same condition. The antifungal spray assay confirmed the yellow colony phenotype described above. Antifungal activity of the H111 wild type, H111 Δ*cepIR*, H111 ΔpC3 and H111 Δ*hamD*/pBBR*hamD* was lowered in the presence of 1 µM additional iron and was completely lost when the bacteria where grown in with 10 µM iron (Figure 12A). H111Δ*cepR*, H111Δ*hamD* and H111Δ*hamD*/pBBR did not exhibit antifungal activity, irrespective of the iron concentration in the agar plate (Figure 12A).

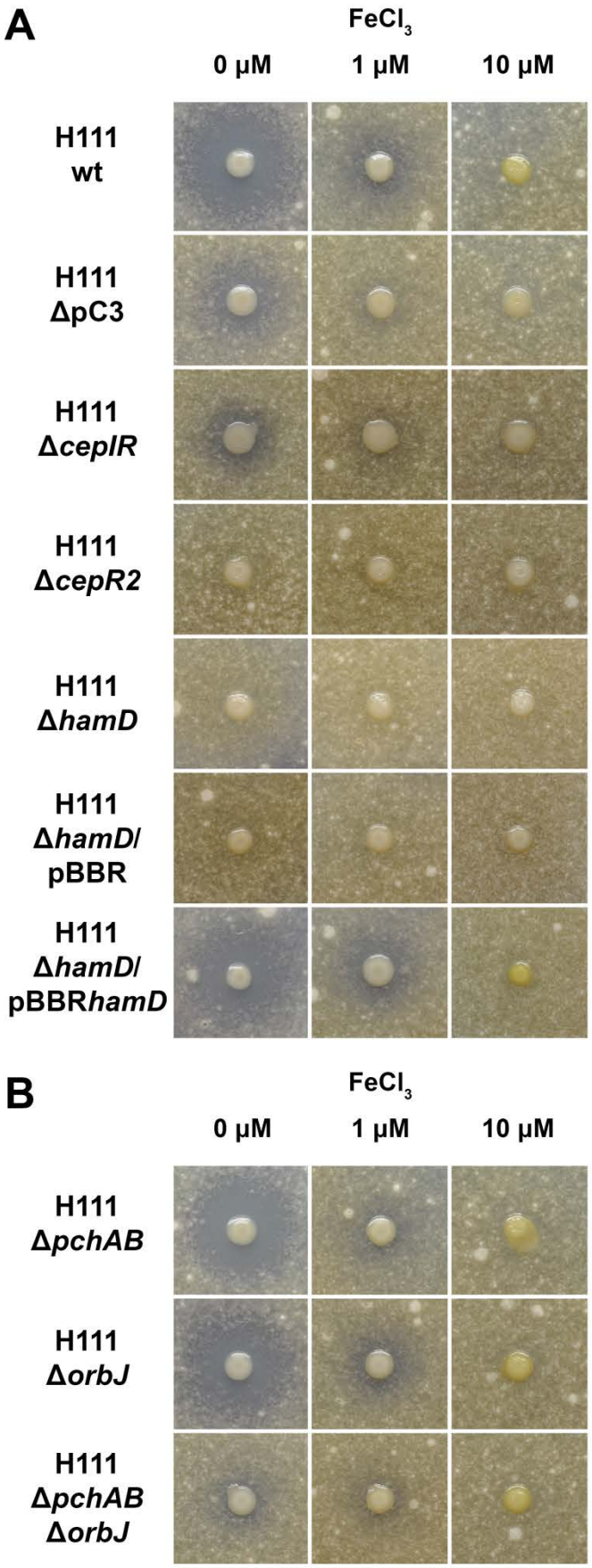

Figure 12: Antifungal activity is lost in the presence of excess amounts of iron. A) Addition of 1 µM $FeCl_3$ diminishes antifungal activity while addition of 10 µM $FeCl_3$ completely abrogates antifungal activity in the wild type strain (H111 wt), the pC3 negative derivative (H111 ΔpC3), the CepIR quorum sensing mutant (H111 Δ*cepIR*) and the complemented *hamD* mutant (H111 Δ*hamD* pBBR*hamD*). B) Mutation of genes involved in pyochelin (H111 Δ*pchAB*) and ornibactin (H111 Δ*orbJ*) biosynthesis resulted in a slight reduction in antifungal activity, while mutation of both siderophores (H111 Δ*pchAB* Δ*orbJ*) resulted in highly reduced antifungal activity. Addition of excess iron led to a reduction of antifungal activity at 1 µM $FeCl_3$, and its complete loss at 10 µM $FeCl_3$ in all three mutant strains. Representative pictures of antifungal spray assays against the fungus *F. solani* are shown.

2.9 Antifungal activity is influenced by the presence of siderophores

Although high iron concentrations lowered antifungal activity (Figure 12A), the iron-induced yellow colony phenotype was not influenced in H111 derivatives deficient for pyochelin and ornibactin production (Figure 11A). Therefore a connection between antifungal activity and siderophore production was not apparent. Nevertheless, siderophores restrict iron availability for competing microbes and the pyochelin precursor dihydro aeruginoic acid (Dha) is a known antifungal compound [219]. Therefore it was of interest to see if pyochelin and ornibactin have an influence on antifungal activity of H111 under the conditions of the antifungal spray assay. While mutation of the pyochelin biosynthesis genes *pchAB* did not influence antifungal activity, mutation of *orbJ*, which is required for ornibactin biosynthesis, clearly reduced antifungal activity (Figure 12B). An H111 mutant strain deficient in the biosynthesis of both siderophores (H111 Δ*pchAB*Δ*orbJ*) was nearly devoid of antifungal activity (Figure 12B). Importantly, supplementation with 1 µM and 10 µM iron diminished antifungal activity even further (Figure 12B), which is in agreement with the observed reduction of antifungal activity in the wild-type strain in the presence of high iron concentrations (Figure 12A). Taken together, the presence of the two siderophores pyochelin and ornibactin is necessary for full antifungal activity of H111. High concentrations of iron have a negative effect on antifungal activity of *B. cenocepacia* H111, probably by downregulating siderophore production.

2.10 Antifungal activity and yellow colony formation are linked in strain K56-2

As previously established, CepR2 is a negative regulator of antifungal activity in *B. cenocepacia* K56-2 and a positive regulator of antifungal activity in *B. cenocepacia* H111. To test whether the yellow colony phenotype was similarly inversely regulated by CepR2, the K56-2 wt and *cepR2* mutant strains thereof were tested for antifungal activity and yellow colony phenotype on standard MEA plates and MEA plates supplemented with 100 µM $FeCl_3$. Antifungal activity was lowered by addition of iron in K56-2 wt and K56-2 Δ*cepR2*. In contrast to H111, the K56-2 wild-type strain

remained white in the presence of 100 µM iron, while the *cepR2* mutant showed the yellow colony phenotype (Figure 13). This supports our finding that the K56-2 *cepR2* mutant exhibits increased antifungal activity (Figure 7) and is in agreement with previously published data showing that CepR2 is a positive regulator of the *ham* cluster in strain H111 [55]. Accordingly, higher amounts of fragin are expected to be produced by H111 wild-type and K56-2 Δ*cepR2* compared to H111 Δ*cepR2* and K56-2 wild-type.

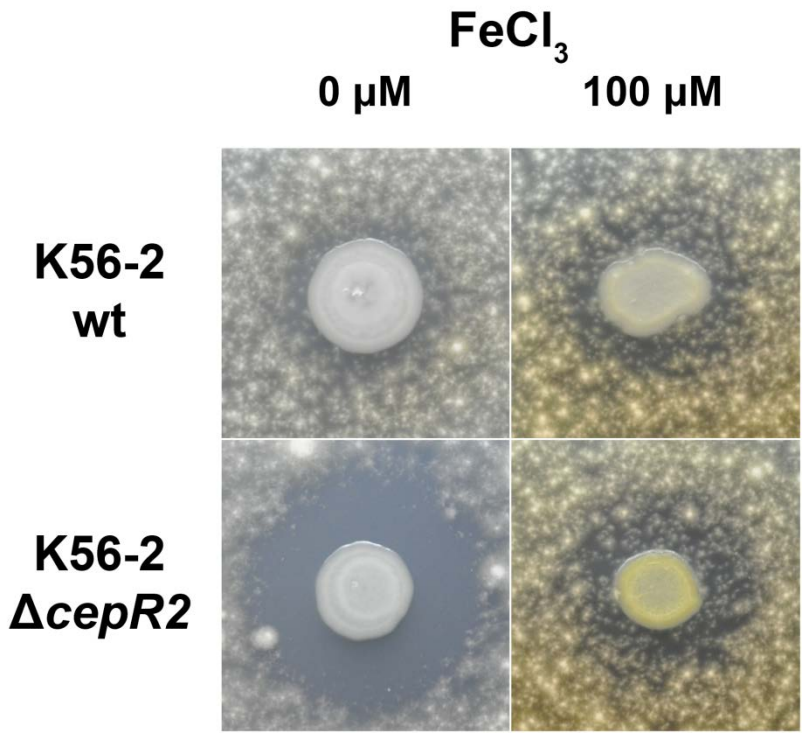

Figure 13: Antifungal activity of strain K56-2 is reduced under high iron concentrations. Addition of 100 µM $FeCl_3$ to agar plates led to the formation of yellow colony phenotype along with a reduction in antifungal activity in the *cepR2* mutant derivative of strain K56-2 (K56-2 Δ*cepR2*). Only a very slightly yellow colony phenotype was observed for the K56-2 wild type (K56-2 wt). Representative pictures of antifungal spray assays against the fungus *F. solani* are shown.

2.11 The antifungal activity of fragin is inhibited by iron *in vitro*

N-nitrosohydroxylamines were shown to chelate metals and inhibit enzymes which have metals in their active center [220, 221]. It is plausible that the antifungal and antibacterial activities of fragin are at least partially due to its metal chelating properties. In this context, reduction of antifungal activity by excess iron might be due

to saturation of fragin with free iron, rendering fragin inactive. To test this possibility, chloroform extracts of H111 wild-type and H111 Δ*hamD* cultures grown under fragin producing conditions, were extracted with chloroform and concentrated 100-fold. The concentrated extracts were either spotted on agar plates containing 100 µM iron or were incubated overnight with different amounts of iron and then spotted on standard MEA plates and tested for antifungal activity. Bacterial extracts spotted on agar plates containing 100 µM additional iron showed lowered antifungal activity compared to extracts spotted on standard agar plates (Figure 14A). Furthermore, overnight incubation of bacterial extracts with high amounts of iron resulted in clearly lowered antifungal activity (Figure 14B). These experiments indicate that iron directly interferes with fragin activity.

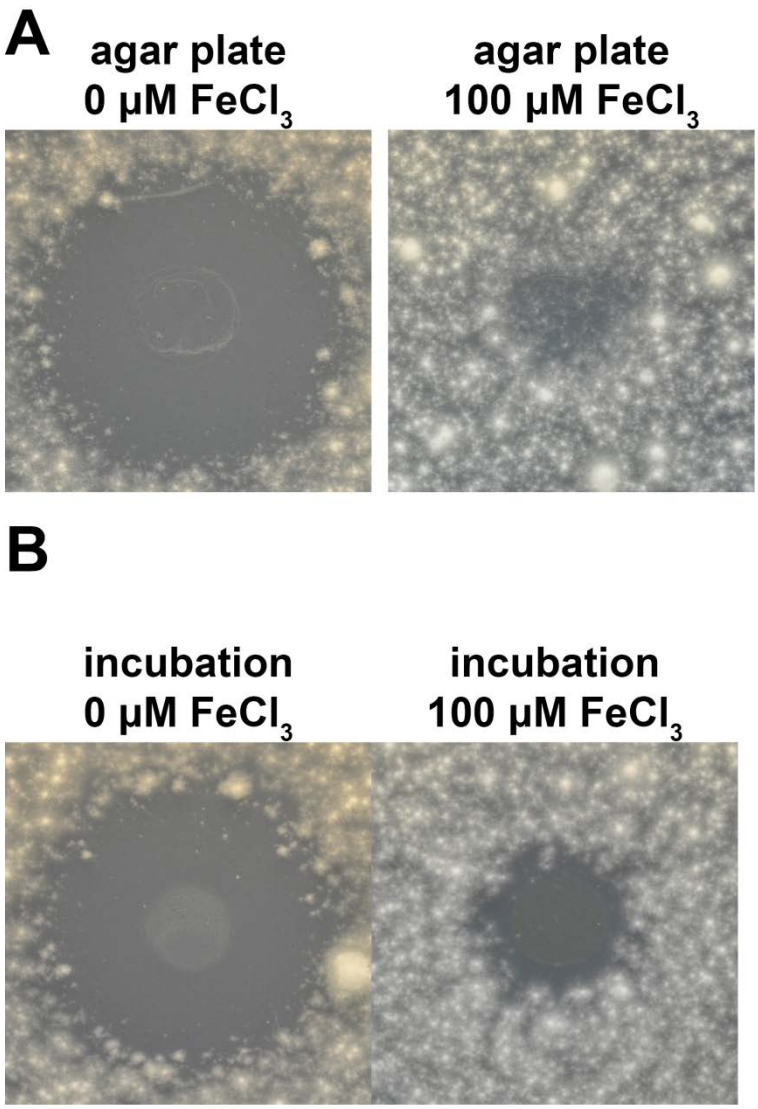

Figure 14: Iron reduces the antifungal activity of fragin *in vitro*. A) Chloroform extracts derived from H111 wild type cultures showed highly reduced antifungal activity when spotted on agar plates containing high amounts of iron (agar plate 100 µM $FeCl_3$) compared to standard agar plates (agar plate 0µM $FeCl_3$). B) Chloroform extracts derived from H111 wild type cultures showed reduced antifungal activity when pre-incubated with iron overnight (supplementation with 100 µM $FeCl_3$) compared to untreated extracts (no $FeCl_3$ supplementation). Representative pictures of antifungal spray assays against the fungus *F. solani* are shown.

2.12 Identification of regulators affecting *ham* gene expression by transposon mutagenesis

All mutants that did not show the yellow colony phenotype in the presence of excess amounts of iron were also reduced in, or completely devoid of, antifungal activity. Therefore the yellow colony phenotype was used as the readout for a transposon mutant library screen. In brief, the transposon mutant library was plated on MEA plates supplemented with 100 µM $FeCl_3$ and screened for white colonies (i.e. putatively fragin negative) and bright yellow colonies (i.e. putatively fragin overproducing). Positive mutants where tested for antifungal activity and their transposon insertion siteswere mapped by arbitrary PCR and sequencing. The transposon insertion sites of the clones derived from white colonies were mapped to *cepS*, *hamF* and I35_0679, a LysR-type regulator encoded on chromosome 1. Three clones showed a bright yellow colony phenotype and the transposon insertion sites for all three mutants were mapped to the gene I35_4197, which encodes an AraC regulator and is located next to the *ham* gene cluster. As expected, the three transposon mutants with the white colony phenotype showed highly reduced antifungal activity while the transposon mutant with the bright yellow colony phenotype showed increased antifungal activity relative to the wild type strain (Figures 15A and 15B).

To further characterize these transposon mutants, they were tested on CAS plates (siderophore production), YEM plates (EPS production) and skim milk plates (protease production). The *hamF* transposon mutant showed clearly reduced siderophore production, slightly reduced protease activity and EPS production comparable to the wild-type strain. Both, the *cepS* and the *lysR* (*I35_0679*) mutants showed reduced siderophore production comparable with the *hamF* mutant, and EPS production similar to the wild-type strain. While the *cepS* transposon mutant showed similar protease activity to the wild-type, the *lysR* mutant had greatly reduced protease activity (Figure 15A).

The *araC* mutant (*I35_4197*) had similar protease activity and EPS production to the wild-type. Siderophore production, as assessed on CAS plates, was clearly increased in the *araC* mutant compared to the wild-type strain (Figure 15B).

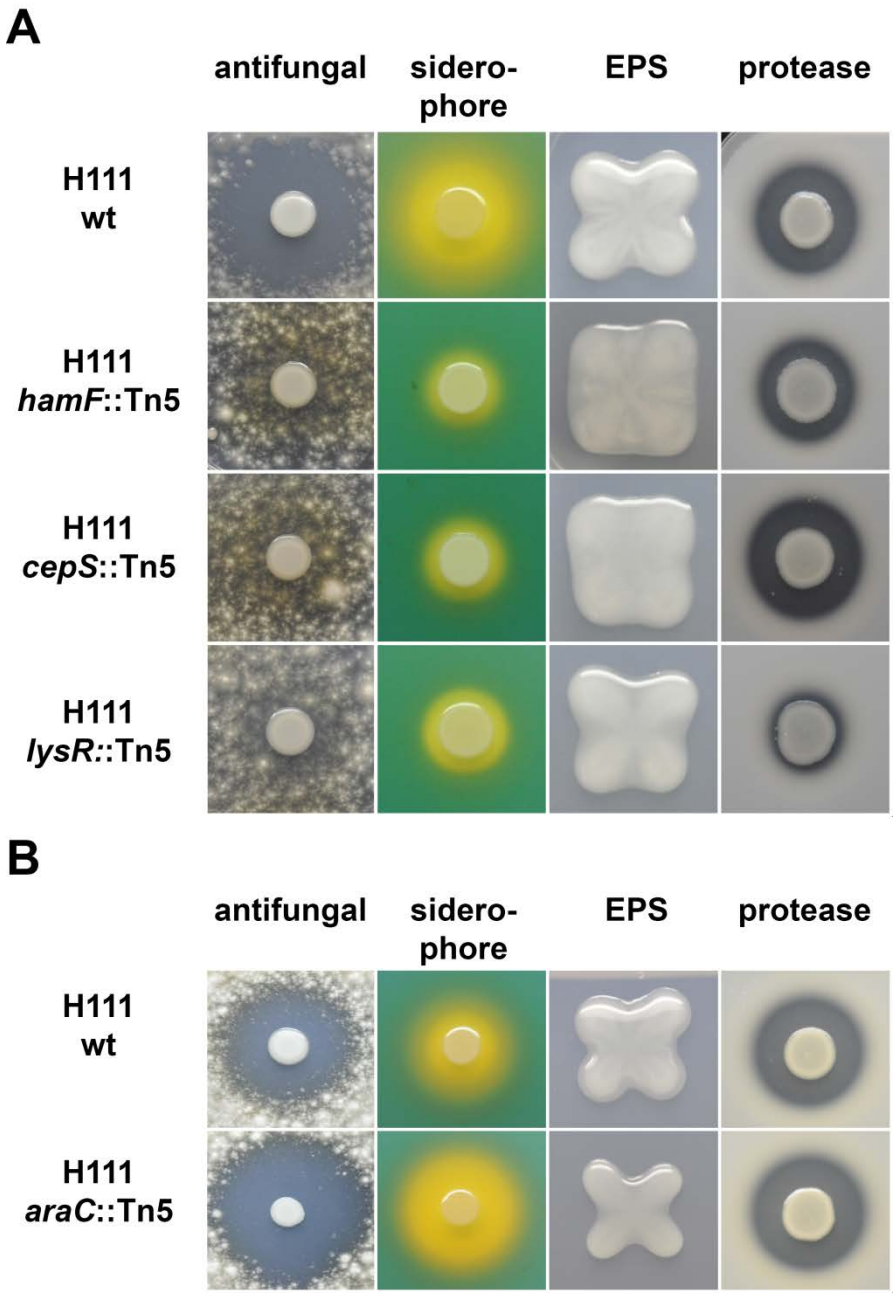

Figure 15 : Altered antifungal activity and additional phenotypic characterization of several transposon mutants. A) Antifungal activity is reduced in a *hamF* (H111 *hamF*::Tn5), a *cepS* (H111 *cepS*::Tn5) and a *lysR* (H111 *lysR*::Tn5) transposon mutant. Phenotypic changes in the transposon *hamF*, *cepS* and *lysR* mutants with regard to siderophore production (CAS plates), EPS production (YEM plates) and protease secretion (skim milk plates) compared to the H111 wild type strain. B) Transposon insertion into I35_4197 (H111 *araC*::Tn5) resulted in elevated antifungal activity. Phenotypic changes in the transposon *araC* mutant with regard to siderophore production (CAS plates), EPS production (YEM plates) and protease secretion (skim milk plates) compared to the H111 wild type strain. Representative pictures are shown.

3 Results II: Cell – Cell Communication

3.1 The *ham* genes are positively regulated by CepR2 and CepS

The solo LuxR-type regulator CepR2 negatively regulates the expression of the *ham* cluster in *B. cenocepacia* K56-2 [55]. In agreement with this, antifungal activity is negatively regulated by CepR2 in strain K56-2, while CepR2 is a positive regulator of antifungal activity in strain H111 (Figure 7A). In addition, CepS is a positive regulator of antifungal activity in strain H111 (Figure 15A). To ascertain the role of CepR2 and CepS in the regulation of the *ham* genes, a transcriptional fusion of the *hamA* promoter (P*hamA*) and the *hamF* promoter (P*hamF*) to *lacZ* were introduced into H111 wild-type (H111/P*hamA–lacZ* and H111/P*hamF–lacZ*), a *cepR2* mutant (H111 *cepR2*::pEX18/P*hamA–lacZ* and H111 *cepR2*::pEX18/P*hamF–lacZ*) and a *cepS* mutant (H111 *cepS*::Tn5Km/P*hamA–lacZ* and H111 *cepS*::Tn5Km/P*hamF–lacZ*) and β-galactosidase activities were determined. The activity of both the *hamA* and the *hamF* promoters was markedly reduced in the *cepR2* and the *cepS* mutants. As expected, the empty vector controls showed no β-galactosidase activity (Figure 16). These data show that both CepR2 and CepS are positive regulators of the *ham* genes in strain H111.

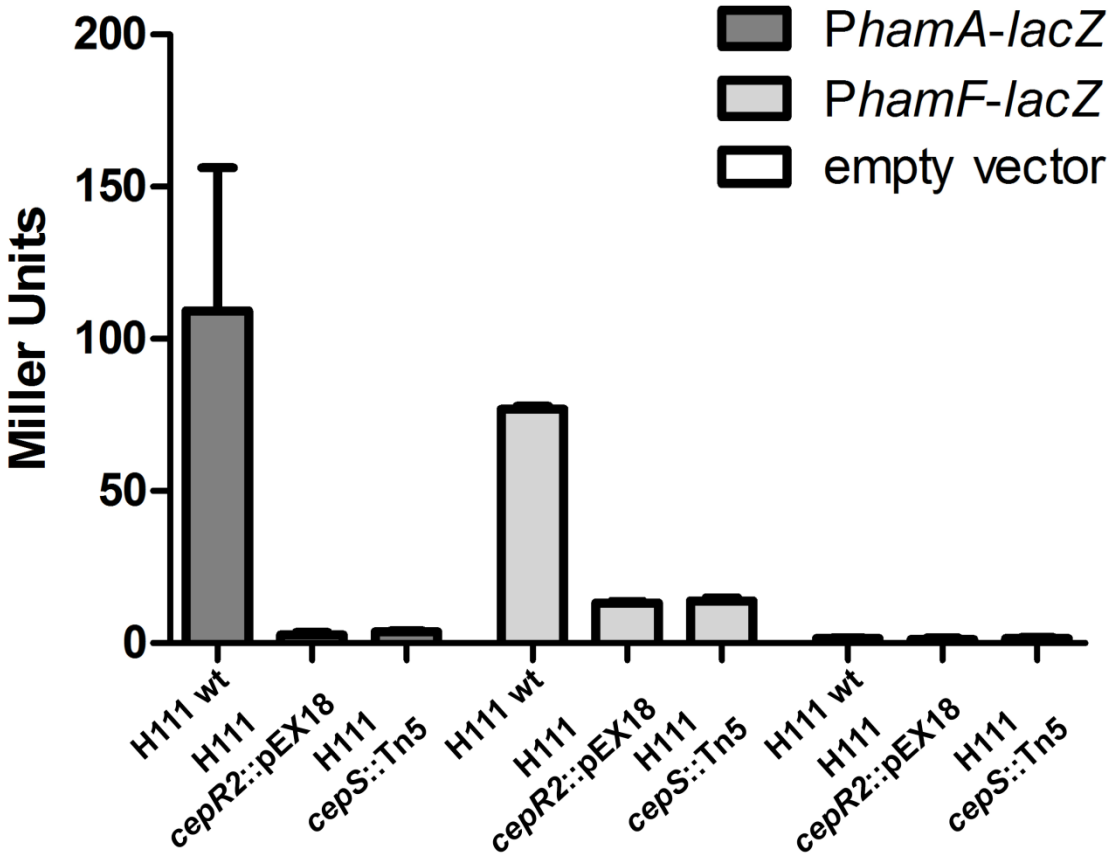

Figure 16 : Both *ham* operons are regulated by CepR2 and CepS. Beta-galactosidase assays of the promoters of the *hamACBDE* (P*hamA-lacZ*) and the *hamFG* (P*hamF-lacZ*) operon in the wild type strain (H111 wt), as well as in a *cepR2* (H111 *cepR2* ::pEX18) and a *cepS* (H111 *cepS* ::Tn5) mutant showed that CepR2 and CepS positively regulate both *ham* operons. Empty vector controls showed no background activity. Results are presented as means ± SD from at least 3 independent biological replicates measured in technical triplicates.

3.2 A subset of the *ham* genes synthesizes a novel autoinducer molecule

The *pvf* cluster of *P. entomophila,* and the *mgo* cluster of *P. syringae pv. syringae* UMAF0158, are homologues of the *ham* cluster, but lack *hamB* and the *hamFG* operon (Figure 4). These clusters were shown to produce an extracellular signaling molecule of unknown structure [216, 217]. This suggested that the expression of the *ham* cluster may be under the control of a self-generated signal which is synthesized by a subset of the *ham* genes. In analogy to the *pvf* and *mgo* clusters, this signaling molecule is predicted to be synthesized by mutants lacking *hamB*, *hamF* or *hamG*,

but not when other *ham* genes are mutated. To test this possibility a transcriptional fusion of the *hamA* promoter (P*hamA*) to *lacZ* was introduced into H111 wild-type and H111 Δ*hamD* and *hamA* promoter activity was estimated on agar plates. The promoter activity was markedly reduced in the *hamD* mutant relative to the wild type strain (Figure 17). Importantly, cross streak experiments showed that *hamA* promoter activity was restored when H111 wild-type was streaked next to H111 Δ*hamD*/P*hamA*–*lacZ*, suggesting that the *ham* cluster synthesizes an extracellular cell-cell signaling molecule (Figure 18A). To ascertain the genes required for synthesis of this extracellular cell-cell signaling molecule, all *ham* mutants were tested for their ability to induce the activity of the *hamA* promoter in cross-streak experiments. In full agreement with published work on the *mgo* and *pvf* clusters of *P. syringae pv syringe* UMAF0158 and *P. entomophila*, mutations in *hamB*, *hamF* and *hamG* did not affect the induction of the *hamA* promoter, while mutants deficient in *hamA*, *hamC, hamD* or *hamE* did not induce the *hamA* promoter (Figure 18A).

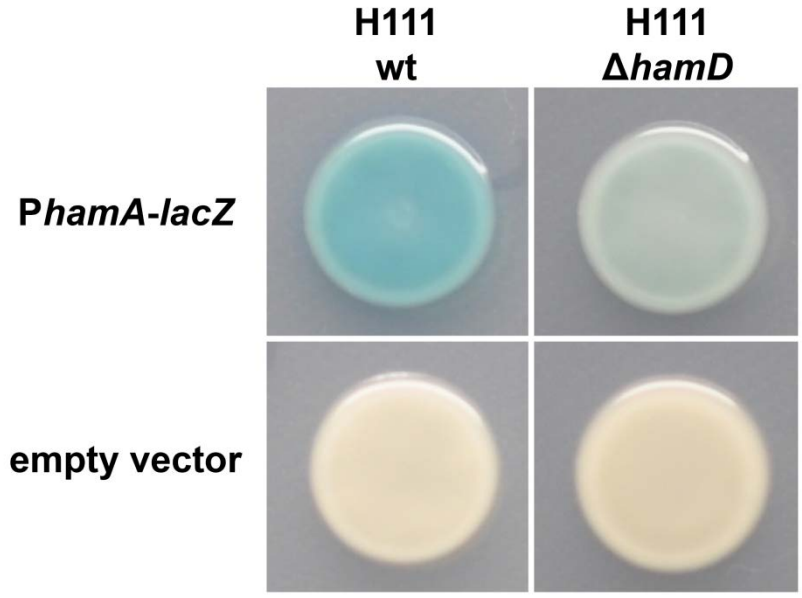

Figure 17: The *ham* genes are regulated by a positive feedback loop. Representative pictures of the promoter activity of the *hamABCDE* operon (P*hamA-lacZ*) in the wild type (H111 wt) and a *hamD* mutant (H111 Δ*hamD*) background observed on agar plates supplemented with 40 µg/ml X-gal as substrate. The promoter activity is clearly higher in the wild type background than in the *hamD* mutant background, as seen by the blue coloration of the wild type bacterial colony. Empty vector controls with pSU11 (empty vector) showed no background promoter activity in both strains.

To visualize the production of the extracellular signaling molecule, a TLC overlay assay was developed. Organic solvent extracts of H111 wild-type and the seven *ham* mutant derivatives were separated by TLC and then overlayed with agar containing the H111Δ*hamD*/P*hamA*–*lacZ* reporter strain. As shown in Figure 18B, extracts from strains H111 wild-type, H111 Δ*hamB*, H111 Δ*hamF* and H111Δ*hamG* showed a distinct spot in the TLC overlay assay, indicating activation of the *hamA* promoter by a diffusible signaling molecule. This confirms the results from the cross-streak experiments, showing that the *ham* gene homologues to the *mgo* and *pvf* genes are essential for the biosynthesis of the uncharacterized signaling molecule. The signaling molecule derived from the *hamF* mutant strain showed a different migration pattern on the TLC plate to those of the wildtype strain and the *hamB* and *hamG* mutants. The concentration of small molecules can influence their migration pattern. Therefore different amounts of H111 wild-type and H111 Δ*hamF* extracts were analyzed. As can be seen in Figure 18C, migration of the signaling molecule is indeed dependent on its concentration. Therefore the difference seen in Figure 18B can be attributed to a higher concentration of the signaling molecule in the *hamF* mutant.

Given that all *ham* genes are required for fragin biosynthesis (Figure 8C), fragin itself cannot be the molecule responsible for induction of the *hamA* promoter, suggesting that the *ham* cluster directs the synthesis of two discrete molecules.

Based on the predicted functions of the HamF and HamG encoded proteins, the putative signaling molecule was thought likely to be structurally similar to fragin, but would lack the acyl chain and the amino group introduced by HamG. We also speculated that fragin might mask the presence of the signaling molecule. H111 Δ*hamF* is fragin-negative (Figure 8), but still induced the *hamA* promoter (Figure 18A). Therefore the H111 Δ*hamF* strain was chosen for the identification of the putative signaling molecule.

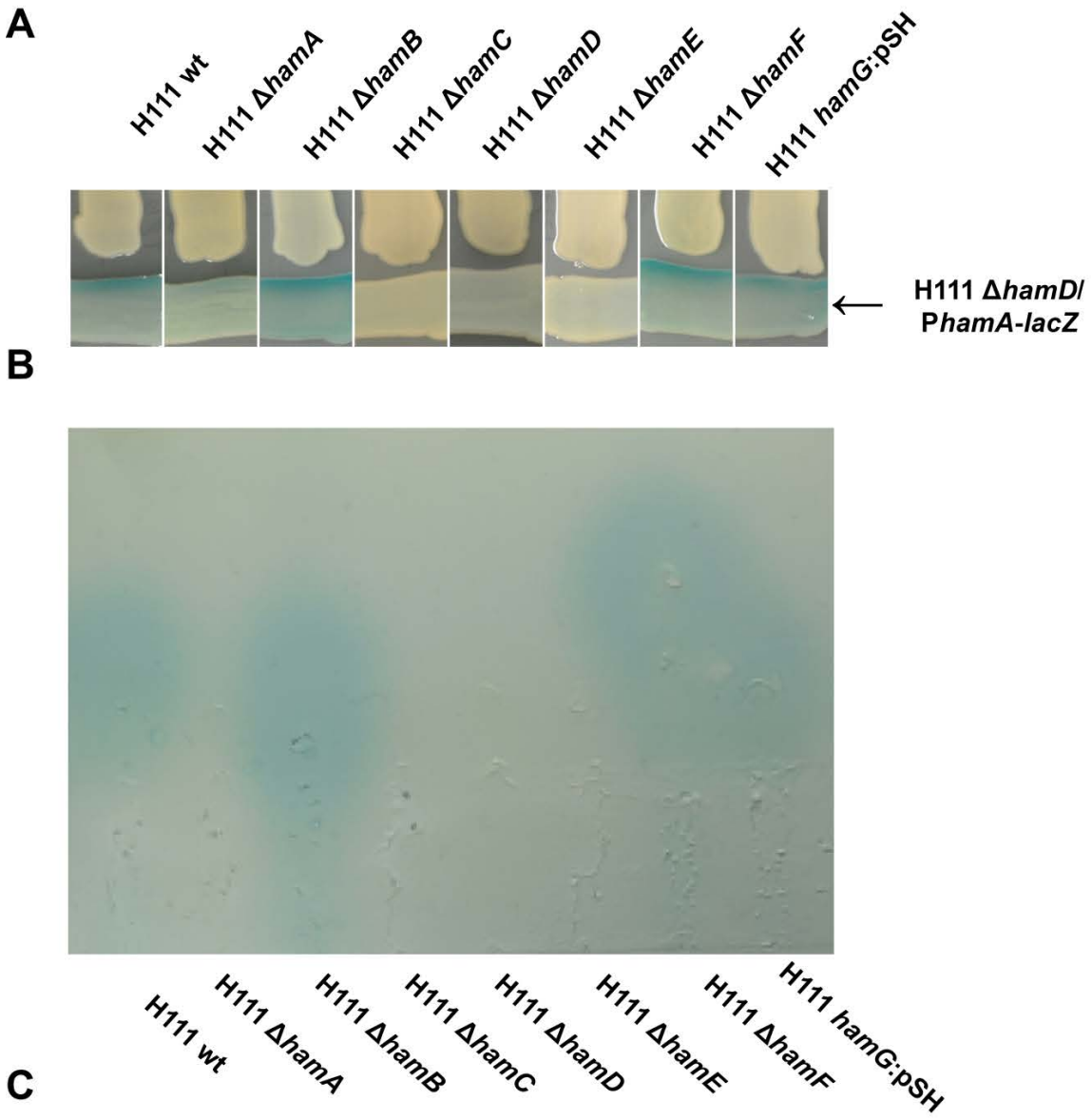
A
H111 wt
H111 ΔhamA
H111 ΔhamB
H111 ΔhamC
H111 ΔhamD
H111 ΔhamE
H111 ΔhamF
H111 hamG:pSH
H111 ΔhamD/
PhamA-lacZ
B
H111 wt
H111 ΔhamA
H111 ΔhamB
H111 ΔhamC
H111 ΔhamD
H111 ΔhamE
H111 ΔhamF
H111 hamG:pSH
C
H111 wt
concentration
H111 ΔhamF
concentration

Figure 18: The *ham* gene cluster synthesizes a signaling molecule which acts in a positive feedback loop. A) Cross-streaks of all seven *ham* gene mutants with the reporter strain (H111 Δ*hamD*/P*hamA-lacZ*) showed that *hamB*, *hamF* and *hamG* are dispensable for the production of the signal molecule. B) TLC overlay assay of dichloromethane extracts from culture supernatants of the wild type strain and all *ham* mutants. C) TLC overlay assay of dichloromethane extracts from the wild type strain (H111 wt) and the *hamF* mutant strain (H111 Δ*hamF*). Different volumes of extracts were spotted on the TLC plates (high to low volumes from left to right), resulting in a concentration gradient of the signaling molecule (indicated by an arrow on the bottom labeled with concentration). The migration pattern of the signaling molecule was dependent on the concentration of the signaling molecule. All TLC plates were overlayed with agar containing 40 µg/ml X-gal and the reporter strain H111 Δ*hamD*/P*hamA-lacZ*. Blue spots indicated the presence of the *ham*-derived signaling molecule.

3.3 Valazole is a novel signaling molecule synthesized by *B. cenocepacia* H111

Attempts to lower the complexity of the H111Δ*hamF* solvent extract by TLC separation and re-extraction of the signaling molecule with subsequent HPLC-MS analysis did not allow us to unequivocally assign a molecular mass to the unknown signaling molecule, due to very low yields after re-extraction from the TLC plate (Figure 19A). Therefore a simple basic-acid work up protocol was established with the help of Simon Sieber (Group Prof. Karl Gademann). Cell-free supernatants of H111 Δ*hamD* and H111 Δ*hamF* were first alkalized to pH 11, and extracted with $CHCl_2$. The aqueous phase was subsequently acidified to pH 5 and extracted again with $CHCl_2$. The organic phase was concentrated and tested for the presence of the *ham* derived signaling molecule with a TLC overlay assay. As shown in Figure 19B, the organic solvent extract derived from the pH 5 aqueous phase contained the signaling molecule as expected. The crude extract was subsequently purified by HPLC and a compound eluting with a retention time of 9.83 minutes was identified as the putative signaling molecule. The structure of the signaling compound was determined by ^{1}H- and ^{13}C-NMR spectroscopy and X-ray crystal structure analysis by Christophe Daeppen (Group Prof. Karl Gademann, University of Zurich). This novel signal molecule was named valazole (Figure 19D). The structure of valazole was confirmed by ^{1}H- and ^{13}C-NMR spectroscopy and X-ray crystal structure analysis of synthetic valazole (synthesis was carried out by Christophe Daeppen, Group Prof. Karl Gademann, University of Zurich).

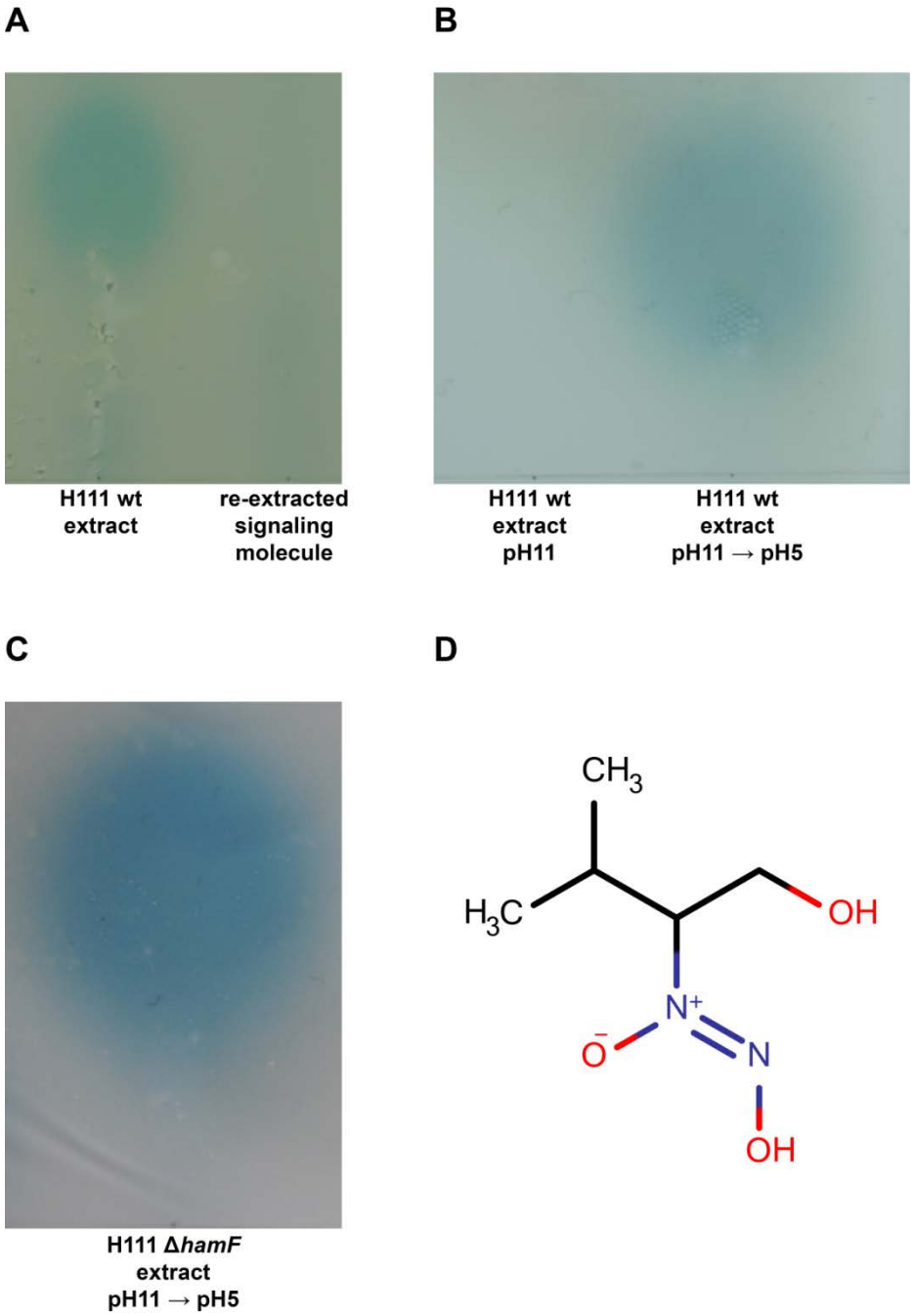

Figure 19 : Extraction and structure of the *ham*-derived signaling molecule valazole. A) Extracted *ham* derived signaling molecule from the H111 wild type strain (H111 wt extract) and the re-extracted signaling molecule from a previously performed TLC separation. B) Chloroform extracts derived from culture supernatants of the H111 wildtype strain alkalized to pH11 (H111 wt extract pH11) and subsequently acidified to pH5 (H111 wt extract pH11 -> pH5). C) Chloroform extract of a *hamF* mutant culture supernatant after acid-base workup shows the presence of the *ham*-derived signaling molecule. All TLC plates were overlayed with agar containing 40 µg/ml X-gal and the reporter strain H111 Δ*hamD*/P*hamA-lacZ*. Blue spots indicated the presence of the *ham*-derived signaling molecule. Representative pictures are shown. D) Structure of valazol, the *ham*-derived signaling molecule, which was determined by ^{1}H-NMR and X-ray crystal structure analysis.

3.4 Valazole regulates the expression of the *ham* cluster and neighboring genes

To confirm that valazole stimulates the activity of the *hamA* promoter and to test whether the *hamFG* operon is also regulated by valazole we measured β-galactosidase activities of respective transcriptional *lacZ* promoter fusions in the wild-type as well as in a *hamD* (fragin and valazole negative) and a *hamF* (fragin negative) mutant background. While the activities of the two promoters were virtually indistinguishable between the wild type and the *hamF* mutant strain, they were greatly reduced in the *hamD* mutant. Addition of D-valazole to the growth medium restored β-galactosidase activities in the *hamD* mutant background in a dose-dependent manner, reaching the level of the wild-type at a concentration of 50 µM (Figure 20). These results demonstrate that valazole is a novel signal molecule that positively regulates its own production.

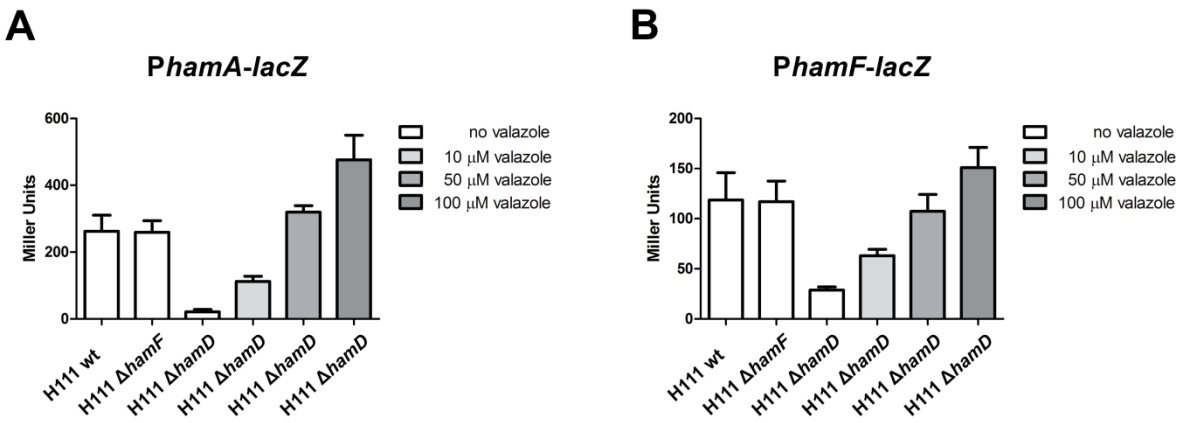

Figure 20 : The *ham* genes are regulated by valazole in a concentration-dependent manner. A) The promoter activity of the *hamABCDE* operon (P*hamA-lacZ*) was comparable in the wild type strain (H111 wt) and the *hamF* mutant strain (H111 Δ*hamF*). The *hamD* mutant strain (H111 Δ*hamD*) showed only very low promoter activity, which could be activitated by the addition of synthetic valazole. B)The promoter activity of the *hamFG* operon (P*hamF-lacZ*) was comparable in the wild type strain (H111 wt) and the *hamF* mutant strain (H111 Δ*hamF*). The *hamD* mutant strain (H111 Δ*hamD*) showed only very low promoter activity which could be activitated by the addtion of synthetic valazole. Results are presented as means ±SD from three independent biological replicates carried out in technical triplactes.

To identify the valazole regulon in *B. cenocepacia* H111 we performed RNA-Seq analyses of the wild-type strain, the *hamD* mutant in the presence and absence of 100 µM D-valazole, and the genetically complemented *hamD* mutant. Expression of 112 genes was found to be > 3-fold lower in the H111 Δ*hamD* mutant relative to the wild-type (Table 5). Most remarkable among these differentially regulated genes was a cluster of sixteen genes consisting of the two *ham* operons plus genes in their vicinity. These valazole-regulated genes code for CepR2 (I35_4186), CepS (I35_4187),a LysR-type regulator (I35_4196), a LeuA homolog (I35_4185), a tripartite multidrug resistance system (I35_4198 – I35_4200), a hypothetical protein (I35_4201) and a TRP repeat protein (I35_4202). CepR2 and CepS are positive regulators of the *ham* cluster and are required for expression of antifungal activity (see above and in [55]). LeuA is a 2-isopropylmalate synthase and catalyzes the first step in leucine biosynthesis at the branching point from valine biosynthesis by converting 3-methyl-2-oxobutanoate to (2*S*)-2-isopropylmalate. The tripartite efflux system might be involved in fragin or valazole secretion, which remains to be investigated in the future.

Moreover, valazole also positively affected the expression of genes that are not physically connected to the *ham* cluster. Several of these genes are either involved in metal transport or homeostasis or rely on metals for their enzymatic activity. The proteins involved in metal transport and homeostasis are the nickel chaperon UreG (I35_0764), a cobalt-zinc-cadmium resistance protein (I35_4611) and a multicopper oxidase (I35_4350). In addition, several proteins that use metals for their enzyme activity are also regulated, among them two putative IlvD homologs (I35_2532 and I35_7391), an L-arabonate dehydratase (I35_6680), a cysteine desulfurase (I35_4435) and the nitrate reductase NirB (I35_5547), all of which have Fe-S clusters in their active center.

Besides the aforementioned LeuA homolog I35_4185, another five valazole-regulated gene products are predicted to be involved in the metabolism of 3-methyl-2-oxobutanoate. Two are putative LeuA homologs (I35_4642 and I35_2881), two are putative IlvD homologs (I35_2532 and I35_7391) and the last one is predicted to be a PanB (I35_4373) homolog. In addition to its role in isoleucine biosynthesis, IlvD also catalyzes the reaction of (2*R*)-2,3-dihydroxy-3-methylbutanoate to 3-methyl-2-oxobutanoate, which is a substrate for LeuA and also for PanB, which converts it to

2-dehydropropantoate.

Table 5: Genes with statistically significant decreased expression (pval<0.1) above the threshold (>3-fold change) in H111 Δ*hamD* (hamD) compared to H111 wildtype (wt). ND: not applicable because read number for hamD was 0.

Name	locus_tag	fold change hamD vs wt
hppD	I35_0198	0.219
paaG	I35_0207	0.246
yrbE	I35_0293	0.298
pilB	I35_0430	0.004
pntAB	I35_0549	0.119
hmpA	I35_0589	0.128
ureG	I35_0764	0.113
ureC	I35_0767	0.104
ureB	I35_0768	0.059
I35_0773	I35_0773	0.104
I35_0775	I35_0775	0.243
I35_0802	I35_0802	ND
I35_0923	I35_0923	0.154
mdtB	I35_1072	0.253
I35_1077	I35_1077	0.111
I35_1214	I35_1214	0.125
I35_1298	I35_1298	0.020
fsr	I35_1349	0.314
truB	I35_1407	0.105
I35_1420	I35_1420	0.131
I35_1421	I35_1421	0.091
I35_1680	I35_1680	0.238
I35_1972	I35_1972	0.090
I35_2020	I35_2020	0.138
aceA	I35_2045	0.169
I35_2050	I35_2050	ND
hutU	I35_2172	0.296
cysNC	I35_2189	0.212
kdpB	I35_2306	0.068
kdpA	I35_2307	0.080
ilvD	I35_2532	0.177
I35_2661	I35_2661	0.302
leuA	I35_2881	0.146
I35_3015	I35_3015	0.235

I35_3278	I35_3278	ND
I35_4013	I35_4013	ND
I35_4014	I35_4014	ND
I35_4113	I35_4113	ND
leuA	I35_4185	0.080
cepR2	I35_4186	0.102
cepS	I35_4187	0.179
I35_4188	I35_4188	0.143
I35_4189	I35_4189	0.146
I35_4191	I35_4191	0.032
I35_4192	I35_4192	0.023
I35_4193	I35_4193	0.026
I35_4194	I35_4194	0.001
I35_4195	I35_4195	0.083
I35_4196	I35_4196	0.038
I35_4198	I35_4198	0.031
emrA	I35_4199	ND
I35_4200	I35_4200	0.028
I35_4201	I35_4201	0.040
I35_4202	I35_4202	0.094
I35_4287	I35_4287	ND
I35_4289	I35_4289	ND
I35_4350	I35_4350	0.079
panB	I35_4373	0.124
I35_4388	I35_4388	ND
I35_4434	I35_4434	0.131
I35_4435	I35_4435	0.216
I35_4500	I35_4500	0.308
I35_4557	I35_4557	ND
I35_4593	I35_4593	0.173
I35_4611	I35_4611	0.316
I35_4625	I35_4625	0.243
I35_4639	I35_4639	0.262
lysR	I35_4640	0.079
lysR	I35_4641	0.201
leuA	I35_4642	0.079
bceC	I35_4769	0.148
I35_5255	I35_5255	0.217
I35_5295	I35_5295	0.319
I35_5296	I35_5296	0.314
I35_5517	I35_5517	ND

I35_5529	I35_5529	0.031
I35_5530	I35_5530	0.149
nirB	I35_5547	0.070
I35_5720	I35_5720	ND
cmeB	I35_5771	0.245
I35_5857	I35_5857	0.316
I35_5869	I35_5869	ND
I35_5874	I35_5874	0.170
I35_5938	I35_5938	0.263
I35_5941	I35_5941	ND
I35_6021	I35_6021	0.252
I35_6175	I35_6175	0.192
I35_6268	I35_6268	0.008
I35_6332	I35_6332	0.161
I35_6416	I35_6416	ND
I35_6430	I35_6430	0.128
ceoB	I35_6448	0.311
I35_6539	I35_6539	0.026
I35_6665	I35_6665	ND
I35_6680	I35_6680	0.107
I35_7021	I35_7021	0.007
sfnR	I35_7049	0.117
I35_7211	I35_7211	0.279
I35_7292	I35_7292	0.248
I35_7336	I35_7336	0.296
I35_7338	I35_7338	0.280
I35_7360	I35_7360	ND
ilvD	I35_7391	0.329
I35_7411	I35_7411	ND
I35_7463	I35_7463	0.314
I35_7529	I35_7529	ND
I35_7706	I35_7706	0.083
I35_7738	I35_7738	ND
I35_7812	I35_7812	0.009
dhT	I35_7854	ND
I35_7855	I35_7855	0.049
I35_7856	I35_7856	ND

We also identified 46 genes that were negatively regulated by valazole (Table 6). Among these genes, two encode proteins that are directly connected to metal

homeostasis, namely a zinc uptake regulation protein (I35_2669) and a zinc-regulated outer membrane receptor (I35_5427). Other genes identified encode proteins which rely on metal ions for their enzymatic activity, including the rubredoxin-type Fe(Cys)4 protein, RubA (I35_2387), an adenosylcobinamide-phosphate guanylyltransferase (I35_2517), which is involved in cobalamin biosynthesis, a quinone oxidoreductase (I35_4578), the taurine catabolism dioxygenase TauD (I35_4965) and FdnI (I35_4938), the gamma subunit of formate dehydrogenase. The only negatively regulated gene cluster is located on pC3 and spans six genes, which encode two proteins from the queuosine biosynthesis pathway (I35_6423; QueD and I35_6424) along with a dihydroorotase (I35_6421; pyrC), a carbonic anhydrase (I35_6422) an acyl-CoA dehydrogenase (I35_6426) and a putative metal chaperone GTPase (I35_6425). Four out of six genes from this gene cluster either use metals in their active center or are involved in metal homeostasis. The cluster could either be involved in queuosine biosynthesis or deazapurine biosynthesis.

Table 6: Genes with statistically significant increased expression (pval<0.1) above the threshold (>3-fold change) in H111 Δ*hamD* (hamD) compared to H111 wildtype (wt). NA: not applicable because read number for wt was 0.

Name	locus_tag	fold change hamD vs wt
cheD	I35_0140	5.588
I35_0178	I35_0178	NA
I35_1157	I35_1157	NA
I35_1212	I35_1212	NA
I35_1679	I35_1679	NA
rubA	I35_2387	NA
I35_2517	I35_2517	NA
I35_2669	I35_2669	3.660
I35_2776	I35_2776	25.078
I35_3066	I35_3066	8.704
I35_3237	I35_3237	3.438
I35_3290	I35_3290	NA
I35_4099	I35_4099	NA
I35_4494	I35_4494	6.371
I35_4532	I35_4532	NA
I35_4578	I35_4578	NA
I35_4579	I35_4579	NA
I35_4691	I35_4691	NA

fdnI	I35_4938	4.676
I35_4965	I35_4965	7.580
xsc	I35_5029	NA
I35_5060	I35_5060	NA
I35_5364	I35_5364	NA
I35_5398	I35_5398	NA
I35_5409	I35_5409	4.071
I35_5427	I35_5427	11.693
I35_5616	I35_5616	NA
I35_5633	I35_5633	NA
I35_5858	I35_5858	NA
I35_5863	I35_5863	9.351
I35_5876	I35_5876	NA
bscK	I35_5886	169.066
I35_5898	I35_5898	NA
I35_6340	I35_6340	NA
pyrC	I35_6421	6.091
I35_6422	I35_6422	12.915
QueD	I35_6423	18.860
I35_6424	I35_6424	19.414
I35_6425	I35_6425	29.852
I35_6426	I35_6426	7.093
fedB	I35_6440	NA
I35_6659	I35_6659	NA
I35_7299	I35_7299	3.997
I35_7638	I35_7638	NA
I35_7795	I35_7795	NA
I35_7876	I35_7876	NA

Comparison of the transcriptome of the wild-type with that of the *hamD* mutant in the presence of 100 µM valazole revealed a strong repression of the pyochelin biosynthesis cluster by valazole (Tables 7 and 8) while in the genetically complemented strain, H111Δ*hamD*/pBBR*hamD,* two additional copper metallo chaperones (I35_1025 and I35_6107) and two cytochrome oxidases (I35_1026 and I35_2071) were found to be repressed (Tables 9 and 10). These genes were not differentially regulated in the *hamD* mutant, suggesting that this effect is likely due to elevated levels of valazole and/or fragin in the genetically or chemically complemented strains.

Table 7: Genes with statistically significant decreased expression (pval<0.1) above the threshhold (>3-fold change) in H111 Δ*hamD* + 100 µM valazole (sig) compared to H111 wt (wt). ND: not applicable because read number for sig was 0.

Name	locus tag	fold change wt vs sig
I35_0064	I35_0064	0.006
I35_0100	I35_0100	ND
hppD	I35_0198	0.304
paaG	I35_0207	0.292
I35_0378	I35_0378	ND
I35_0708	I35_0708	ND
dfrA	I35_0948	0.071
I35_1133	I35_1133	ND
I35_1147	I35_1147	0.186
I35_1273	I35_1273	ND
I35_1420	I35_1420	0.266
I35_1421	I35_1421	0.199
cysP	I35_1562	0.309
I35_1669	I35_1669	ND
I35_1976	I35_1976	0.012
I35_2183	I35_2183	ND
cysNC	I35_2189	0.070
kdpA	I35_2307	0.326
gp36	I35_2423	ND
I35_2487	I35_2487	0.084
I35_2544	I35_2544	0.330
I35_3012	I35_3012	0.115
potG	I35_3071	ND
I35_3177	I35_3177	0.164
I35_4006	I35_4006	ND
I35_4014	I35_4014	ND
I35_4047	I35_4047	ND
I35_4090	I35_4090	0.291
I35_4194	I35_4194	ND
I35_4227	I35_4227	ND
I35_4350	I35_4350	0.327
I35_4351	I35_4351	ND
I35_4374	I35_4374	ND
I35_4401	I35_4401	0.239
I35_4438	I35_4438	ND
I35_4593	I35_4593	0.225
I35_4681	I35_4681	ND

I35_4689	I35_4689	ND
I35_4841	I35_4841	0.209
I35_5045	I35_5045	ND
I35_5066	I35_5066	0.182
I35_5131	I35_5131	0.007
I35_5228	I35_5228	ND
I35_5281	I35_5281	ND
I35_5464	I35_5464	ND
I35_5487	I35_5487	ND
I35_5529	I35_5529	0.226
I35_5631	I35_5631	0.229
I35_5733	I35_5733	ND
I35_5787	I35_5787	ND
I35_5874	I35_5874	0.214
I35_5996	I35_5996	0.121
fptA	I35_6116	0.289
pchI	I35_6117	0.197
pchH	I35_6118	0.127
pchG	I35_6119	0.147
pchF	I35_6120	0.162
pchE	I35_6121	0.238
pchD	I35_6123	0.146
pchC	I35_6124	0.297
pchB	I35_6125	0.223
pchA	I35_6126	0.149
I35_6127	I35_6127	0.222
I35_6197	I35_6197	0.008
I35_6265	I35_6265	ND
I35_6268	I35_6268	0.008
I35_6316	I35_6316	ND
I35_6317	I35_6317	0.275
I35_6332	I35_6332	0.329
I35_6383	I35_6383	ND
I35_6430	I35_6430	0.135
I35_6509	I35_6509	ND
I35_6514	I35_6514	0.309
I35_6550	I35_6550	0.258
I35_6561	I35_6561	ND
I35_6674	I35_6674	0.021
I35_6680	I35_6680	0.315
I35_7124	I35_7124	0.011

I35_7190	I35_7190	0.059
I35_7225	I35_7225	ND
I35_7275	I35_7275	ND
I35_7292	I35_7292	0.136
I35_7320	I35_7320	ND
I35_7336	I35_7336	0.320
I35_7338	I35_7338	0.184
I35_7393	I35_7393	0.074
I35_7431	I35_7431	ND
I35_7630	I35_7630	0.177
I35_7824	I35_7824	ND

Table 8: Genes with statistically significant increased expression (pval<0.1) above the threshhold (>3-fold change) in H111 Δ*hamD* + 100 µM valazole (sig) compared to H111 wt (wt). NA: not applicable because read number for wt was 0.

Name	**locus tag**	**fold change wt vs sig**
I35_0178	I35_0178	NA
I35_0350	I35_0350	NA
hmpA	I35_0589	7.883
I35_1102	I35_1102	4.004
I35_1157	I35_1157	NA
I35_1369	I35_1369	NA
I35_2254	I35_2254	3.512
cobC	I35_2519	6.297
glcC	I35_2816	NA
I35_3290	I35_3290	NA
I35_4639	I35_4639	5.020
I35_4640	I35_4640	5.874
I35_4641	I35_4641	4.158
I35_4684	I35_4684	NA
I35_4695	I35_4695	NA
I35_4857	I35_4857	4.223
I35_5060	I35_5060	NA
I35_5133	I35_5133	NA
I35_5250	I35_5250	3.203
rdgC	I35_5414	5.793
I35_5518	I35_5518	267.347
I35_5817	I35_5817	179.374
I35_5898	I35_5898	NA
I35_6161	I35_6161	NA
I35_6340	I35_6340	NA

I35_6397	I35_6397	NA
ceoA	I35_6449	7.803
I35_6602	I35_6602	4.666
I35_6603	I35_6603	4.298
ampC	I35_7154	NA
I35_7324	I35_7324	NA
I35_7327	I35_7327	NA
I35_7410	I35_7410	NA
I35_7413	I35_7413	NA
I35_7638	I35_7638	NA
I35_7703	I35_7703	NA
I35_7715	I35_7715	NA
I35_7820	I35_7820	10.283

Table 9: Genes with statistically significant decreased expression (pval<0.1) above the threshhold (>3-fold change) in H111 Δ*hamD* pBBR*hamD* (comp) compared to H111 wt (wt). ND: not applicable because read number for comp was 0.

Name	**locus tag**	**fold change wt vs comp**
I35_0020	I35_0020	0.052
I35_0533	I35_0533	0.006
ureC	I35_0767	0.203
ureB	I35_0768	ND
I35_0775	I35_0775	0.116
hemN	I35_0780	0.108
I35_0868	I35_0868	0.066
I35_0869	I35_0869	0.060
I35_0870	I35_0870	0.003
rpmF	I35_0987	ND
I35_1025	I35_1025	0.123
I35_1026	I35_1026	0.291
gudD	I35_1034	0.248
I35_1077	I35_1077	0.111
I35_1147	I35_1147	0.226
I35_1214	I35_1214	0.227
cysP	I35_1562	0.318
cysT	I35_1563	0.306
fimA	I35_1588	0.141
I35_1589	I35_1589	0.230
I35_1590	I35_1590	0.153
I35_1591	I35_1591	0.137

I35_1686	I35_1686	ND
I35_1899	I35_1899	ND
I35_1976	I35_1976	ND
aceA	I35_2045	0.193
cyoB	I35_2071	0.031
hutU	I35_2172	0.176
kdpB	I35_2306	0.128
kdpA	I35_2307	0.022
I35_2661	I35_2661	0.092
I35_2905	I35_2905	0.313
tlpA	I35_2940	0.277
I35_3276	I35_3276	ND
fliP	I35_3283	0.123
I35_4048	I35_4048	0.152
I35_4049	I35_4049	0.246
I35_4227	I35_4227	ND
I35_4350	I35_4350	0.133
I35_4383	I35_4383	ND
I35_4384	I35_4384	0.012
I35_4385	I35_4385	0.011
I35_4386	I35_4386	0.110
I35_4434	I35_4434	0.095
I35_4435	I35_4435	0.003
I35_4591	I35_4591	0.282
I35_4631	I35_4631	0.235
I35_4669	I35_4669	ND
I35_4841	I35_4841	0.323
I35_4867	I35_4867	0.256
I35_4868	I35_4868	0.023
lipA	I35_4869	0.149
I35_5045	I35_5045	ND
mhbH	I35_5121	ND
I35_5195	I35_5195	ND
I35_5196	I35_5196	0.092
I35_5197	I35_5197	0.122
I35_5198	I35_5198	0.188
I35_5200	I35_5200	ND
I35_5255	I35_5255	0.043
I35_5278	I35_5278	0.014
I35_5295	I35_5295	0.147
I35_5296	I35_5296	0.329

I35_5372	I35_5372	0.008
I35_5450	I35_5450	0.230
I35_5466	I35_5466	ND
I35_5468	I35_5468	ND
I35_5537	I35_5537	0.314
nirB	I35_5547	0.050
I35_5683	I35_5683	0.280
I35_5776	I35_5776	ND
I35_5833	I35_5833	ND
I35_5950	I35_5950	ND
I35_6104	I35_6104	0.056
I35_6105	I35_6105	0.030
I35_6106	I35_6106	0.022
I35_6107	I35_6107	0.039
I35_6108	I35_6108	0.020
I35_6109	I35_6109	0.213
I35_6110	I35_6110	0.060
I35_6174	I35_6174	0.020
I35_6175	I35_6175	0.174
I35_6317	I35_6317	0.233
I35_6332	I35_6332	0.163
metE	I35_6384	0.014
I35_6389	I35_6389	0.080
I35_6416	I35_6416	ND
ceoB	I35_6448	0.271
hmuT	I35_6524	0.304
I35_6605	I35_6605	0.027
I35_6680	I35_6680	0.019
glcG	I35_6700	ND
I35_7124	I35_7124	ND
I35_7209	I35_7209	ND
I35_7289	I35_7289	ND
I35_7292	I35_7292	0.141
I35_7354	I35_7354	0.049
I35_7411	I35_7411	0.028
I35_7462	I35_7462	ND
I35_7812	I35_7812	0.005
I35_7855	I35_7855	ND
I35_7873	I35_7873	0.011
bpeB	I35_7888	0.048
I35_0020	I35_0020	0.052

I35_0533	I35_0533	0.006
ureC	I35_0767	0.203
ureB	I35_0768	ND
I35_0775	I35_0775	0.116
hemN	I35_0780	0.108
I35_0868	I35_0868	0.066
I35_0869	I35_0869	0.060
I35_0870	I35_0870	0.003
rpmF	I35_0987	ND
I35_1025	I35_1025	0.123
I35_1026	I35_1026	0.291
gudD	I35_1034	0.248
I35_1077	I35_1077	0.111
I35_1147	I35_1147	0.226
I35_1214	I35_1214	0.227
cysP	I35_1562	0.318
cysT	I35_1563	0.306
fimA	I35_1588	0.141
I35_1589	I35_1589	0.230
I35_1590	I35_1590	0.153
I35_1591	I35_1591	0.137
I35_1686	I35_1686	ND
I35_1899	I35_1899	ND
I35_1976	I35_1976	ND
aceA	I35_2045	0.193
cyoB	I35_2071	0.031
hutU	I35_2172	0.176
kdpB	I35_2306	0.128
kdpA	I35_2307	0.022
I35_2661	I35_2661	0.092
I35_2905	I35_2905	0.313
tlpA	I35_2940	0.277
I35_3276	I35_3276	ND
fliP	I35_3283	0.123
I35_4048	I35_4048	0.152
I35_4049	I35_4049	0.246
I35_4227	I35_4227	ND
I35_4350	I35_4350	0.133
I35_4383	I35_4383	ND
I35_4384	I35_4384	0.012
I35_4385	I35_4385	0.011

I35_4386	I35_4386	0.110
I35_4434	I35_4434	0.095
I35_4435	I35_4435	0.003
I35_4591	I35_4591	0.282
I35_4631	I35_4631	0.235
I35_4669	I35_4669	ND
I35_4841	I35_4841	0.323
I35_4867	I35_4867	0.256
I35_4868	I35_4868	0.023
lipA	I35_4869	0.149
I35_5045	I35_5045	ND
mhbH	I35_5121	ND
I35_5195	I35_5195	ND
I35_5196	I35_5196	0.092
I35_5197	I35_5197	0.122
I35_5198	I35_5198	0.188
I35_5200	I35_5200	ND
I35_5255	I35_5255	0.043
I35_5278	I35_5278	0.014
I35_5295	I35_5295	0.147
I35_5296	I35_5296	0.329
I35_5372	I35_5372	0.008
I35_5450	I35_5450	0.230
I35_5466	I35_5466	ND
I35_5468	I35_5468	ND
I35_5537	I35_5537	0.314
nirB	I35_5547	0.050
I35_5683	I35_5683	0.280
I35_5776	I35_5776	ND
I35_5833	I35_5833	ND
I35_5950	I35_5950	ND
I35_6104	I35_6104	0.056
I35_6105	I35_6105	0.030
I35_6106	I35_6106	0.022
I35_6107	I35_6107	0.039
I35_6108	I35_6108	0.020
I35_6109	I35_6109	0.213
I35_6110	I35_6110	0.060
I35_6174	I35_6174	0.020
I35_6175	I35_6175	0.174
I35_6317	I35_6317	0.233

I35_6332	I35_6332	0.163
metE	I35_6384	0.014
I35_6389	I35_6389	0.080
I35_6416	I35_6416	ND
ceoB	I35_6448	0.271
hmuT	I35_6524	0.304
I35_6605	I35_6605	0.027
I35_6680	I35_6680	0.019
glcG	I35_6700	ND
I35_7124	I35_7124	ND
I35_7209	I35_7209	ND
I35_7289	I35_7289	ND
I35_7292	I35_7292	0.141
I35_7354	I35_7354	0.049
I35_7411	I35_7411	0.028
I35_7462	I35_7462	ND
I35_7812	I35_7812	0.005
I35_7855	I35_7855	ND
I35_7873	I35_7873	0.011
bpeB	I35_7888	0.048

Table 10: Genes with statistically significant increased expression (pval<0.1) above the threshold (>3-fold change) in H111 Δ*hamD* pBBR*hamD* (comp) compared to H111 wt (wt). NA: not applicable because read number for wt was 0.

Name	**locus tag**	**fold change wt vs comp**
I35_0046	I35_0046	NA
I35_0178	I35_0178	NA
I35_0349	I35_0349	4.593
I35_1369	I35_1369	NA
I35_1520	I35_1520	NA
lipA	I35_1827	5.607
cobC	I35_2519	4.874
ilvD	I35_2532	3.394
I35_2741	I35_2741	4.721
phbB	I35_2838	3.643
I35_2840	I35_2840	3.584
I35_2891	I35_2891	3.341
I35_2892	I35_2892	3.463
I35_2893	I35_2893	3.994
I35_2894	I35_2894	3.204

I35_2895	I35_2895	4.339
I35_3177	I35_3177	3.263
gspM	I35_3297	NA
I35_4074	I35_4074	3.565
I35_4099	I35_4099	NA
I35_4194	I35_4194	5.638
I35_4198	I35_4198	3.142
I35_4618	I35_4618	15.119
I35_4684	I35_4684	NA
I35_4691	I35_4691	NA
I35_4730	I35_4730	NA
I35_5364	I35_5364	NA
I35_5529	I35_5529	6.207
I35_5530	I35_5530	4.371
I35_5875	I35_5875	4.205
I35_5876	I35_5876	NA
I35_5878	I35_5878	5.573
I35_5879	I35_5879	6.281
I35_5880	I35_5880	4.442
bscL	I35_5885	NA
bscK	I35_5886	766.641
I35_5888	I35_5888	8.570
bscD	I35_5890	5.757
bscC	I35_5891	7.500
I35_6161	I35_6161	NA
I35_6180	I35_6180	3.755
rhlC	I35_6229	10.413
rhlA	I35_6233	3.312
pqqB	I35_6259	3.875
fedB	I35_6440	NA
I35_6655	I35_6655	6.655
I35_6659	I35_6659	NA
I35_7574	I35_7574	3.018
I35_7590	I35_7590	NA
I35_7595	I35_7595	3.280
I35_7603	I35_7603	9.031
I35_7604	I35_7604	3.838
I35_7610	I35_7610	3.411
I35_7620	I35_7620	6.715
I35_7638	I35_7638	NA
I35_7703	I35_7703	NA

3.5 Regulatory elements in the *ham* promoter region

Ryan and colleagues [55] mapped the CepR2 binding site in the bidirectional promoter region of the *ham* cluster. Additional prediction of putative promoter regions with the BPROM online tool revealed three -10 and -35 boxes which could act as promoter sites for the expression of the *hamABCDE* operon and placed one of the putative promoters (P2) next to the CepR2 binding site (Figure 21A). In addition to the previously constructed transcriptional fusion of the full *hamA* promoter region to *lacZ* (P*hamA*-*lacZ*), which contains all three putative promoters (P1 – P3) along with the CepR2 binding site, three truncated *hamA* promoter fragments were constructed. P*hamA*122-*lacZ* only contained the -10 box of P1, P*hamA*222-*lacZ* contained the full P1 promoter, and P*ham*A281-l*acZ* contained the P1 promoter and the CepR2 binding site. The three truncated transcriptional *hamA* promoter fusions were introduced into H111 and H111 Δ*hamD* and β-galactosidase activities were measured. No promoter activity was present in any of the four tested constructs in the *hamD* mutant background (Figure 21B). In the wild-type background, P*hamA*122-*lacZ* showed no activity. This was expected, as the construct only contained the -10 box of the first putative promoter. The activity of the P*hamA*281-*lacZ* construct was comparable to the full length construct. The highest activity was observed in the P*hamA*222-*lacZ* construct (Figure 21B). This implies that the P1 promoter is both necessary and sufficient to drive expression of the *hamABCDE* operon. In addition, an element which negatively affects the *hamA* promoter activity seems to be present in the region spanning the -222 to -281 region, which contains the CepR2 binding site. This is surprising, as CepR2 was clearly necessary for *hamA* promoter activity. Although no other regulatory elements were predicted for the region between position -222 and -281, it might be possible that a so far unknown regulatory element in this region is responsible for the observed difference of *hamA* promoter activities.

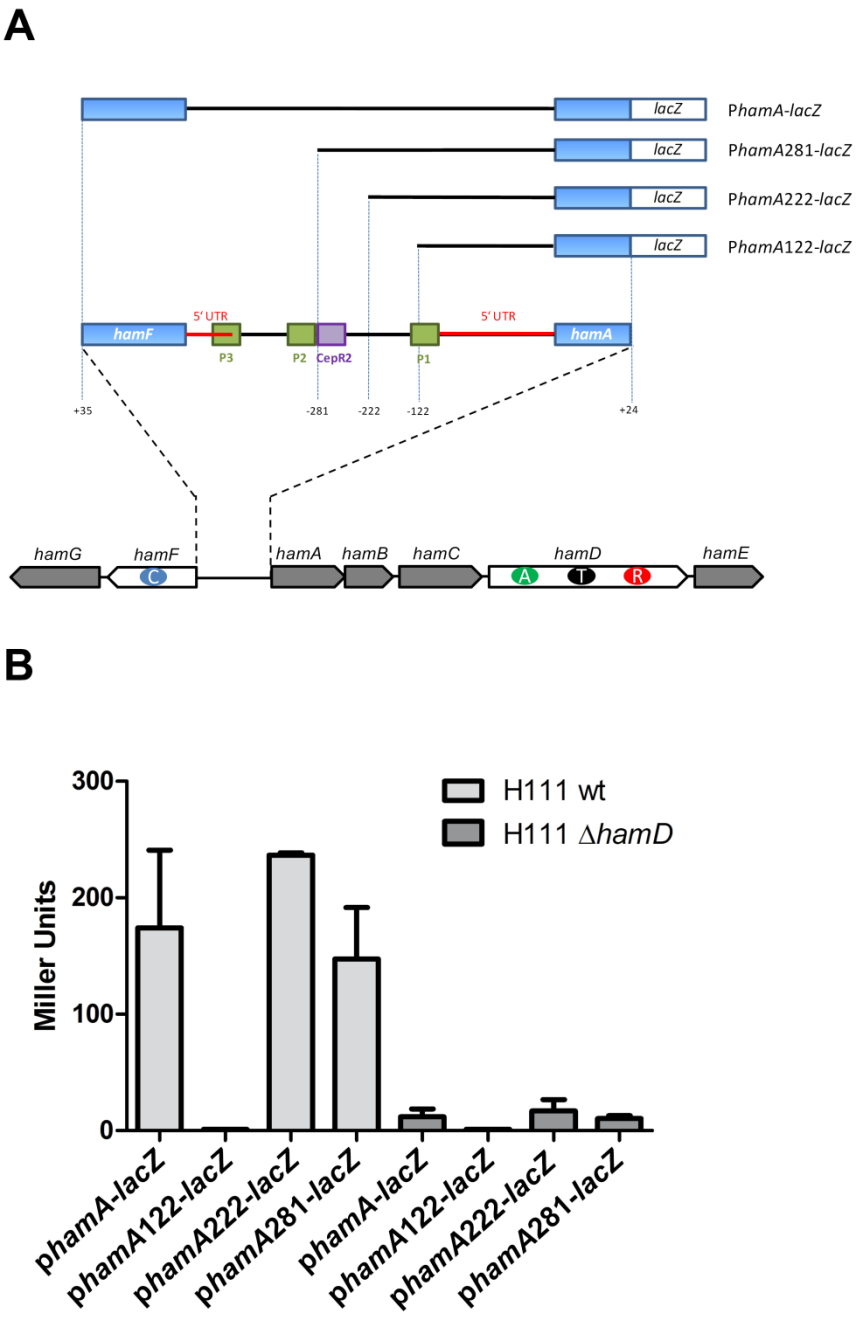

Figure 21: The presence of the CepR2 binding box is not necessary for the *hamA* promoter activity. A) Schematic depiction of the truncated *hamA* promoter fusions. P1, P2, P3: putative promoter regions (-10 box and -35 box) ; CepR2: CepR2 binding box ; 5'UTR: 5' untranslated region. B) The *hamA* promoter activity derived from the full promoter region (P*hamA-lacZ*) and the three truncated constructs (P*hamA*122-*lacZ*, P*hamA*222-*lacZ* and P*hamA*281-*lacZ*) was tested in the wild type (H111 wt) and the *hamD* mutant (H111 Δ*hamD*) background. No promoter activity was observed in the H111 Δ*hamD* background. No promoter activity was present in the shortest construct (P*hamA122-lacZ*). The highest activity was observed in theP*hamA*222-*lacZ* construct followed by P*hamA-lacZ* and P*hamA*281-*lacZ*. Results are presented as means ± SD from three independent biological replicates carried out in technical triplactes.

3.6 Iron positively regulates expression of the *ham* cluster

We have shown that iron reduces antifungal activity by directly interfering with the antifungal activity of fragin *in vitro* (Figure 14). Nevertheless, this does not exclude the possibility that iron might also influence *ham* gene transcription. This would not be surprising, as production of other metal chelating molecules is tightly controlled by iron. Siderophores like pyochelin and ornibactin, for example, are downregulated in the presence of free iron.

To examine if the *ham* genes are also downregulated in the presence of high iron concentrations, the *hamA* promoter activity was measured in the presence of increasing amounts of iron in the growth medium. An approximately 20-fold increase of promoter activity was seen when the cultures were grown with 1 µM iron compared to 100 nM iron. This trend was also observed in a culture grown with 10 µM iron, which resulted in a 10-fold higher promoter activity compared to 1 µM iron (Figure 22). At the same time, the cultures reached similar OD_{600} values, independent of the iron concentration in the medium, demonstrating that the observed difference in promoter activities is not due to differences in growth.

Chapter III: Discussion and future Prospects

4 Discussion

In this study, we identified an NPRS-like gene cluster in *B. cenocepacia* H111, the so-called *ham* cluster, which directs the synthesis of two distinct molecules, the antifungal molecule fragin and a novel signal molecule which we have named valazole.

The initial *ham* cluster-derived molecule identified in this study was the antifungal molecule fragin, which was first isolated in 1967 in a screen for novel plant growth inhibitors [218]. Fragin was reported to be synthesized by *Pseudomonas fragi*, but subsequent studies on *P. fragi* were unable to confirm the production of fragin [222]. Currently there is one whole shotgun sequence of *P. fragi* B25 deposited at GenBank (accession number NZ_AHZX01000000). Thorough investigation of the eleven scaffolds (NZ_JH604622.1 – NZ_JH604632.1) showed that no gene cluster with similarity to the *ham* cluster is present in the sequenced *P. fragi* genome. Also, there are no sequenced bacterial strains besides *B. cenocepacia* deposited at public databases that harbor both *ham* operons (Figure 2), which are essential for fragin biosynthesis. Based on this, the strain from which fragin was originally isolated might have been a *B. cenocepacia* strain, misidentified as *P. fragi*.

4.1 Antimicrobial activity of fragin

The most outstanding feature of fragin and valazole is their nitrosohydroxylamine group, also described as an *N*-hydroxy-*N*-nitrosamine group in the literature [220]. Molecules bearing this functional group are rarely found in nature, but all of them show potent biological activities, including antifungal, antibacterial, antiviral and antitumor activities (reviewed in [220, 221]), which makes this group of molecules an interesting source for drug development.

The first described natural product with a nitrosohydroxylamine group was alanosine, isolated in 1966 from *Streptomyces alanosinicus* [223]. Alanosine was shown to have

antibiotic activity against *Candida albicans*, *Mycobacterium marinum* and *Saccharomyces cerevisiae* [224]. Besides its antibiotic activity, it also exhibited antiviral properties and had immunosuppressive effects in several animal models [225, 226]. Most notably, alanosine was investigated in clinical trials as a potential chemotherapy drug due to its antitumor activity [227]. In 1967, the antifungal molecule fragin, the biosynthesis of which is investigated in this study, was isolated in a screen for novel plant growth inhibitors. This compound was shown to inhibit the growth of Gram-positive and Gram-negative bacteria, algae, yeast and fungi [218]. The reported activity of fragin against the Gram-negative bacterium *E.coli* is of particular interest for this study, as no growth inhibition of Gram-negative bacteria, including two different *E. coli* strains, was observed in the present study. In the study of Tamura and Murayama [218] the amount of fragin reported to inhibit the growth of *E. coli* was 100 ppm, which equates to 100 µg/ml. In our study, we used a maximum of 40 µg fragin spotted on filter discs to test antibacterial activity (Figures 10C and 10D show the results with 20 µg fragin). To clearly determine if fragin can inhibit Gram-negative bacteria, additional disc diffusion assays with higher amounts of fragin would be required.

While the precise mode of action is not known for any naturally occurring nitrosohydroxylamine, alanosine has been shown to interfere with aspartate utilizing enzymes of the purine and pyrimidine biosynthesis pathway, by serving as a structural analog of carboxylic acid [228]. In addition, alanosine was found to chelate copper and zinc [229] and the synthetic nitrosohydroxylamine cupferron is commonly used as a metal chelator [230-233]. Interestingly, mushroom tyrosinase, which uses copper in its active center [234], is inhibited by dopastin and cupferron [235-237]. Dopamine beta-hydroxylase, another copper dependent enzyme [238] is also inhibited by dopastin [239], while 5-lipoxygenase, which has iron in its active center [240], is inhibited by nitrosoxacins A, B and C [241]. The presence of the nitrosohydroxylamine group in the fragin structure, in addition to the observed loss of antifungal activity in the presence of iron, suggests that fragin, like other nitrosohydroxylamines might inhibit the growth of other microbes, either by metal chelation or by inactivating enzymes that rely on metals for their activity.

Several fungal enzymes, including superoxide dismutase (SOD) and cytochrome C oxidase are copper-dependent [242]. SODs protect the fungal cell against oxidative

stress, especially against the oxidative burst of phagocytic cells [243]. Cytochrome C oxidase is the terminal enzyme in the mitochondrial respiratory chain [243]. Importantly, iron uptake in fungi is partially depend on copper via a high-affinity Cu-dependent iron transporter [244]. Therefore copper chelation by fragin could potentially disrupt the respiratory chain and leave the fungus more susceptible to oxidative stress, while at the same time it could also restrict iron uptake.

4.2 Gene regulation by the novel signaling molecule valazole

In addition to the identification of fragin as the major antifungal compound of *B. cenocepacia* H111, we also identified valazole, a second nitrosohydroxylamine compound, which is synthesized by a sub-set of the *ham* genes. Valazole shows remarkable structural similarity to fragin, only lacking an amino group and the acyl-chain which is attached to the valine core. Valazole acts as a signaling molecule in a positive feedback loop, driving its own expression as well as that of fragin (Figures 20A and 20B, Tables 5 and 6). Interestingly, several studies in *P. syringae pv. syringae* UMAF0158 and *P. entomophila* have identified a gene cluster responsible for the production of a putative extracellular signaling molecule. The identified gene clusters, *mgo* in *P. syringae pv. syringae* UMAF0158 and *pvf* in *P. entomophila* show striking similarity to the *hamABCDE* operon, only lacking a *hamB* homolog , which is not required for valazole biosynthesis in *B. cenocepacia* H111. The *mgo*-derived signaling molecule was shown to regulate expression of the biosynthetic genes for mangotoxin production in *P. syringae pv. syringae* UMAF0158 [217], while *pvf* was shown to be involved in *P. entomophila* virulence in a *drosophila* model [216]. Examination of the A domain substrate binding pockets of PvfC, MgoC and HamD showed that PvfC and HamD share the same amino acid sequence (DALFVGIV), while PvfC has a different binding pocket sequence (DSIFMGLV) (Table 3). Nevertheless, prediction of the amino acid substrates using NRPSpredictor 2 and NRPSsp online tools suggested that all three enzymes incorporate the same amino acid as a building block for the signaling molecule. Taken together, valazole might be the prototype of a new class of signaling molecules which are produced by members of the genera *Burkholderia*, *Pseudomonas* and *Pandorae* (Figure 4). Valazole controls expression of the transcriptional regulators CepS and CepR2, which in turn

regulate expression of the *ham* gene cluster. Interestingly, a tripartite multidrug resistance system located next to the *ham* cluster is also regulated by valazole, indicating a putative role as a fragin and/or valazole transporter. Further investigations are required to elucidate the role, if any, of this system in fragin or valazole transport. The most unexpected valazole-regulated functions identified by global RNA-Seq analysis were those with a putative role in 3-methyl-2-oxobutanoate metabolism (Table 5). 3-methyl-2-oxobutanoate is the intermediate metabolite at the branching point of the valine and leucine biosynthesis pathways. Based on the RNA-Seq data, valazole specifically upregulated six genes (I35_2532, I35_2881, I35_4185, I35_4642, I35_7391 and I35_4373) involved in the metabolism of 3-methyl-2-oxobutanoate. Two of these genes encode IlvD homologs, which can potentially shunt 3-methyl-2-oxobutanoate away from valine biosynthesis. Restricting valine biosynthesis might be a mechanism to regulate fragin and valazole biosynthesis.

At present it is not known whether valazole binds to a specific receptor, but CepR2 and CepS are encoded by genes adjacent to the *ham* cluster and thus are good candidates. CepR2 is a solo LuxR-type regulator. These have been shown to not only bind AHL molecules but also pyrones and dialkylresorcinols [52, 53]. Sequence alignments of LuxR-type regulators have shown that six amino acid residues in the signal binding domain (SBD) are conserved in 95 % of LuxR proteins and these residues are involved in binding their cognate AHL molecules [245]. As these amino acid residues (WYDPG) are fully conserved in CepR2, and AHL binding has been experimentally proven for CepR2 from *B. cenocepacia* K56-2 [55], it is unlikely that CepR2 is a valazole receptor. Therefore, the AraC-type regulator CepS remains the best candidate valazole receptor and additional work will be required to test this possibility.

Valazole could also alter transcription of the *ham* genes by binding to a riboswitch. Riboswitches are metabolite sensing RNA elements found in 5'UTR regions, which can alter the transcription of their respective mRNAs. They recognize a broad range of metabolites including amino acids, vitamin cofactors, amino sugars, metal ions and secondary messengers (reviewed in [246]). Therefore the unusually long 5'UTR of the *hamABCDE* operon might contain a riboswitch which controls *ham* gene expression. Nevertheless, thorough investigation of the 5'UTR did not identify any

putative riboswitches in this area. In addition, both the *hamABCDE* and *hamFG* operons, are regulated by valazole, and therefore the presence of a riboswitch in the 5'UTR of *hamABCDE* would not explain the observed regulation of the *hamFG* operon. As CepR2 and CepS are both necessary for full activity of both *ham* operons and both regulators were positively regulated by valazole in our global RNA-seq analysis, valazole might not directly regulate the expression of the *ham* genes, but rather drive the expression of CepR2 and CepS.

4.3 Biological activity of valazole beyond bacterial signaling

It is also important to mention that our data supports a role of valazole beyond its function as a signaling molecule. One clear indication is the amount of valazole which is necessary to induce *ham* promoter activity to a level similar to that of the wild-type strain. The required valazole concentration of 50 µM is much higher than that determined for dedicated signaling molecules like AHLs or BDSF, which are in the range of 5 nM to 5 µM. Further evidence that valazole is a multifunctional molecule is the finding that it affects transcription of genes involved in metal transport/homeostasis as well as those encoding metal dependent enzymes. Several of these genes are not associated with iron, but rather with copper, which suggests that fragin and valazole affect gene transcription by copper chelation. The signaling function of valazole together with the metal chelating ability of both fragin and valazole is reminiscent of the quinolone quorum sensing system of *Pseudomonas*. The *Pseudomonas aeruginosa* QS signal molecule known as Pseudomonas quinolone signal (PQS) and its immediate precursor 2-heptyl-4-quinolone (HHQ) are both employed as signaling molecules [66, 71] that drive expression of their own biosynthesis genes *via* the regulator PqsR. In addition, PQS was shown to regulate several virulence factors, including pyocyanin and the siderophores pyochelin and pyoverdin [73]. PQS was also shown to chelate iron and to possibly function as an iron trap at the cell surface. This is thought to create a shortage of free iron, leading to an up-regulation of pyochelin and pyoverdin production. As both siderophores have a higher affinity for iron than PQS, ferric iron can be transferred from membrane-associated PQS to either of the two siderophores [71]. Here it is of special interest to mention, that the complementation of a fragin and valazole negative strain

with synthetic valazole resulted in a strong down-regulation of the pyochelin biosynthesis cluster (Table 10). This indicates that valazole might be used to supply the cell with iron and possibly other metals (e.g. copper), either directly or by interacting with pyochelin or ornibactin.

4.4 The influence of iron on antifungal activity and the *ham* cluster

The addition of excess iron to agar plates resulted in the development of a yellow colony phenotype which was independent of the two siderophores pyochelin and ornibactin, but was directly connected to the presence and expression of the *ham* gene cluster. Mutants bearing single gene deletions of several *ham* genes as well as of the positive *ham* cluster regulators CepR2 and CepS did not develop the yellow colony phenotype and remained white, while deletion of an AraC regulator (I35_4197) encoded immediately downstream of the *hamABCDE* operon, resulted in a bright yellow colony phenotype, which was accompanied by increased antifungal activity, implying that it is a positive regulator of the *ham* cluster. Given that the *hamF* mutant does not produce fragin, but is still capable of valazole biosynthesis, the yellow colony phenotype seems to be dependent on fragin but not valazole. As fragin and valazole have the same nitrosohydroxylamine functional group, both molecules should be able to bind metals. Based on the determined structures of the two compounds, valazole is more likely to freely diffuse in and out of the cell, while the fatty acid tail of fragin might prevent it from freely diffusing through the cell wall. Therefore, the yellow colony phenotype might be explained by iron chelation by fragin and subsequent precipitation of the fragin-iron complex in the culture supernatant, or its association with the cell envelope, in a similar manner to that reported for PQS, as discussed above.

In agreement with the proposed function of CepR2 as negative regulator of the *ham* cluster in strain K56-2 and positive regulator in strain H111, the K56-2 wild type strain did not show a yellow colony phenotype, while the CepR2 mutant did. This not only supports the idea of diametrically opposed roles of CepR2 in the two *B. cenocepacia* strains, but also indicates involvement of the *ham* cluster in formation of the yellow colony phenotype.

Further support comes from the successful exploitation of the yellow colony phenotype as a screening tool for genes involved in antifungal activity and *ham* cluster regulation. Mutants in the *ham* cluster, as well as several regulators some of which were not known to regulate antifungal activity at the time of the transposon screen were identified based on the yellow colony phenotype and all of them have been confirmed to be involved in antifungal activity or *ham* gene regulation.

Another important mechanism by which iron influences antifungal activity is through the siderophores pyochelin and ornibactin. While mutations in each of the siderophore biosynthesis genes had little effect on antifungal activity, a very strong reduction was observed in a strain that is deficient in both pyochelin and ornibactin biosynthesis. As high iron concentrations lead to lowered expression of siderophores, the observed loss of antifungal activity is possibly connected to a down-regulation of siderophore expression.

4.5 Positive regulation of the *ham* genes by iron

Antifungal activity was reduced in the presence of excess iron in the medium. In contrast to this, expression of the *ham* genes was activated by iron. Although this seems counterintuitive, we have established that iron lowers the activity of extracted fragin *in vitro* (Figure 15). Hence, elevated fragin production in the presence of high amounts of iron may allow the cell to reserve parts of the available iron for later use, when iron becomes scarce in the environment. This strategy might give *B. cenocepacia* an advantage over other microbes competing for available iron. The same is most likely true for copper. Fragin as well as valazole bind copper in vitro (personal communication, Christophe Daeppen) and therefore it is possible, that both molecules might serve as copper storage system for the cell, either intra- or extracellularly. Therefore it would also be very interesting to see, if copper can stimulate *ham* gene expression, as we have shown for iron.

4.6 Fragin and valazole biosynthesis

Despite the fact that nitrosohydroxylamines have great potential for drug development, with alanosine under investigation in clinical trials as a potential chemotherapeutic drug [247], no information is available on the biosynthesis of this functional group. This is in part owed to the fact that no genomic sequence data is available for microbes which have been shown to produce nitrosohydroxylamine derivatives. Therefore this is the first report linking a molecule with a nitrosohydroxylamine group to its biosynthetic gene cluster.

The data obtained for the structural elucidation of fragin showed that the naturally occurring enantiomer is D-fragin. Feeding studies with C^{13}- and N^{15}-labeled L-leucine and L-valine showed the highest incorporation rate was for C^{13}-labeled L-valine into fragin (Table 4) Accordingly, L-valine is the most likely substrate of the HamD A domain.

Although the observed incorporation rate of C^{13}-labeled L-valine was not much higher than those of the other three isotopically labeled amino acids (10 % vs 4 – 5 %), one must bear in mind that for L-valine all five carbon atoms were C^{13}-labeled and therefore the observed mass shift (+5 *m/*z) is very specific and cannot be explained by any mechanism other than incorporation. The C^{13}-labeled L-leucine, as well as the N^{15}-labeled L-leucine and L-valine, were only labeled on a single carbon or nitrogen atom. Therefore it is possible that the labeled residues entered the bacterial metabolism *via* leucine or valine degradation and the observed mass shifts resultfrom the incorporation of C^{13} or N^{15} atoms and not leucine or valine. This hypothesis is supported by the fact that feeding studies with the N^{15}-labeled amino acids also showed incorporation of N^{15} into the siderophore pyochelin (personal communication by Simon Sieber, unpublished data), which does not contain a valine or a leucine residue. Together with the relatively low incorporation rate of < 5 %, it is most likely that L-leucine is not specifically incorporated into fragin.

Many NRPS-derived secondary metabolites have non-proteinogenic amino acids incorporated into their structures. Nearly 500 non-proteinogenic amino acids are known to date and they are synthesized either from pre-existing proteinogenic amino acids or by *de novo* biosynthesis [248]. D-amino acids are synthesized from their L enantiomers by racemases or epimerases, which are part of their respective NRPS

megaenzymes [171, 184]. As no epimerase or racemase domain is encoded within the *ham* locus, the enzymes required for epimerization of L-valine to D-fragin remain to be identified. While isolated fragin is exclusively in the D-configuration, valazole was found to be a racemic mixture (personal communication by Christophe Daeppen, unpublished results). This suggests that epimerization occurs at the branching point of the valazole and fragin biosynthesis pathways. A more thorough discussion of the possible epimerization reaction will be provided in the biosynthesis section later in this chapter.

4.7 Biosynthesis of the bioactive nitrosohydroxylamine group

Biosynthesis of the nitrosohydroxylamine group of valazole and fragin requires the modification of the native valine amino group. This might be accomplished by a post-assembly or an on-line tailoring reaction. The latter include alkylation, hydroxylation and heterocyclization reactions as well as the synthesis of various ring systems [182]. To date, no nitrosylation reaction has been describedas an on-line tailoring reaction. Despite the lack of literature on this subject, there are several reasons why the formation of the nitrosohydroxylamine group of fragin and valazole is probably an on-line tailoring reaction. We were unable to identify intermediates of fragin or valazole biosynthesis in supernatants of any of the *ham* gene mutants (personal communication by Simon Sieber, unpublished data). If fragin or valazole had undergone post-assembly tailoring, one would expect to find intermediates of either of the two molecules lacking the nitrosohydroxylamine group. Furthermore, the fatty acid chain of fragin is attached to the valine moiety via an amino group most likely introduced by the putative amino transferase HamG. So far, all natural products which are acylated by a starter condensation domain have their acyl chain attached to the native amino group of the first amino acid in the assembly line. If the native valine amino group were still present when fragin was released from HamD, acylation could theoretically take place on this amino group and a corresponding molecule should be detectable in the organic solvent extracts. Therefore, it is most likely that the nitrosohydroxylamine group is the result of on-line tailoring reactions.

4.8 Acylation of the fragin precursor

Another unique feature of the fragin structure, as briefly mentioned above, is the localization of its acyl chain. Acylation by starter condensation domains has only been reportedto take place at the native amino group of the first amino acid in the peptide chain [159, 249]. In this respect, the *ham* cluster clearly differs from other NRPS assembly lines, as its starter condensation domain is not the first module on the NRPS enzyme (HamD), but is located on a separate protein (HamF). Furthermore, the *ham* cluster does not synthesize a peptide, but rather synthesizes a single modified amino acid (valazole) and its acylated derivative (fragin). The unique positioning of the acyl chain on the final molecule (fragin) is either a pre-requisite for the formation of the nitrosohydroxylamine group or a consequence thereof.

4.9 A unified model for fragin and valazole biosynthesis

The structural information obtained for fragin and valazole (Figures 10A and 19C,) along with the *in silico* predicted enzymatic function of the *ham* cluster encoded proteins (Figure 3B) allows us topropose a model for the biosynthesis of fragin and valazole (Figure 23). As already discussed above, the nitrosohydroxylamine group is most likely synthesized by on-line tailoring of the valine amino group. Formation of the nitrosohydroxylamine group probably involves HamC. Owing to the high conservation of residues responsible for substrate specificity between HamC and PsAAO (Figure 3C), it is likely that HamC oxidizes an aromatic amine to an aryl nitro compound as demonstrated for PsAAO [214]. The resulting aryl nitro compound might serve as an NO_2 donor for the formation of the nitrosohydroxylamine group. A similar mechanism was recently proposed for diazo group formation in cremeomycin biosynthesis [250]. Unpublished results obtained by the group of Prof. Karl Gademann have demonstrated that a synthetic hydroxyl amine derivative of fragin reacts spontaneously with $NaNO_2$ to give rise to fragin (personal communication by Simon Sieber, unpublished data), which is in good agreement with an aryl nitro compound as NO_2 donor. HamA and HamE are essential for both fragin and valazole biosynthesis and therefore they are likely to be involved in the formation of the nitrosohydroxylamine group. The branching point of valazole and fragin biosynthesis

seems to be the reductive release of the precursor from HamD. As has been demonstrated for myxochelin A and B biosynthesis, R domain catalyzed release of NRPS-bound amino acids proceeds in two 2-electron reduction steps, which can be competitively transaminated during the second reduction step [180]. The first R domain catalyzed 2-electron reduction results in an aldehyde intermediate, which can then undergo a second R domain catalyzed 2-electron reduction to yield valazole, or alternatively can be transaminated by HamG. The resulting amino derivative could then be acylated by HamF to yield fragin (Figure 7). While we have shown that L-valine is incorporated into fragin, the naturally occurring stereoisomer of fragin is D-fragin and the isolated valazole was racemic (D-valazole and L-valazole). As no epimerases or racemases are encoded by the *ham* genes, formation of the fragin and valazole D-enantiomers seem to derive from another tailoring reaction. The fact that fragin is only found as the D-enantiomer could be explained by enantioselectivity of the transamination (HamG) reaction or the acylation reaction (HamF). In fact, it has been shown that the binding pockets of C domains are enantioselective [251]. In this scenario, the biosynthetic precursor at the branching point of valazole and fragin biosynthesis is likely to be racemic, but only the D-enantiomer can be further processed to fragin due to the enantioselectivity of HamF. Such a system would also assure the production of enough valazole to drive the expression of the *ham* genes.

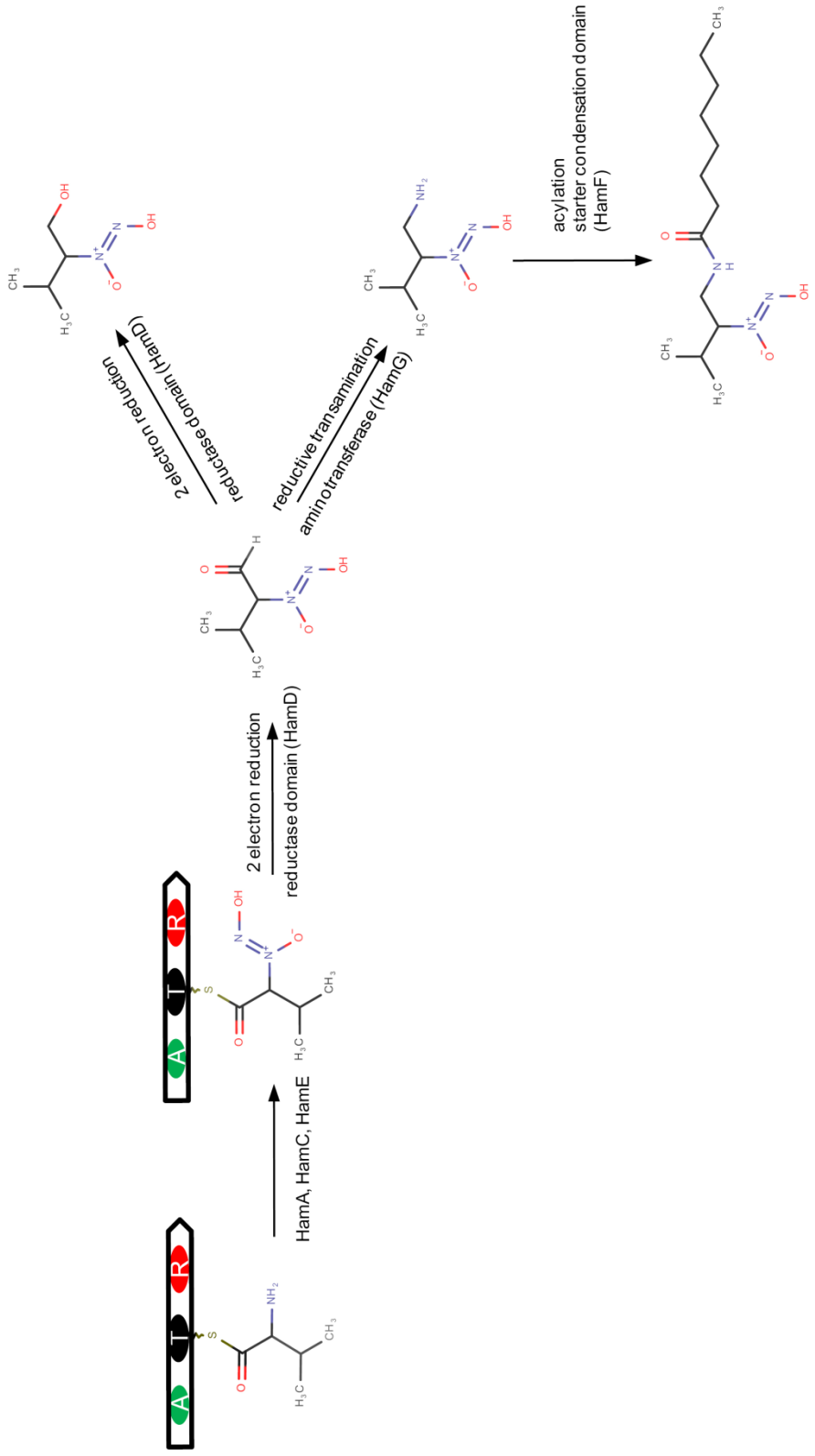

Figure 21 : Proposed model for fragin and valazole biosynthesis.

4.10 Regulation of the *ham* cluster by CepR2 and CepS

CepR2 is essential for antifungal activity of *B. cenocepacia* H111 (Figure 7A). In a recent paper, Ryan and colleagues investigated the regulatory role of the solo LuxR-type regulator CepR2 and the AraC-type regulator CepS in the regulation of the *ham* gene cluster in *B. cenocepacia* K56-2. In contrast to the findings of Mallott and colleagues [54], they showed that CepR2 can bind AHLs and is a negative regulator of *ham* gene expression. They also showed that CepS acts as a positive regulator of the *ham* genes. In their regulatory model, the DNA binding sites of CepR2 and CepS in the *ham* promoter region overlap. Apo-CepR2 binds to the promoter region of the *ham* genes, thereby blocking access for the positive regulator CepS. When QS is triggered, CepR2 binds AHLs, and is released from its binding site allowing CepS to bind and induce transcription of the *ham* genes. As we showed that the *ham* cluster is responsible for the antifungal activity of *B. cenocepacia* H111 and that a *cepR2* mutant is completely devoid of antifungal activity, this model is not valid for strain H111. Mutation of CepR2 in strain K56-2 lead to an increase in antifungal activity, which is in good agreement with CepR2 acting as a negative regulator of *ham* gene expression. Hence, CepR2 acts as a negative regulator of *ham* gene expression in K56-2, while it is a positive regulator of *ham* gene expression in strain H111. As there is only one nucleotide difference between the predicted CepR2 binding site of K56-2 and H111, it is not clear how CepR2 can have a diametrically opposite regulatory function in the two *B. cenocepacia* strains. Nevertheless, the *ham*-dependent development of a yellow colony phenotype on agar plates supplemented with high amounts of iron supports the different regulatory roles of CepR2 in K56-2 and H111 (Figure 13). The promoter activity of the *hamABCDE* operon in H111 was found to be clearly downregulated in an H111 *cepR2* mutant, again supporting its role as a positive regulator of the *ham* genes in this strain.

5 Future prospects

In this study, we identified an NRPS-like gene cluster which synthesizes two distinct molecules, fragin and valazole, which are involved in microbial antagonism and cell-cell communication.

5.1 Molecular mechanisms of fragin and valazole biosynthesis

As this is the first study which links a biosynthesis gene cluster to the production of a nitrosohydroxylamine molecule, it lays the ground for detailed studies on the biosynthesis of nitrosohydroxylamines. A recent study has shown that diazo group formation in cremeomycin biosynthesis is most likely accomplished by a spontaneous reaction of nitrous acid with a cremeomycin precursor [250]. Given the fact, that the two HamC homologues AurF and PsAAO both have aryl amines as substrates, it is likely that HamC does not have a fragin or valazole precursor as substrate, but rather an aryl amine compound. In this model the nitrosohydroxylamine group is formed spontaneously with the help of an NO donor, which is synthesized by HamC. *In vitro* enzyme assays of purified HamC will show whether nitro aryl compounds can be synthesized by HamC. Further studies will then be required to show whether these molecules are suitable NO donors for spontaneous nitrosohydroxylamine formation.

5.2 The role of fragin and valazole in copper homeostasis

Nitrosohydroxylamines are well known for their ability to chelate copper and our transcriptomics data suggests that valazole regulates several genes which use copper in their active center or are involved in copper homeostasis. It will be of great interest to further explore the role of fragin and valazole in copper homeostasis. Transcriptomics of the *B. cenocepacia* H111 wild type and its *hamF* (fragin negative, valazole positive) and *hamD* (fragin negative, valazole negative) mutant derivatives grown in the presence of different copper concentrations will help to clarify the importance of fragin and valazole in copper homeostasis.

5.3 Antimicrobial activity of fragin

It will also be important to unravel the molecular mechanism of the antifungal activity of fragin. As discussed before, it is very likely that fragin restricts competing organisms for iron or copper or directly interferes with essential enzymes which rely on metals for their enzymatic functions. The cytochrom C oxidase for example is located in the mitochondrial membrane while fungal SODs were shown to be located within the cell, but have also been found associated with the cell membrane and in the supernatant [242, 243]. In this context it will be important to investigate if fragin exerts its activity within the target cell or in the extracellular environment.

5.4 Gene regulation by valazole

Currently it is not known how valazole regulates gene expression in *B. cenocepacia* H111. Valazole might either bind to a riboswitch or to a specific receptor. As no putative riboswitches could be predicted in the *ham* promoter region, gene regulation by a riboswitch seems to be very unlikely. We have identified several receptors which are involved in the regulation of the *ham* genes. One of them, CepR2, was shown to bind AHLs [55] and is therefore not a promising candidate. In contrast, it is not known which molecules are bound by the AraC-type regulator CepS, making it the most promising valazole receptor candidate. Promoter activity studies in a heterologues host, with CepS expressed from a plasmid and external addition of synthetic valazole would be a possible strategy to clarify the possible role of CepS as valazole receptor.

Chapter IV: Material and Methods

6 Material and Methods

6.1 Bacterial strains, plasmids and growth conditions

Strains and plasmids used in this study are listed in Table 11. Primers used in this study are listed in Table 12. The model strains used in this study were *Burkholderia cenocepacia* H111, a cystic fibrosis isolate from Germany [43] and *B. cenocepacia* K56-2, a cystic fibrosis isolate from Canada [252]. Both strains were routinely grown at 37°C in Luria-Bertani medium (BD^{Tm}Difco, USA). For extraction of fragin and/or valazole, as well as promoter activity measurements, strains were grown in ABG minimal medium. Yeast extract (0.005 %) was routinely added to boost growth, except when the effect of iron on the activity of the *ham* promoter was tested. *E. coli* strains were grown in LB medium at 37 °C. When required, media were supplemented with antibiotics at the following concentrations: Kanamycin (Km) at 100 µg/ml, gentamycin (Gm) at 20 µg/ml, trimethoprim (Tp) at 25 µg/ml, chloramphenicol (Cm) 20 µg/ml. Antibiotics resuspended in water were filter sterilised (0.44 µm). All media were sterilized by autclavation unless stated otherwise.

ABG minimal medium

<u>component A (A-10x)</u>

16 g $(NH_4)_2SO_4$

48 g Na_2HPO_4

24 g KH_2PO_4

24 g NaCl

dH_2O to a final volume of 800 ml

component B

2 ml 1 M $MgCl_2$ x 6 H_2O

0.2 ml 0.5 M $CaCl_2$ x 2 H_2O

0.3 ml 0.01 M $FeCl_3$ x 6 H_2O

dH_2O to a final volume of 800 ml

component G (carbon source)

20 % glycerol v/v in dH_2O

ABG:

800 ml component B

100 ml component A

100 ml component G

Feeding studies with isotopically labeled amino acids

Bacterial strains were grown in ABG minimal medium at 37 °C with agitation (220 rpm). Isotopically labeled amino acids, L-leucine-2-^{13}C, L-leucine-^{15}N, L-valine-^{15}N (Sigma-Aldrich, Switzerland) and L-valine-^{13}C5 (Cambridge Isotope Laboratories, USA) were added to 1 mM final concentration after 24 and 48 hours of incubation. After 72 hours incubation, fragin extraction was performed as described in the 'Extraction of fragin and valazole' section. Subsequent ESI-MS analysis to determine the incorporation rate of isotopically labeled amino acids into fragin was carried out by Simon Sieber from the Group of Prof. Karl Gademann, University of Basel and University of Zurich) the mass spectrometry service of the University of Zurich.

6.2 Molecular Methods

Preparation of electrocompetent cells

E. coli was grown at 37 °C with agitation (220 rpm) in LB broth to exponential growth phase. The cells were harvested by centrifugation and washed with 1 volume of ice cold 10 % glycerol. After two more washes with 0.5 and 0.2 volumes of ice cold 10 % glycerol, the cells were centrifuged and the resulting cell pellet was resuspended in 1 ml 10 % ice cold glycerol, aliquoted and stored at – 80 °C.

Electroporation of electrocompetent *E. coli*

7 µl of the ligation reaction mix was incubated with 70 µl electrocompetent *E. coli* cells for 10 minutes on ice. The mixture was subsequently transferred to electroporation cuvettes (BIO-RAD, Gene Pulser Cuvette, 0.2 cm) chilled on ice. The cells were subsequently electroporated (25 µF; 200 Ohm ; 2,5 kV) using a BIO-RAD GenePulser. Immediately after electroporation, the cells were mixed with warm SOC medium [253], incubated with shaking at 37 °C for 1 hour and plated on LB agar plates containing the appropriate antibiotic for the selection of positive clones. Successful electroporation was confirmed by PCR.

Plasmid transfer

Plasmids were transferred from *E. coli* strains to *B. cenocepacia* strains by tri-parental mating. *E. coli* HB101 pRK600 was used as helper strain in all conjugations. *E. coli* strains (donor and helper strain) and *B. cenocepacia* (recipient strain) were grown in LB overnight with agitation (220 rpm) at 37 °C. The donor and helper strain were mixed and incubated at room temperature for 10 minutes before the donor strain was added. The bacterial mixture was then spotted on LB agar plates and incubated at 37 °C for 4 to 7 hours, washed off with saline (0.9 % NaCl solution) and plated on Pseudomonas Isolation Agar (PIA ;BD^{Tm}Difco, USA) containing the respective antibiotic and incubated overnight at 37 °C. Colonies were picked, patched on PIA containing the respective antibiotic and again incubated overnight at 37 °C. Successful transconjugation was confirmed by PCR with the plasmid specific primers listed in Table 12.

Bacterial genetics

B. cenocepacia H111 mutants were constructed using three different systems. Mutation of *hamG* was accomplished by single cross-over with a homologous region of the *hamG* (I35_4188) gene cloned into the pSHAFT2Gm plasmid. An internal fragment of *hamG* was amplified with Phusion polymerase (New England Biolabs) using the primers listed in Table 12 and purified by the QIAquick gel extraction kit (Qiagen, Germany). The DNA fragment was digested with the respective restriction enzymes (indicated in table 12), purified using the QIAquick PCR purificaton kit (Qiagen, Germany) and subsequently cloned into pSHAFT2Gm. The resulting plasmid was electroporated into *E. coli* Top10 and the homology region was sequenced at Microsynth AG, Switzerland. The plasmid was subsequently transferred into *B. cenocepacia* H111 by tri-parental mating. Correct insertion into the chromosome was verified by PCR.

Markerless mutations were either introduced using the pGPI-SceI/pDAI system or a FRT/Flp based system.

Targeted unmarked deletions with the pGPI-SceI/pDAI system were carried out as described in the literature [254]. In brief, upstream and downstream regions (approximately 1 kb in size), flanking the region targeted for deletion, were amplified with Phusion Polymerase using the primers listed in Table 12. The PCR product was purified using the QIAquick gel extraction kit, digested with the enzymes indicated in Table 12 and purified with the QIAquick PCR purification kit. After triple ligation of pGPI-SceI with the two homology arms upstream and downstream of the targeted deletion region, the up- and downstream regions were sequenced at Microsynth AG. The resulting plasmid was electroporated into *E. coli* SY327 and subsequently transferred into the target strain (*B. cenocepacia*) by tri-parental mating. Correct integration of the plasmid by homologous recombination was verified by PCR. To stimulate a second homologous recombination event by double-strand break, plasmid pDAI-SceI was transferred into the target strain. The second homologous recombination event either restored the wildtype or deleted the sequence between the two flanking regions, the latter of which resulted in the desired unmarked mutant.

Successful mutant generation was verified by PCR. Mutations in *hamA*, *hamB* and *hamF* were introduced with the pGPI-SceI/pDAI system

For targeted unmarked deletions with the FRT/FLP system, upstream and downstream regions of approximately 1 kb in size were amplified using Phusion Polymerase and the primers listed in Table 12. The PCR products were purified with the QIAquick gel extraction kit, digested with the appropriate restriction enzymes and again purified with the QIAquick PCR purification kit. The upstream fragment was cloned into plasmid pSHAFT-FRT and electroporated into *E. coli* CC118λpir. The downstream fragment was cloned into plasmid pEX-FRT and electroporated into *E. coli* MC1061. The up- and downstream fragments were sequenced at Microsynth AG. Both resulting plasmids were sequentially transferred into the target strain by conjugation. Integration of both plasmids into the chromosome via homologous recombination was verified by PCR. Plasmid pBBR5-FLP was introduced into the target strain and deletion of the targeted DNA region was verified by PCR. Mutants carrying the deletion were subsequently incubated on M9 minimal medium agar plates with 10 % sucrose as sole carbon source to enforce plasmid loss (pBBR5-FLP). Plasmid loss was verified by sensitivity of the strain to gentamycin (20 µg/ml). Mutations in *hamC*, *hamD*, *hamE* and *afcA* were introduced with the FRT/FLP system.

M9 minimal medium

<u>M9 salts (10 x)</u>

60 g Na_2HPO_4 anhydrous

30 g KH_2PO_4 anhydrous

5 g NaCl

10 g NH_4Cl

dH_2O to a final volume of 1000 ml

M9 agar plates with sucrose

90 ml dH_2O

1.5 % agar w/v

10 % sucrose w/v

10 ml M9 salts (10 x)

100 µl 0,1M $CaCl_2$

100 µl 1M $MgSO_4$

Transcriptional lacZ fusions

DNA fragments containing the putative promoters of the *hamABCDE* and *hamFG* operon were amplified with Phusion Polymerase using theprimers listed in Table 12. The promoter fragments were purified by the QIAquick gel extraction kit, digested with the restriction enzymes indicated in Table 12, purified by the QIAquick PCR purification kit and cloned into pSU11 [54] or pSU11Tp [63]. The resulting plasmids were electroporated into *E. coli* Top10 and subsequently transferred into the target strain by tri-parental mating with selection on PIA plates containing gentamycin (20 µg/ml) for the pSU11 backbone or trimethoprim (25 µg/ml) for the pSU11Tp backbone.

Assessment of promoter activity in liquid culture

Promoter activity of transcriptional *lacZ* fusions in liquid cultures was assessed by β-galactosidase assays as described before [255] with minor modifications. Briefly, bacterial cells were grown overnight in ABG minimal medium. If necessary, synthetic valazole resuspended in methanol was added to the cultures. To assess the influence of iron on promoter activity, no yeast extract was added to the ABG medium and the standard concentration of $FeCl_3$ for ABG medium was replaced with higher or lower concentrations as indicated in the results section of this thesis. Bacterial overnight cultures were routinely set to an OD_{600} of 2, centrifuged at 16,000 rpm for 5 minutes and resuspended in 2 ml Z-buffer. 1 ml of the bacterial suspension was used to determine the exact OD_{600} value. To permeabilize the cell membrane, 25 µl of

chloroform and 0.1 % SDS were added to the residual 1 ml of bacterial suspension, vortexed for 10 seconds and incubated at 28 °C for 10 minutes. 200 µl of o-nitrophenyl-β-D-galactoside (ONPG) solution (4 mg/ml in Z-buffer) were added to each sample, vortexed briefly and incubated at room temperature. The reaction was stopped by the addition of 500 µl 1 M Na_2CO_3after the development of a satisfactory yellow color, or after 30 minutes if this did not occur. The samples were centrifuged at 16,000 rpm for 10 minutes and 1 ml of cell-debris free supernatant was used to measure the absorbance at 420 nm and 550 nm with a. For every β-galactosidase assay, a sample containing only the growth medium was processed as described above and used as a blank. To determine the promoter activity in the sample, Miller Units were calculated with the following formula:

1 Miller Unit = $1000*(OD_{420}-1.75*OD_{550})/(t*v*OD_{600})$

t = reaction time in minutes

v = volume of assayed sample in milliliters

Assessment of promoter activity on agar plates

The promoter activity was determined qualitatively on LB, ABG or Malt Extract Agar (MEA ; BD^{Tm} Difco) plates containing 40 µg/ml 5-Bromo-4-chloro-3-indoxyl-beta-D-galactopyranoside (X-Gal; Gold Biotechnology, USA). Blue coloration of the bacterial colonies indicated promoter activity.

To determine the production of signaling molecules and their ability to induce promoter activity in reporter strains, the reporter strain was streaked next to the bacterial strain to be tested on LB, ABG or MEA plates containing 40 µg/ml X-Gal. Blue coloration of the reporter strain indicated production of a diffusible signaling molecule by the tested bacterial strain.

Preparation for RNAseq analysis

Starter cultures of *B. cenocepacia* strains for RNA extraction were setup in 5 ml LB broth and incubated overnight at 37 °C with agitation (220 rpm).

50 ml ABG aliquots were inoculated from the starter cultures to OD_{600} of 0.03 and incubated at 37 °C with shaking (220 rpm). Synthetic valazole resuspended in methanol was added to a final concentration of 100 µM when appropriate. An equal volume of methanol was added to all cultures not containing synthetic valazole. All strains were grown to an OD_{600} of 0.9 to 1. 50 ml Falcon tubes containing 5 ml stop solution (10 % phenol buffered with 10 mMTris-HCl pH 8) were kept on ice and 45 ml of bacterial cultures were added and mixed by inversion. Bacterial cells were pelleted by centrifugation (5,000 rpm, 15 minutes at 4 °C), the supernatant was decanted and the cell pellet was flash frozen using liquid nitrogen. Cells were stored at – 80 °C.

RNA isolation and cDNA synthesis was carried out by Dr.Yilei Liu as described previously [256]. RNA sequencing was carried out at the Functional Genomics Center Zurich. RNAseq data analysis was performed byDr. Gabriella Pessi and Martina Lardi with the DESeq software [257].

6.3 Chemical methods

Extraction of fragin and valazole

Bacterial strains were grown in ABG minimal medium containing 0.005 % yeast extract for 72 hours with agitation (220 rpm) at 37 °C. Bacterial cultures were centrifuged at 5000 rpm with an Eppendorf Centrifuge 5804R. To remove all bacterial cells, supernatants were subsequently filtered with a Millipore Express^{Tm} Plus 0.22 µm system. To extract fragin, the cell free supernatant was extracted twice with 0.5 volumes chloroform in a separation funnel. The two chloroform phases were combined, dried with anhydrous magnesium sulfate (Sigma-Aldrich, Switzerland) and filtered through folded filters (grade: 3 hw; Sartorius, Switzerland). Alternatively, bacterial cells from an overnight culture grown in LB were spotted on MEA plates covered with a cellophane membrane (Sigma-Aldrich, Switzerland) for 7 days. Bacteria were removed together with the cellophane membrane and the agar plates were cut into small pieces. The agar pieces were mixed with an equal volume of chloroform and extractedfor 2h at room temperature in the dark with 90 rpm shaking in a glass bottle. The chloroform phase was decanted, filtered through folded filters, dried using anhydrous magnesium sulphate and again filtered through folded filters. The chloroform extracts were stored at 4 °C.

To extract valazole, the cell free supernatant was alkalised to pH11with 10M NaOH and extracted twice with 0.5 volumes dichloromethane. The dichloromethane phases were discarded and the water phase was subsequently acidified to pH 5 with 10 M HCl and extracted twice with 0.5 volumes dichloromethane. The two dichloromethane phases were combined, dried using anhydrous magnesium sulphate and filtered through a folded filter. The dichloromethane extracts were stored at 4 °C.

Chloroform and dichloromethane extracts were dried using an Eppendorf Concentrator 5301 under vacuum and routinely resuspended in 0.01 volumes methanol. The concentrated extracts were stored at -20 °C.

Thin layer chromatography (TLC) of fragin and valazole

Concentrated fragin or valazole extracts were spotted on TLC silica gel 60 F_{254} plates (Merck Millipore, Germany). For separation of fragin, a mixture of chloroform:methanol (8:2) was used as mobile phase. For separation of valazole, a mixture of chloroform:methanol (3.5 :6.5) with 1 % triethylamine (TEA ; Sigma-Aldrich, Switzerland) was used as mobile phase. The TLC chambers were allowed to become saturated with mobile phase vapour for 30 minutes before the start of TLC. Separation was stopped when the mobile phase had reached approximately 2 cm below the upper edge of the TLC plate. The TLC plates were dried at room temperature for at least 2 hours to ensure complete evaporation of the mobile phase.

After separation, fragin was extracted from TLC plates for subsequent mass spectrometry analysis. For extraction from TLC plates, the stationary phase was scraped off the TLC plate, mixed with methanol and vortexed for 1 hour at room temperature. After centrifugation (13,000 rpm, 1 minute), the clear methanol supernatant was removed and stored at 4 °C.

TLC overlay assays

To visualize valazole, TLC plates were overlayed with top-agar (ABG with 0.4 % agar) containing the appropriate reporter strain and 40 µg/ml X-Gal. The overlayed TLC plates were incubated in a wet chamber at 37 °C until clear blue spots, indicating the presence of the signaling molecule (valazole), developed. The agar

was subsequently dried at room temperature for 2 days and pictures were taken with a Nikon D90 camera with AF-S Micro Nikkor 60 mm objective.

6.4 Phenotypic assays

Dual culture plate assay.

Bacteria from overnight LB cultures were pelleted, washed and resuspended to an OD_{600} of 1. Between 10 or 20 µl of bacterial suspension were spotted at three points at the edge of the MEA plates, equidistant from the center and each other, and the suspension was allowed to dry for 10 minutes. The spotted bacteria were incubated overnight at 37 °C. Fungi were prepared by placing a fungal plug in the middle of a MEA plate. After 3 days (*Rhizoctonia solani*) or 8 days (*Fusarium solani*), plugs from the edge of the plates were taken and placed placed in the center of the MEA plates with the spotted bacteria. The plates were sealed with parafilm and incubated at room temperature in the dark. Plates with the fungus *F. solani* were incubated for 8 days and plates with the fungus *R. solani*, were incubated for 3 days. MEA plates with fungal plugs but lacking bacteria were used as controls to determine fungal growth. Pictures were taken with a Nikon D90 camera with AF-S Micro Nikkor 60 mm objective and used to determine the antifungal activity of each bacterial strain. The fungal surface area (mm^2) was calculated from pictures using the ImageJ software. Antifungal activity was calculated by subtracting the fungal surface area (mm^2) from plates grown with bacteria from the fungal surface (mm^2) area of control plates.

Fungal spray assay

One agar plug of *F. solani* was incubated in LB with 70 rpm shaking at room temperature for 2 to 3 days. The liquid *F. solani* culture was homogenised with glass beads by thorough vortexing.

Bacterial strains to be tested were grown overnight at 37 °C with 220 rpm shaking, resuspended to an OD_{600} of 1 and 10 or 20 µl of the bacterial suspension were spotted on MEA plates. After preincubation of the spotted bacteria at 37 °C for 20 hours, the homogenized fungus was sprayed on the MEA plates with a perfume

spray bottle purchased at a supermarket. The plates were sealed with parafilm and incubated in the dark at room temperature for 48 hours. Antifungal activity of the bacterial strains resulted in a fungus-free halo around the bacterial colony. Pictures were taken with a Nikon D90 camera with a AF-S Micro Nikkor 60 mm objective.

Siderophore production

Bacteria were screened for the production of metal chelating molecules on Chrome Azurol S (CAS) agar plates as described by Schwyn and Neilands[258]. Briefly, bacterial cultures grown overnight in either LB or ABG medium were resuspended to an OD_{600} of 1 and 10 µl were spotted on CAS agar plates and incubated at 37 °C overnight. CAS agar plates were examined for an orange or yellow halo around the bacterial cultures which indicated the production and secretion of iron chelating molecules. Pictures were taken with a Nikon D90 camera with AF-S Micro Nikkor 60 mm objective.

EPS production

Bacteria were screened for EPS production on YEM agar plates (yeast extract 0.05 %; mannitol 0.4 %, agar 1.5 %). Bacteria were grown overnight in LB or ABG medium, then resuspended to an OD_{600} of 1 and streaked on YEM agar plates in a cross shape. After incubation at 37 °C for 2 days, the bacteria were examined for EPS production. Pictures were taken with a Nikon D90 camera with AF-S Micro Nikkor 60 mm objective.

Protease production

Bacteria were screened for protease production on skim milk LB agar plates. In brief, bacteria were grown overnight in LB or ABG medium, then resuspended to an OD_{600} of 1 and 10 µl of the bacterial cultures were spotted on skim milk agar plates (LB agar plates with 2 % w/v skim milk). The bacteria were incubated for 2 days at 37 °C and then screened for a clear halo around the bacterial colonies, which denoted the

production and secretion of proteases. Pictures were taken with a Nikon D90 camera with AF-S Micro Nikkor 60 mm objective.

6.5 Transposon mutagenesis

Preparation of a transposon mutant library

To construct a pooled transposon library, the donor strain (*E. coli* S17/pUT-miniTn5) and the recipient strain (*B. cenocepacia* H111) were grown to mid-log phase. To mobilize pUT-miniTn5 into the recipient strain multiple parallel conjugations were setup. 100 µl donor strain were mixed with 200 µl recipient strain and spotted in 50 µl aliquots on LB agar plates and incubated overnight at 37 °C. The bacterial mix was washed off with saline and the bacterial mixtures from all parallel conjugations were pooled and plated on PIA plates containing 100 µg/ml kanamycin. After overnight incubation at 37 °C, colonies were counted, washed off the plates with saline and mixed with 0.33 volume 50 % glycerol. The transposon library was aliquoted (1 ml per aliquot) and stored at -80 °C.

Screening for transposon mutants deficient in yellow colony formation/antifungal activity

One aliquot of the pooled transposon library was regenerated in 8 ml LB for 30 minutes at 50 rpm agitation at 37 °C, centrifuged at 5,000 rpm and resuspended in 10 ml saline. The bacteria were subsequently diluted to allow the growth of single colonies on agar plates. The diluted bacteria were plated on MEA plates containing 100 µM $FeCl_3$ and incubated for 24 hours. Colonies showing either a white or bright yellow colony phenotype were patched on a new MEA plate containing 100 µM $FeCl_3$ to confirm the phenotype. Clones which showed a consistent phenotype were used for further investigation and the transposon insertion site was mapped by arbitrary PCR.

Mapping of the transposon insertion site

Selected clones from the transposon mutant library were lysed by heating at 90 °C in a thermocycler and the transposon insertion site was mapped by arbitrary PCR. Primers used for the arbitrary PCR are listed in Table 12.

1st round PCR:

- PCR reaction mix:
  - DNA (from lysed colony) 5 µl
  - dNTPs (10 mM each) 2 µl
  - 5xbuffer (GoTaqFlexi) 10 µl
  - DMSO 4 µl
  - $MgCl_2$ (25 mM) 6 µl
  - ARB6 (50 µM) 4 µl
  - specific internal (5 µM) 4 µl
  - GoTaq (Promega) 0.5 µl
  - MQ H_2O 14.5 µl
- Thermocycler program:
  - 95°C 5 min
  - 95°C 0.5 min
  - 30°C 0.5 min
  - 72°C 1 min

    (6 x)
  - 95°C 0.5 min
  - 45°C 0.5 min
  - 72°C 1 min

    (30x)
  - 72°C 5 min
  - 12°C forever
- Purification of PCR product with QIAquick PCR purification kit (Qiagen).

2nd round PCR:

- PCR reaction mix:
  - purified 1st round PCR product 5 µl
  - dNTPs (10 mM each) 2 µl
  - 5xbuffer (GoTaq, Flexi) 10 µl
  - DMSO 4 µl
  - MgCl2 (25 mM) 6 µl
  - ARB2 (50 µM) 4 µl
  - specific external (5 µM) 4 µl
  - GoTaq (Promega) 0.5 µl
  - MQ H_2O 14.5 µl
- Thermocycler program:
  - 95°C 5 min
  - 95°C 0.5 min
  - 50°C 0.5 min
  - 72°C 1 min

  (30 x)
  - 72°C 5 min
  - 12°C Hold

The PCR products were separated on a 0.8 % agarose gel. Bands were cut out from the gel, purified using the QIAquick gel extraction kit (Qiagen) and sequenced at Microsynth AG. If multiple bands were derived from a single arbitrary PCR reaction, all bands were sequenced separately.

Table 11: Bacterial strains and plasmids used in this study

Strain or plasmid	Characteristics/Information	Source/Reference
Burkholderia		
H111	CF isolate, (Germany)	[43]
H111 ∆*cepIR*	Unmarked deletion of a region spanning from *cepI* to *cepR*	Straincollection Eberl lab
H111 Δ*hamA*	unmarked *hamA* deletion mutant	This study
H111 Δ*hamB*	unmarked *hamB* deletion mutant	This study
H111 Δ*hamC*	unmarked *hamC* deletion mutant	This study
H111 Δ*hamD*	unmarked *hamD* deletion mutant	This study
H111 Δ*hamE*	unmarked *hamE* deletion mutant	This study
H111 Δ*hamF*	unmarked *hamF* deletion mutant	This study
H111 *hamG* ::pSH	*hamG* interrupted by pSHAFT2Gm insertion	This study
H111 Δ*pchAB*	unmarked *pchAB* deletion mutant	[259]
H111 Δ*orbJ*	unmarked *orbJ* deletion mutant	[259]
H111 Δ*pchAB* Δ*orbJ*	unmarked *pchAB* and *orbJ* double deletion mutant	[259]
H111 ΔpC3	H111 after loss of megaplasmid pC3	[110]
H111 *cepR2*::pEX18	*cepR2* interrupted by pEX18Gm insertion	[54]
H111 *cepS*::Tn5	H111 transposon mutant with *cepS* interrupted	This study
H111 *lysR* ::Tn5	H111 transposon mutant with I35_0679 interrupted	This study
H111 *araC* ::Tn5	H111 tarnsposon mutant with I34_4197 interrupted	This study
K56-2	CF sputum isolate, (Canada) ; ET12 lineage	[252]
K56-2 Δ*cepR2*	*cepR2* interrupted by trimethoprim cassette ; Tp^R	Sokol lab
Escherichia coli		
Top 10	F^- *mcrA* Δ(*mrr-hsdRMS-mcrBC*) Φ80*lacZ*ΔM15 ΔlacX74 nupG recA1 araD139 Δ(*ara-leu*)$_{7697}$ *galE*15 *galK*16 r*psL*(Str^R) *endA*1 λ^-	Invitrogen
CC118λpir	Δ(*ara,leu*)$_{7697}$ *araD*139 Δ*lacX*74 *galE galK phoA*20 *thi-1 rpsE rpoB*(RF^R) *argE*(am) *recA1* λpir^+	[260]

MC1061	*hsdR araD*139 Δ(*ara-leu*)$_{7697}$ Δ*lacX*74 *galU galK rpsL* (Sm^R)	[261]
SY327	*araD* Δ(*lac pro*) *argE*(am) *recA*56 Rif^R *nalA* λpir	[262]
DH5α	F$^-$Φ80d*lacZ*Δ*M15* Δ(*lacZYA-argF*)$_{U169}$ *recA1 endA1 hsdR17* (r_K^-, m_K^+) *supE44 thi-1 relA1 gyrA96*	[253]
ATCC25922	recomended reference strain for antibiotic susceptibility testing	ATCC®
K-12	F- λ$^-$ rph-1 *ilvG- rfb*-50; MG1655	Straincollection Eberl lab
S17	*thi recA pro hsdR$^-$ hsdM$^+$* RP4-2-Tc::Mu-Km::Tn7	[263]
HB101	*recA thi pro leu hsd M$^+$* ; Sm^R	[264]
Additional bacteria		
Klebsiella oxytoca	wild type	Straincollection Eberl lab
Bacillus cereus	wild type	Straincollection Eberl lab
Bacillus thuringiensis	wild type	Straincollection Eberl lab
Staphylococcus aureus	wild type	Straincollection Eberl lab
Pseudomonas syringae	Bean pathogen; Rif^R	[265]
Chromobacterium	wild type	Straincollection Eberl lab
Yeast		
Saccharomyces cerevisae BY4741	MATa his3Δ1 leu2Δ0 met15Δ0 ura3Δ0	Undine Krügel, Grossniklaus lab
Plasmids		
pBBR	pBBR1MCS2 ; expression vector	[266]
pSU11	vector for lacZ fusion	[267]
pSU11Tp	pSU11 carrying a trimethoprim resistance	[63]
pEX ::FRT	pEX18TP containing a FRT site ; Gm^R	Kirsty Agnoli, Eberl lab
pSHAFT ::FRT	pUTmini-Tn5Cm with deleted BglII fragment; contains the *tnp* gene and I end of mini-Tn5; containig a FRT site ; Cm^R	Kirsty Agnoli, Eberl lab
pBBR5-FLP	pBBR1MCS5 encoding flippase	[110]

pSHAFT2Gm	pUTmini-Tn5Cm with deleted BglII fragment; contains the *tnp* gene and I end of mini-Tn5; Gm^R	[268]
pDAI-SceI	pDAI17 carrying the I-SceI gene	[254]
pGPI-SceI	pGPI-SceI from [254] with Tp^R	Elisabeth Steiner, Eberl
pRK600	RK2-*mob*$^+$ RK2-*tra*$^+$, *ori* ColE1	[269]
pUT-miniTn5	transposon delivery vector	[260]
pBBR*hamA*	pBBR1MCS2 expressing *hamA*	This study
pBBR*hamB*	pBBR1MCS2 expressing *hamB*	This study
pBBR*hamC*	pBBR1MCS2 expressing *hamC*	This study
pBBR*hamD*	pBBR1MCS2 expressing *hamD*	This study
pBBR*hamE*	pBBR1MCS2 expressing *hamE*	This study
pBBR*hamF*	pBBR1MCS2 expressing *hamF*	This study
pBBR*hamG*	pBBR1MCS2 expressing *hamG*	This study
P*hamA-lacZ*	pSU11 containing the full *hamA*	This study
P*hamA*122-*lacZ*	pSU11 containing 122 bp of the	This study
P*hamA*222-*lacZ*	pSU11 containing 222 bp of the	This study
P*hamA*281-*lacZ*	pSU11 containing 281 bp of the	This study
P*hamF-lacZ*	pSU11 containing the full *hamF*	This study
P*hamA-lacZ*Tp	pSU11Tp containing the full *hamA*	This study
P*hamF-lacZ*Tp	pSU11Tp containing the full *hamF*	This study

Table 12: Oligonucleotides used in this study (nucleotide sequences of restriction sites are underlined).

Primer	Sequence (5`-3`)	restriction site
***hamA* mutant**		
hamA_SceI_up_rv	ggggccatggCTCCAGCCCTTCCAGTTGA	NcoI
hamA_SceI_up_fw	ggggtctagaCGCGTCTTCGTCCAGTT	XbaI
hamA_SceI_d_fw	ggggccatggGATGCGATCGACGAG	NcoI
hamA_SceI_d_rv	ggggggaattcATCCAGAACGCCGAG	EcoRI
***hamB* mutant**		
hamB_SceI_up_fw	ggggtctagaAGGAGAGTCCCGTGAATCAA	XbaI
hamB_SceI_up_rv	ggggccatggTATCGACGAGCACGACCTG	NcoI
hamB_SceI_d_fw	ggggccatggTGCTGCTCGAAATCCATTACT	NcoI
hamB_SceI_d_rv	ggggggaattcAAGAACTGCCGGATGTTGAC	EcoRI
***hamC* mutant**		
hamC_FRT_u_rv	ggggagatctTAGTAGCGCAGTTCGTCGT	BglII
hamC_FRT_u_fw	ggggagatctGGATTTCATGTCGCTCGT	BglII
hamC_FRT_d_fw	gggggatccTGAGTCACGTCGATGAA	BamHI
hamC_FRT_d_rv	ggggggaattcAGGTCGGGAACATGTC	EcoRI
***hamD* mutant**		
hamD_FRT_down_fw	ggggctcgagCGTACCCCGTTTGATCAAT	PstI
hamD_FRT_down_rv	gggggatccGCGTATCACGAGCGCAT	BamHI
hamD_FRT_up_fw	ggggctcgagATCGGGAAGGCAGCTACT	XhoI
hamD_FRT_up_rv	ggggagatcttagCCGCCGATCGCAATGAT	BglII
***hamE* mutant**		
hamE_FRT_u_fw	ggggctcgagCTTCTTGGGCAGCTTCATC	XhoI
hamE_FRT_u_rv	ggggctcgagGATGAATGATGCGATGACAG	XhoI

hamE_FRT_d_fw	ggggctcgagTCAAGCCGCAGTAACCGT	PstI
hamE_FRT_d_rv	ggggaattcCCAGCCGGAGGTTTCGTTA	EcoRI
***hamF* mutant**		
hamF_SceI_up_fw	ggggtctagaCGTGCAGGTACAGGTCGTAG	XbaI
HamF_SceI_up_rv	ggggccatggCACGTCGTTTCTCCTGGAA	NcoI
hamF_SceI_d_fw	ggggccatggTTCCTGACTTTCATGCGTGT	NcoI
hamF_SceI_d_rv	ggggaattcACCCTGGAACAGGATCTCG	EcoRI
***hamG* mutant**		
hamG_ins_fw	ggggtctagaATCGGGACCCTGGAACA	XbaI
hamG_ins_rv	ggggctcgagGGCGGGAAATCAAGGAA	XhoI
***hamA* expression**		
hamA_expr_fw	ggggaagcttctaaCGAGCGGACATTACTAGGAGA	HindIII
hamA_expr_rv	ggggtctagattagcTATCGACGAGCACGACCTG	XbaI
***hamB* expression**		
hamB_expr_fw	ggggaagcttctaaTAGGAGATGCCGGCATGAACG	HindIII
hamB_expr_rv	ggggtctagattatGGGTAGTAGCGCAGTTCGTC	XbaI
***hamC* expression**		
hamC_expr_fw	ggggctcgagctaaCCATTACTACGGTTCCCC	XhoI
hamC_expr_rv_XbaI	ggggtctagaCTCACAGGTAGTCGGACA	XbaI
***hamD* expression**		
hamD_expr_fw	ggggaagcttctaaTGTCCGACTACCTGTGAG	HindIII
hamD_expr_rv	ggggtctagaATCAAACGGGGTACGTC	XbaI
***hamE* expression**		
hamE_expr_fw	ggggctcgagctaaGTCATCGCATCATTCATCAAG	XhoI

hamE_expr_rv	ggggtctagaCGGTTACTGCGGCTTGA	XbaI
***hamF* expression**		
hamF_expr_fw	ggggaagcttctaaTGCCCCGTCAAACCGAAT	HindIII
hamF_expr_rv	ggggtctagaGCCGACGAACTGAGCGAACT	XbaI
***hamG* expression**		
hamG_expr_fw	ggggaagcttctaaCCAGGAGAAACGACGTGA	HindIII
hamG_expr_rv	ggggtctagaTGATTCGGTTTGACGGGG	XbaI
***lacZ* fusions**		
hamA_prom_fw	ggggctcgagGCGGACAGCGGCAATTGAA	XhoI
hamA_prom122_fw	ggggctcgagATCGACGCCTGAAATTGCT	XhoI
hamA_prom222_fw	ggggctcgagCATGACGGTAAAGGCTTTGG	XhoI
hamA_prom281_fw	ggggctcgagTAGACAGCCCGATTTG	XhoI
hamA_prom_rv	ggggaagcttaCTCCAGCCCTTCCAGTTGA	HindIII
hamF_prom_fw	ggggctcgaGCTCCAGCCCTTCCAGTT	XhoI
hamF_prom_rv	ggggaagcttaGGACAGCGGCAATTGAA	HindIII
***afcA* mutant**		
afcA_FRT_up_fw	ggggctcgagGATAGTTGTTGCCGTTCGTGA	XhoI
afcA_FRT_up_rv	ggggagatcttaCAGGCGGTGAATGGTGGAA	BglII
afcA_FRT_d_rv	gggggatccATAGTCGAAGAAGCCGGG	BamHI
afcA_FRT_d_fw	ggggaattcAGGATCTGTGTTTCGTCGAG	EcoRI
transposon mutagenesis		
ARB6	GGCCACGCGTCGACTAGTACNNNNNNNNNNACGCC	
specific internal	GACCTTGCC ATC ATGACTGTGCTG	
ARB2	GGC CACGCGTCGACTAGTAC	
specific external	AAC GCGTATTCAGGCTGACC	

arb-seq	ATG AATGTTCCGTTGCGCTG	
plasmid specific		
pSHAFTseq_fw4	GAACACTTAACGGCTGACAT	
pSHAFTFor2	AAGGTGACCGCGTATTATTA	
M13 fw (-21)	TGTAAAACGACGGCCAGT	
lacZrv	TGCTGCAAGGCGATTAAG	
pSU11trm_rv	GTGCTGCAAGGCGATTAAGT	

Chapter V: Bibliography

7 References

1. Coenye, T. and P. Vandamme, *Diversity and significance of Burkholderia species occupying diverse ecological niches.* Environ Microbiol, 2003. **5**(9): p. 719-29.
2. Vandamme, P. and C. Peeters, *Time to revisit polyphasic taxonomy.* Antonie Van Leeuwenhoek, 2014. **106**(1): p. 57-65.
3. Depoorter, E., et al., *Burkholderia: an update on taxonomy and biotechnological potential as antibiotic producers.* Appl Microbiol Biotechnol, 2016.
4. Compant, S., et al., *Diversity and occurrence of Burkholderia spp. in the natural environment.* FEMS Microbiol Rev, 2008. **32**(4): p. 607-26.
5. Suarez-Moreno, Z.R., et al., *Common features of environmental and potentially beneficial plant-associated Burkholderia.* Microb Ecol, 2012. **63**(2): p. 249-66.
6. Scherlach, K., et al., *Antimitotic rhizoxin derivatives from a cultured bacterial endosymbiont of the rice pathogenic fungus Rhizopus microsporus.* J Am Chem Soc, 2006. **128**(35): p. 11529-36.
7. Partida-Martinez, L.P., et al., *Burkholderia rhizoxinica sp. nov. and Burkholderia endofungorum sp. nov., bacterial endosymbionts of the plant-pathogenic fungus Rhizopus microsporus.* Int J Syst Evol Microbiol, 2007. **57**(Pt 11): p. 2583-90.
8. Carlier, A.L. and L. Eberl, *The eroded genome of a Psychotria leaf symbiont: hypotheses about lifestyle and interactions with its plant host.* Environ Microbiol, 2012. **14**(10): p. 2757-69.
9. Carlier, A., et al., *The genome analysis of Candidatus Burkholderia crenata reveals that secondary metabolism may be a key function of the Ardisia crenata leaf nodule symbiosis.* Environ Microbiol, 2015.
10. Limmathurotsakul, D. and S.J. Peacock, *Melioidosis: a clinical overview.* Br Med Bull, 2011. **99**: p. 125-39.
11. Whitlock, G.C., D.M. Estes, and A.G. Torres, *Glanders: off to the races with Burkholderia mallei.* FEMS Microbiol Lett, 2007. **277**(2): p. 115-22.
12. Naughton, L.M., et al., *Functional and genomic insights into the pathogenesis of Burkholderia species to rice.* Environ Microbiol, 2016. **18**(3): p. 780-90.
13. De Smet, B., et al., *Burkholderia stagnalis sp. nov. and Burkholderia territorii sp. nov., two novel Burkholderia cepacia complex species from environmental and human sources.* Int J Syst Evol Microbiol, 2015. **65**(7): p. 2265-71.
14. Parke, J.L. and D. Gurian-Sherman, *Diversity of the Burkholderia cepacia complex and implications for risk assessment of biological control strains.* Annu Rev Phytopathol, 2001. **39**: p. 225-58.
15. Mahenthiralingam, E., T.A. Urban, and J.B. Goldberg, *The multifarious, multireplicon Burkholderia cepacia complex.* Nat Rev Microbiol, 2005. **3**(2): p. 144-56.
16. Mahenthiralingam, E. and P. Vandamme, *Taxonomy and pathogenesis of the Burkholderia cepacia complex.* Chron Respir Dis, 2005. **2**(4): p. 209-17.
17. Hauser, A.R., et al., *Clinical significance of microbial infection and adaptation in cystic fibrosis.* Clin Microbiol Rev, 2011. **24**(1): p. 29-70.
18. Vandamme, P., et al., *Burkholderia cenocepacia sp. nov.--a new twist to an old story.* Res Microbiol, 2003. **154**(2): p. 91-6.
19. Shafiq, I., et al., *Cepacia syndrome in a cystic fibrosis patient colonised with Burkholderia multivorans.* BMJ Case Rep, 2011. **2011**.

20. Sokol, P.A., et al., *The CepIR quorum-sensing system contributes to the virulence of Burkholderia cenocepacia respiratory infections.* Microbiology, 2003. **149**(Pt 12): p. 3649-58.
21. Huber, B., et al., *The cep quorum-sensing system of Burkholderia cepacia H111 controls biofilm formation and swarming motility.* Microbiology, 2001. **147**(Pt 9): p. 2517-28.
22. Malott, R.J., et al., *Characterization of the cciIR quorum-sensing system in Burkholderia cenocepacia.* Infect Immun, 2005. **73**(8): p. 4982-92.
23. Schmidt, S., et al., *Production of the antifungal compound pyrrolnitrin is quorum sensing-regulated in members of the Burkholderia cepacia complex.* Environ Microbiol, 2009. **11**(6): p. 1422-37.
24. Waters, C.M. and B.L. Bassler, *Quorum sensing: cell-to-cell communication in bacteria.* Annu Rev Cell Dev Biol, 2005. **21**: p. 319-46.
25. Thoendel, M., et al., *Peptide signaling in the staphylococci.* Chem Rev, 2011. **111**(1): p. 117-51.
26. Le, K.Y. and M. Otto, *Quorum-sensing regulation in staphylococci-an overview.* Front Microbiol, 2015. **6**: p. 1174.
27. Fuqua, C. and E.P. Greenberg, *Self perception in bacteria: quorum sensing with acylated homoserine lactones.* Curr Opin Microbiol, 1998. **1**(2): p. 183-9.
28. Whitehead, N.A., et al., *Quorum-sensing in Gram-negative bacteria.* FEMS Microbiol Rev, 2001. **25**(4): p. 365-404.
29. Withers, H., S. Swift, and P. Williams, *Quorum sensing as an integral component of gene regulatory networks in Gram-negative bacteria.* Curr Opin Microbiol, 2001. **4**(2): p. 186-93.
30. Nealson, K.H., T. Platt, and J.W. Hastings, *Cellular control of the synthesis and activity of the bacterial luminescent system.* J Bacteriol, 1970. **104**(1): p. 313-22.
31. Eberhard, A., et al., *Structural identification of autoinducer of Photobacterium fischeri luciferase.* Biochemistry, 1981. **20**(9): p. 2444-9.
32. Fuqua, W.C., S.C. Winans, and E.P. Greenberg, *Quorum sensing in bacteria: the LuxR-LuxI family of cell density-responsive transcriptional regulators.* J Bacteriol, 1994. **176**(2): p. 269-75.
33. Williams, P., *Quorum sensing, communication and cross-kingdom signalling in the bacterial world.* Microbiology, 2007. **153**(Pt 12): p. 3923-38.
34. Williams, P., et al., *Look who's talking: communication and quorum sensing in the bacterial world.* Philos Trans R Soc Lond B Biol Sci, 2007. **362**(1483): p. 1119-34.
35. Suppiger, A., et al., *Two quorum sensing systems control biofilm formation and virulence in members of the Burkholderia cepacia complex.* Virulence, 2013. **4**(5): p. 400-9.
36. Engebrecht, J., K. Nealson, and M. Silverman, *Bacterial bioluminescence: isolation and genetic analysis of functions from Vibrio fischeri.* Cell, 1983. **32**(3): p. 773-81.
37. Engebrecht, J. and M. Silverman, *Identification of genes and gene products necessary for bacterial bioluminescence.* Proc Natl Acad Sci U S A, 1984. **81**(13): p. 4154-8.
38. Bottomley, M.J., et al., *Molecular insights into quorum sensing in the human pathogen Pseudomonas aeruginosa from the structure of the virulence regulator LasR bound to its autoinducer.* J Biol Chem, 2007. **282**(18): p. 13592-600.
39. Zhang, R.G., et al., *Structure of a bacterial quorum-sensing transcription factor complexed with pheromone and DNA.* Nature, 2002. **417**(6892): p. 971-4.
40. Eberl, L., *N-acyl homoserinelactone-mediated gene regulation in gram-negative bacteria.* Syst Appl Microbiol, 1999. **22**(4): p. 493-506.
41. Lutter, E., et al., *Distribution of quorum-sensing genes in the Burkholderia cepacia complex.* Infect Immun, 2001. **69**(7): p. 4661-6.
42. Venturi, V., et al., *Quorum sensing in the Burkholderia cepacia complex.* Res Microbiol, 2004. **155**(4): p. 238-44.
43. Gotschlich, A., et al., *Synthesis of multiple N-acylhomoserine lactones is wide-spread among the members of the Burkholderia cepacia complex.* Syst Appl Microbiol, 2001. **24**(1): p. 1-14.

44. Lewenza, S., et al., *Quorum sensing in Burkholderia cepacia: identification of the LuxRI homologs CepRI.* J Bacteriol, 1999. **181**(3): p. 748-56.
45. Case, R.J., M. Labbate, and S. Kjelleberg, *AHL-driven quorum-sensing circuits: their frequency and function among the Proteobacteria.* ISME J, 2008. **2**(4): p. 345-9.
46. Fuqua, C., *The QscR quorum-sensing regulon of Pseudomonas aeruginosa: an orphan claims its identity.* J Bacteriol, 2006. **188**(9): p. 3169-71.
47. Subramoni, S. and V. Venturi, *LuxR-family 'solos': bachelor sensors/regulators of signalling molecules.* Microbiology, 2009. **155**(Pt 5): p. 1377-85.
48. Hudaiberdiev, S., et al., *Census of solo LuxR genes in prokaryotic genomes.* Front Cell Infect Microbiol, 2015. **5**: p. 20.
49. Sabag-Daigle, A. and B.M. Ahmer, *ExpI and PhzI are descendants of the long lost cognate signal synthase for SdiA.* PLoS One, 2012. **7**(10): p. e47720.
50. Chugani, S. and E.P. Greenberg, *An evolving perspective on the Pseudomonas aeruginosa orphan quorum sensing regulator QscR.* Front Cell Infect Microbiol, 2014. **4**: p. 152.
51. Gonzalez, J.F. and V. Venturi, *A novel widespread interkingdom signaling circuit.* Trends Plant Sci, 2013. **18**(3): p. 167-74.
52. Brachmann, A.O., et al., *Pyrones as bacterial signaling molecules.* Nat Chem Biol, 2013. **9**(9): p. 573-8.
53. Brameyer, S., et al., *Dialkylresorcinols as bacterial signaling molecules.* Proc Natl Acad Sci U S A, 2015. **112**(2): p. 572-7.
54. Malott, R.J., et al., *A Burkholderia cenocepacia orphan LuxR homolog is involved in quorum-sensing regulation.* J Bacteriol, 2009. **191**(8): p. 2447-60.
55. Ryan, G.T., Y. Wei, and S.C. Winans, *A LuxR-type repressor of Burkholderia cenocepacia inhibits transcription via antiactivation and is inactivated by its cognate acylhomoserine lactone.* Mol Microbiol, 2013. **87**(1): p. 94-111.
56. Barber, C.E., et al., *A novel regulatory system required for pathogenicity of Xanthomonas campestris is mediated by a small diffusible signal molecule.* Mol Microbiol, 1997. **24**(3): p. 555-66.
57. Wang, L.H., et al., *A bacterial cell-cell communication signal with cross-kingdom structural analogues.* Mol Microbiol, 2004. **51**(3): p. 903-12.
58. Boon, C., et al., *A novel DSF-like signal from Burkholderia cenocepacia interferes with Candida albicans morphological transition.* ISME J, 2008. **2**(1): p. 27-36.
59. Deng, Y., et al., *Differential modulation of Burkholderia cenocepacia virulence and energy metabolism by the quorum-sensing signal BDSF and its synthase.* J Bacteriol, 2009. **191**(23): p. 7270-8.
60. Deng, Y., et al., *Cis-2-dodecenoic acid receptor RpfR links quorum-sensing signal perception with regulation of virulence through cyclic dimeric guanosine monophosphate turnover.* Proc Natl Acad Sci U S A, 2012. **109**(38): p. 15479-84.
61. Udine, C., et al., *Phenotypic and genotypic characterisation of Burkholderia cenocepacia J2315 mutants affected in homoserine lactone and diffusible signal factor-based quorum sensing systems suggests interplay between both types of systems.* PLoS One, 2013. **8**(1): p. e55112.
62. Ryan, R.P., et al., *Intraspecies signaling involving the diffusible signal factor BDSF (cis-2-dodecenoic acid) influences virulence in Burkholderia cenocepacia.* J Bacteriol, 2009. **191**(15): p. 5013-9.
63. Schmid, N., et al., *The AHL- and BDSF-dependent quorum sensing systems control specific and overlapping sets of genes in Burkholderia cenocepacia H111.* PLoS One, 2012. **7**(11): p. e49966.
64. Vial, L., et al., *Burkholderia pseudomallei, B. thailandensis, and B. ambifaria produce 4-hydroxy-2-alkylquinoline analogues with a methyl group at the 3 position that is required for quorum-sensing regulation.* J Bacteriol, 2008. **190**(15): p. 5339-52.

65. Gallagher, L.A., et al., *Functions required for extracellular quinolone signaling by Pseudomonas aeruginosa.* J Bacteriol, 2002. **184**(23): p. 6472-80.
66. Pesci, E.C., et al., *Quinolone signaling in the cell-to-cell communication system of Pseudomonas aeruginosa.* Proc Natl Acad Sci U S A, 1999. **96**(20): p. 11229-34.
67. Cao, H., et al., *A quorum sensing-associated virulence gene of Pseudomonas aeruginosa encodes a LysR-like transcription regulator with a unique self-regulatory mechanism.* Proc Natl Acad Sci U S A, 2001. **98**(25): p. 14613-8.
68. Deziel, E., et al., *The contribution of MvfR to Pseudomonas aeruginosa pathogenesis and quorum sensing circuitry regulation: multiple quorum sensing-regulated genes are modulated without affecting lasRI, rhlRI or the production of N-acyl-L-homoserine lactones.* Mol Microbiol, 2005. **55**(4): p. 998-1014.
69. Reen, F.J., et al., *The Pseudomonas quinolone signal (PQS), and its precursor HHQ, modulate interspecies and interkingdom behaviour.* FEMS Microbiol Ecol, 2011. **77**(2): p. 413-28.
70. Deziel, E., et al., *Analysis of Pseudomonas aeruginosa 4-hydroxy-2-alkylquinolines (HAQs) reveals a role for 4-hydroxy-2-heptylquinoline in cell-to-cell communication.* Proc Natl Acad Sci U S A, 2004. **101**(5): p. 1339-44.
71. Diggle, S.P., et al., *The Pseudomonas aeruginosa 4-quinolone signal molecules HHQ and PQS play multifunctional roles in quorum sensing and iron entrapment.* Chem Biol, 2007. **14**(1): p. 87-96.
72. Oglesby, A.G., et al., *The influence of iron on Pseudomonas aeruginosa physiology: a regulatory link between iron and quorum sensing.* J Biol Chem, 2008. **283**(23): p. 15558-67.
73. Bredenbruch, F., et al., *The Pseudomonas aeruginosa quinolone signal (PQS) has an iron-chelating activity.* Environ Microbiol, 2006. **8**(8): p. 1318-29.
74. Royt, P.W., et al., *4-hydroxy-2-nonylquinoline: a novel iron chelator isolated from a bacterial cell membrane.* Bioorg Chem, 2001. **29**(6): p. 387-97.
75. Newman, D.J. and G.M. Cragg, *Natural products as sources of new drugs over the 30 years from 1981 to 2010.* J Nat Prod, 2012. **75**(3): p. 311-35.
76. Fleming, A., *On the Antibacterial Action of Cultures of a Penicillium, with Special Reference to their Use in the Isolation of B. influenzæ.* British journal of experimental pathology, 1929. **10**(3): p. 226-236.
77. Walsh, C.T. and T.A. Wencewicz, *Prospects for new antibiotics: a molecule-centered perspective.* J Antibiot (Tokyo), 2014. **67**(1): p. 7-22.
78. Walsh, C., *Molecular mechanisms that confer antibacterial drug resistance.* Nature, 2000. **406**(6797): p. 775-81.
79. Davies, J., *Bacteria on the rampage.* Nature, 1996. **383**(6597): p. 219-20.
80. Vial, L., et al., *Burkholderia diversity and versatility: an inventory of the extracellular products.* J Microbiol Biotechnol, 2007. **17**(9): p. 1407-29.
81. Knappe, T.A., et al., *Isolation and structural characterization of capistruin, a lasso peptide predicted from the genome sequence of Burkholderia thailandensis E264.* J Am Chem Soc, 2008. **130**(34): p. 11446-54.
82. Seyedsayamdost, M.R., et al., *Quorum-sensing-regulated bactobolin production by Burkholderia thailandensis E264.* Org Lett, 2010. **12**(4): p. 716-9.
83. Duerkop, B.A., et al., *Quorum-sensing control of antibiotic synthesis in Burkholderia thailandensis.* J Bacteriol, 2009. **191**(12): p. 3909-18.
84. Ishida, K., et al., *Induced biosynthesis of cryptic polyketide metabolites in a Burkholderia thailandensis quorum sensing mutant.* J Am Chem Soc, 2010. **132**(40): p. 13966-8.
85. Biggins, J.B., M.A. Ternei, and S.F. Brady, *Malleilactone, a polyketide synthase-derived virulence factor encoded by the cryptic secondary metabolome of Burkholderia pseudomallei group pathogens.* J Am Chem Soc, 2012. **134**(32): p. 13192-5.
86. Franke, J., K. Ishida, and C. Hertweck, *Genomics-driven discovery of burkholderic acid, a noncanonical, cryptic polyketide from human pathogenic Burkholderia species.* Angew Chem Int Ed Engl, 2012. **51**(46): p. 11611-5.

87. Kim, J., et al., *Quorum sensing and the LysR-type transcriptional activator ToxR regulate toxoflavin biosynthesis and transport in Burkholderia glumae.* Mol Microbiol, 2004. **54**(4): p. 921-34.
88. Suzuki, F., et al., *Identification of Proteins Involved in Toxin Production by Pseudomonas glumae.* Japanese Journal of Phytopathology, 1998. **64**(2): p. 75-79.
89. Moebius, N., et al., *Biosynthesis of the respiratory toxin bongkrekic acid in the pathogenic bacterium Burkholderia gladioli.* Chem Biol, 2012. **19**(9): p. 1164-74.
90. Ross, C., et al., *Biosynthesis of antifungal and antibacterial polyketides by Burkholderia gladioli in coculture with Rhizopus microsporus.* Mycoses, 2014. **57 Suppl 3**: p. 48-55.
91. Partida-Martinez, L.P. and C. Hertweck, *Pathogenic fungus harbours endosymbiotic bacteria for toxin production.* Nature, 2005. **437**(7060): p. 884-8.
92. Partida-Martinez, L.P., et al., *Rhizonin, the first mycotoxin isolated from the zygomycota, is not a fungal metabolite but is produced by bacterial endosymbionts.* Appl Environ Microbiol, 2007. **73**(3): p. 793-7.
93. Sieber, S., et al., *Isolation and Total Synthesis of Kirkamide, an Aminocyclitol from an Obligate Leaf Nodule Symbiont.* Angew Chem Int Ed Engl, 2015. **54**(27): p. 7968-70.
94. Hammer, P.E., et al., *Conservation of the pyrrolnitrin biosynthetic gene cluster among six pyrrolnitrin-producing strains.* FEMS Microbiol Lett, 1999. **180**(1): p. 39-44.
95. Kirner, S., et al., *Functions encoded by pyrrolnitrin biosynthetic genes from Pseudomonas fluorescens.* J Bacteriol, 1998. **180**(7): p. 1939-43.
96. Elander, R.P., et al., *Metabolism of tryptophans by Pseudomonas aureofaciens. VI. Production of pyrrolnitrin by selected Pseudomonas species.* Appl Microbiol, 1968. **16**(5): p. 753-8.
97. el-Banna, N. and G. Winkelmann, *Pyrrolnitrin from Burkholderia cepacia: antibiotic activity against fungi and novel activities against streptomycetes.* J Appl Microbiol, 1998. **85**(1): p. 69-78.
98. Burkhead, K.D., D.A. Schisler, and P.J. Slininger, *Pyrrolnitrin Production by Biological Control Agent Pseudomonas cepacia B37w in Culture and in Colonized Wounds of Potatoes.* Appl Environ Microbiol, 1994. **60**(6): p. 2031-9.
99. Gonzalez, M., et al., *Tobacco leaf spot and root rot caused by Rhizoctonia solani Kuhn.* Mol Plant Pathol, 2011. **12**(3): p. 209-16.
100. Bisacchi, G.S., et al., *Xylocandin: a new complex of antifungal peptides. II. Structural studies and chemical modifications.* J Antibiot (Tokyo), 1987. **40**(11): p. 1520-9.
101. Lee, C.H., et al., *Cepacidine A, a novel antifungal antibiotic produced by Pseudomonas cepacia. I. Taxonomy, production, isolation and biological activity.* J Antibiot (Tokyo), 1994. **47**(12): p. 1402-5.
102. Lee, C.-H., J.-W. Suh, and Y.-H. Cho, *Immunosuppressive Activity of Cepacidine A , a Novel Antifungal Antibiotic Produced by Pseudomonas cepacia.* J. Microbiol. Biotechnol., 1999. **9**(5): p. 672-674.
103. Tawfik, K.A., et al., *Burkholdines 1097 and 1229, Potent Antifungal Peptides from Burkholderia ambifaria 2.2N.* Organic Letters, 2010. **12**(4): p. 664-666.
104. Wang, X.Q., et al., *Occidiofungin is an important component responsible for the antifungal activity of Burkholderia pyrrocinia strain Lyc2.* J Appl Microbiol, 2016. **120**(3): p. 607-18.
105. Lu, S.E., et al., *Occidiofungin, a unique antifungal glycopeptide produced by a strain of Burkholderia contaminans.* Biochemistry, 2009. **48**(35): p. 8312-21.
106. Gu, G., et al., *Genetic and biochemical map for the biosynthesis of occidiofungin, an antifungal produced by Burkholderia contaminans strain MS14.* Appl Environ Microbiol, 2011. **77**(17): p. 6189-98.
107. Krishnan-Natesan, S. and P.H. Chandrasekar, *Current and future therapeutic options in the management of invasive aspergillosis.* Drugs, 2008. **68**(3): p. 265-82.
108. Thomson, E.L. and J.J. Dennis, *A Burkholderia cepacia complex non-ribosomal peptide-synthesized toxin is hemolytic and required for full virulence.* Virulence, 2012. **3**(3): p. 286-98.

109. Kang, Y., et al., *Characterization of genes involved in biosynthesis of a novel antibiotic from Burkholderia cepacia BC11 and their role in biological control of Rhizoctonia solani.* Appl Environ Microbiol, 1998. **64**(10): p. 3939-47.
110. Agnoli, K., et al., *Exposing the third chromosome of Burkholderia cepacia complex strains as a virulence plasmid.* Mol Microbiol, 2012. **83**(2): p. 362-78.
111. O'Grady, E.P., et al., *The Burkholderia cenocepacia LysR-type transcriptional regulator ShvR influences expression of quorum-sensing, protease, type II secretion, and afc genes.* J Bacteriol, 2011. **193**(1): p. 163-76.
112. Subramoni, S., et al., *Role of Burkholderia cenocepacia afcE and afcF genes in determining lipid-metabolism-associated phenotypes.* Microbiology, 2013. **159**(Pt 3): p. 603-14.
113. Crosa, J.H., *Genetics and molecular biology of siderophore-mediated iron transport in bacteria.* Microbiol Rev, 1989. **53**(4): p. 517-30.
114. Weinberg, E.D., *Iron and infection.* Microbiol Rev, 1978. **42**(1): p. 45-66.
115. Thomas, M.S., *Iron acquisition mechanisms of the Burkholderia cepacia complex.* Biometals, 2007. **20**(3-4): p. 431-52.
116. Ratledge, C. and L.G. Dover, *Iron metabolism in pathogenic bacteria.* Annu Rev Microbiol, 2000. **54**: p. 881-941.
117. Cox, C.D., et al., *Pyochelin: novel structure of an iron-chelating growth promoter for Pseudomonas aeruginosa.* Proc Natl Acad Sci U S A, 1981. **78**(7): p. 4256-60.
118. Ankenbauer, R.G., et al., *Synthesis and biological activity of pyochelin, a siderophore of Pseudomonas aeruginosa.* J Bacteriol, 1988. **170**(11): p. 5344-51.
119. Schlegel, K., K. Taraz, and H. Budzikiewicz, *The stereoisomers of pyochelin, a siderophore of Pseudomonas aeruginosa.* Biometals, 2004. **17**(4): p. 409-14.
120. Tseng, C.F., et al., *Bacterial siderophores: the solution stoichiometry and coordination of the Fe(III) complexes of pyochelin and related compounds.* J Biol Inorg Chem, 2006. **11**(4): p. 419-32.
121. Visca, P., et al., *Metal regulation of siderophore synthesis in Pseudomonas aeruginosa and functional effects of siderophore-metal complexes.* Appl Environ Microbiol, 1992. **58**(9): p. 2886-93.
122. Baysse, C., et al., *Vanadium interferes with siderophore-mediated iron uptake in Pseudomonas aeruginosa.* Microbiology, 2000. **146 (Pt 10)**: p. 2425-34.
123. Brandel, J., et al., *Pyochelin, a siderophore of Pseudomonas aeruginosa: physicochemical characterization of the iron(III), copper(II) and zinc(II) complexes.* Dalton Trans, 2012. **41**(9): p. 2820-34.
124. Mathew, A., et al., *The role of siderophores in metal homeostasis of members of the genus Burkholderia.* Environ Microbiol Rep, 2016. **8**(1): p. 103-9.
125. Quadri, L.E., et al., *Assembly of the Pseudomonas aeruginosa nonribosomal peptide siderophore pyochelin: In vitro reconstitution of aryl-4, 2-bisthiazoline synthetase activity from PchD, PchE, and PchF.* Biochemistry, 1999. **38**(45): p. 14941-54.
126. Sokol, P.A., *Production and utilization of pyochelin by clinical isolates of Pseudomonas cepacia.* J Clin Microbiol, 1986. **23**(3): p. 560-2.
127. Darling, P., et al., *Siderophore production by cystic fibrosis isolates of Burkholderia cepacia.* Infect Immun, 1998. **66**(2): p. 874-7.
128. Stephan, H., et al., *Ornibactins--a new family of siderophores from Pseudomonas.* Biometals, 1993. **6**(2): p. 93-100.
129. Meyer, J.M., et al., *Ornibactin production and transport properties in strains of Burkholderia vietnamiensis and Burkholderia cepacia (formerly Pseudomonas cepacia).* Biometals, 1995. **8**(4): p. 309-17.
130. Agnoli, K., et al., *The ornibactin biosynthesis and transport genes of Burkholderia cenocepacia are regulated by an extracytoplasmic function sigma factor which is a part of the Fur regulon.* J Bacteriol, 2006. **188**(10): p. 3631-44.

131. Uehlinger, S., et al., *Identification of specific and universal virulence factors in Burkholderia cenocepacia strains by using multiple infection hosts.* Infect Immun, 2009. **77**(9): p. 4102-10.
132. Yang, H.M., W. Chaowagul, and P.A. Sokol, *Siderophore production by Pseudomonas pseudomallei.* Infect Immun, 1991. **59**(3): p. 776-80.
133. Franke, J., et al., *Nitro versus hydroxamate in siderophores of pathogenic bacteria: effect of missing hydroxylamine protection in malleobactin biosynthesis.* Angew Chem Int Ed Engl, 2013. **52**(32): p. 8271-5.
134. Vargas-Straube, M.J., et al., *Genetic and Functional Analysis of the Biosynthesis of a Non-Ribosomal Peptide Siderophore in Burkholderia xenovorans LB400.* PLoS One, 2016. **11**(3): p. e0151273.
135. Meyer, J.M., D. Hohnadel, and F. Halle, *Cepabactin from Pseudomonas cepacia, a new type of siderophore.* J Gen Microbiol, 1989. **135**(6): p. 1479-87.
136. Barelmann, I., et al., *Cepaciachelin, a new catecholate siderophore from Burkholderia (Pseudomonas) cepacia.* Z. Naturforsch., 1996. **51C**: p. 627-630.
137. Mahenthiralingam, E., et al., *Enacyloxins are products of an unusual hybrid modular polyketide synthase encoded by a cryptic Burkholderia ambifaria Genomic Island.* Chem Biol, 2011. **18**(5): p. 665-77.
138. Gu, G., et al., *Biosynthesis of an antifungal oligopeptide in Burkholderia contaminans strain MS14.* Biochem Biophys Res Commun, 2009. **380**(2): p. 328-32.
139. Gu, G., et al., *AmbR1 is a key transcriptional regulator for production of antifungal activity of Burkholderia contaminans strain MS14.* FEMS Microbiol Lett, 2009. **297**(1): p. 54-60.
140. Chapalain, A., et al., *Identification of quorum sensing-controlled genes in Burkholderia ambifaria.* Microbiologyopen, 2013. **2**(2): p. 226-42.
141. Lewenza, S. and P.A. Sokol, *Regulation of ornibactin biosynthesis and N-acyl-L-homoserine lactone production by CepR in Burkholderia cepacia.* J Bacteriol, 2001. **183**(7): p. 2212-8.
142. Behnken, S. and C. Hertweck, *Anaerobic bacteria as producers of antibiotics.* Appl Microbiol Biotechnol, 2012. **96**(1): p. 61-7.
143. Cragg, G.M., P.G. Grothaus, and D.J. Newman, *Impact of natural products on developing new anti-cancer agents.* Chem Rev, 2009. **109**(7): p. 3012-43.
144. Cragg, G.M. and D.J. Newman, *Natural products: a continuing source of novel drug leads.* Biochim Biophys Acta, 2013. **1830**(6): p. 3670-95.
145. Newman, D.J. and G.M. Cragg, *Natural products as sources of new drugs over the last 25 years.* J Nat Prod, 2007. **70**(3): p. 461-77.
146. Felnagle, E.A., et al., *Nonribosomal peptide synthetases involved in the production of medically relevant natural products.* Mol Pharm, 2008. **5**(2): p. 191-211.
147. Hur, G.H., C.R. Vickery, and M.D. Burkart, *Explorations of catalytic domains in non-ribosomal peptide synthetase enzymology.* Nat Prod Rep, 2012. **29**(10): p. 1074-98.
148. Marahiel, M.A., *Working outside the protein-synthesis rules: insights into non-ribosomal peptide synthesis.* J Pept Sci, 2009. **15**(12): p. 799-807.
149. Smith, J.L., G. Skiniotis, and D.H. Sherman, *Architecture of the polyketide synthase module: surprises from electron cryo-microscopy.* Curr Opin Struct Biol, 2015. **31**: p. 9-19.
150. Staunton, J. and K.J. Weissman, *Polyketide biosynthesis: a millennium review.* Nat Prod Rep, 2001. **18**(4): p. 380-416.
151. Weissman, K.J. and R. Muller, *Protein-protein interactions in multienzyme megasynthetases.* Chembiochem, 2008. **9**(6): p. 826-48.
152. Weissman, K.J. and R. Muller, *Crystal structure of a molecular assembly line.* Angew Chem Int Ed Engl, 2008. **47**(44): p. 8344-6.
153. Mootz, H.D., D. Schwarzer, and M.A. Marahiel, *Ways of assembling complex natural products on modular nonribosomal peptide synthetases.* Chembiochem, 2002. **3**(6): p. 490-504.
154. Gehring, A.M., I. Mori, and C.T. Walsh, *Reconstitution and characterization of the Escherichia coli enterobactin synthetase from EntB, EntE, and EntF.* Biochemistry, 1998. **37**(8): p. 2648-59.

155. Kohli, R.M., et al., *Generality of peptide cyclization catalyzed by isolated thioesterase domains of nonribosomal peptide synthetases.* Biochemistry, 2001. **40**(24): p. 7099-108.
156. Marahiel, M.A. and L.O. Essen, *Chapter 13. Nonribosomal peptide synthetases mechanistic and structural aspects of essential domains.* Methods Enzymol, 2009. **458**: p. 337-51.
157. Du, L. and L. Lou, *PKS and NRPS release mechanisms.* Nat Prod Rep, 2010. **27**(2): p. 255-78.
158. Winn, M., et al., *Recent advances in engineering nonribosomal peptide assembly lines.* Nat Prod Rep, 2016. **33**(2): p. 317-47.
159. Rausch, C., et al., *Phylogenetic analysis of condensation domains in NRPS sheds light on their functional evolution.* BMC Evol Biol, 2007. **7**: p. 78.
160. Arima, K., A. Kakinuma, and G. Tamura, *Surfactin, a crystalline peptidelipid surfactant produced by Bacillus subtilis: isolation, characterization and its inhibition of fibrin clot formation.* Biochem Biophys Res Commun, 1968. **31**(3): p. 488-94.
161. Horowitz, S. and W.M. Griffin, *Structural analysis of Bacillus licheniformis 86 surfactant.* J Ind Microbiol, 1991. **7**(1): p. 45-52.
162. Tosato, V., et al., *Sequence completion, identification and definition of the fengycin operon in Bacillus subtilis 168.* Microbiology, 1997. **143 (Pt 11)**: p. 3443-50.
163. Morikawa, M., et al., *A new lipopeptide biosurfactant produced by Arthrobacter sp. strain MIS38.* J Bacteriol, 1993. **175**(20): p. 6459-66.
164. Lambalot, R.H., et al., *A new enzyme superfamily - the phosphopantetheinyl transferases.* Chem Biol, 1996. **3**(11): p. 923-36.
165. Quadri, L.E., et al., *Characterization of Sfp, a Bacillus subtilis phosphopantetheinyl transferase for peptidyl carrier protein domains in peptide synthetases.* Biochemistry, 1998. **37**(6): p. 1585-95.
166. Weber, T., et al., *Solution structure of PCP, a prototype for the peptidyl carrier domains of modular peptide synthetases.* Structure, 2000. **8**(4): p. 407-18.
167. Reuter, K., et al., *Crystal structure of the surfactin synthetase-activating enzyme sfp: a prototype of the 4'-phosphopantetheinyl transferase superfamily.* EMBO J, 1999. **18**(23): p. 6823-31.
168. Stachelhaus, T., et al., *Peptide bond formation in nonribosomal peptide biosynthesis. Catalytic role of the condensation domain.* J Biol Chem, 1998. **273**(35): p. 22773-81.
169. Sieber, S.A. and M.A. Marahiel, *Molecular mechanisms underlying nonribosomal peptide synthesis: approaches to new antibiotics.* Chem Rev, 2005. **105**(2): p. 715-38.
170. Finking, R. and M.A. Marahiel, *Biosynthesis of nonribosomal peptides1.* Annu Rev Microbiol, 2004. **58**: p. 453-88.
171. Clugston, S.L., et al., *Chirality of peptide bond-forming condensation domains in nonribosomal peptide synthetases: the C5 domain of tyrocidine synthetase is a (D)C(L) catalyst.* Biochemistry, 2003. **42**(41): p. 12095-104.
172. Balibar, C.J., F.H. Vaillancourt, and C.T. Walsh, *Generation of D amino acid residues in assembly of arthrofactin by dual condensation/epimerization domains.* Chem Biol, 2005. **12**(11): p. 1189-200.
173. Miller, D.A., et al., *Yersiniabactin synthetase: a four-protein assembly line producing the nonribosomal peptide/polyketide hybrid siderophore of Yersinia pestis.* Chem Biol, 2002. **9**(3): p. 333-44.
174. Hubbard, B.K. and C.T. Walsh, *Vancomycin assembly: nature's way.* Angew Chem Int Ed Engl, 2003. **42**(7): p. 730-65.
175. Grunewald, J., S.A. Sieber, and M.A. Marahiel, *Chemo- and regioselective peptide cyclization triggered by the N-terminal fatty acid chain length: the recombinant cyclase of the calcium-dependent antibiotic from Streptomyces coelicolor.* Biochemistry, 2004. **43**(10): p. 2915-25.
176. Khosla, C., et al., *Structure and mechanism of the 6-deoxyerythronolide B synthase.* Annu Rev Biochem, 2007. **76**: p. 195-221.

177. Ehmann, D.E., A.M. Gehring, and C.T. Walsh, *Lysine biosynthesis in Saccharomyces cerevisiae: mechanism of alpha-aminoadipate reductase (Lys2) involves posttranslational phosphopantetheinylation by Lys5.* Biochemistry, 1999. **38**(19): p. 6171-7.
178. Kessler, N., et al., *The linear pentadecapeptide gramicidin is assembled by four multimodular nonribosomal peptide synthetases that comprise 16 modules with 56 catalytic domains.* J Biol Chem, 2004. **279**(9): p. 7413-9.
179. Schracke, N., et al., *Synthesis of linear gramicidin requires the cooperation of two independent reductases.* Biochemistry, 2005. **44**(23): p. 8507-13.
180. Li, Y., K.J. Weissman, and R. Muller, *Myxochelin biosynthesis: direct evidence for two- and four-electron reduction of a carrier protein-bound thioester.* J Am Chem Soc, 2008. **130**(24): p. 7554-5.
181. Read, J.A. and C.T. Walsh, *The lyngbyatoxin biosynthetic assembly line: chain release by four-electron reduction of a dipeptidyl thioester to the corresponding alcohol.* J Am Chem Soc, 2007. **129**(51): p. 15762-3.
182. Sundaram, S. and C. Hertweck, *On-line enzymatic tailoring of polyketides and peptides in thiotemplate systems.* Curr Opin Chem Biol, 2016. **31**: p. 82-94.
183. Walsh, C.T., et al., *Tailoring enzymes that modify nonribosomal peptides during and after chain elongation on NRPS assembly lines.* Curr Opin Chem Biol, 2001. **5**(5): p. 525-34.
184. Stachelhaus, T. and C.T. Walsh, *Mutational analysis of the epimerization domain in the initiation module PheATE of gramicidin S synthetase.* Biochemistry, 2000. **39**(19): p. 5775-87.
185. Hoffmann, K., et al., *Purification and characterization of eucaryotic alanine racemase acting as key enzyme in cyclosporin biosynthesis.* J Biol Chem, 1994. **269**(17): p. 12710-4.
186. Cheng, Y.Q. and J.D. Walton, *A eukaryotic alanine racemase gene involved in cyclic peptide biosynthesis.* J Biol Chem, 2000. **275**(7): p. 4906-11.
187. Kahne, D., et al., *Glycopeptide and lipoglycopeptide antibiotics.* Chem Rev, 2005. **105**(2): p. 425-48.
188. Solenberg, P.J., et al., *Production of hybrid glycopeptide antibiotics in vitro and in Streptomyces toyocaensis.* Chem Biol, 1997. **4**(3): p. 195-202.
189. Losey, H.C., et al., *Tandem action of glycosyltransferases in the maturation of vancomycin and teicoplanin aglycones: novel glycopeptides.* Biochemistry, 2001. **40**(15): p. 4745-55.
190. Mulichak, A.M., et al., *Crystal structure of vancosaminyltransferase GtfD from the vancomycin biosynthetic pathway: interactions with acceptor and nucleotide ligands.* Biochemistry, 2004. **43**(18): p. 5170-80.
191. Mulichak, A.M., et al., *Structure of the TDP-epi-vancosaminyltransferase GtfA from the chloroeremomycin biosynthetic pathway.* Proc Natl Acad Sci U S A, 2003. **100**(16): p. 9238-43.
192. van Wageningen, A.M., et al., *Sequencing and analysis of genes involved in the biosynthesis of a vancomycin group antibiotic.* Chem Biol, 1998. **5**(3): p. 155-62.
193. He, X.M. and H.W. Liu, *Formation of unusual sugars: mechanistic studies and biosynthetic applications.* Annu Rev Biochem, 2002. **71**: p. 701-54.
194. Blanchard, S. and J.S. Thorson, *Enzymatic tools for engineering natural product glycosylation.* Curr Opin Chem Biol, 2006. **10**(3): p. 263-71.
195. Chen, H., et al., *Deoxysugars in glycopeptide antibiotics: enzymatic synthesis of TDP-L-epivancosamine in chloroeremomycin biosynthesis.* Proc Natl Acad Sci U S A, 2000. **97**(22): p. 11942-7.
196. Byford, M.F., et al., *The Mechanism of ACV Synthetase.* Chem Rev, 1997. **97**(7): p. 2631-2650.
197. Roach, P.L., et al., *Structure of isopenicillin N synthase complexed with substrate and the mechanism of penicillin formation.* Nature, 1997. **387**(6635): p. 827-30.
198. Schofield, C.J., et al., *Proteins of the penicillin biosynthesis pathway.* Curr Opin Struct Biol, 1997. **7**(6): p. 857-64.
199. Bischoff, D., et al., *The biosynthesis of vancomycin-type glycopeptide antibiotics--a model for oxidative side-chain cross-linking by oxygenases coupled to the action of peptide synthetases.* Chembiochem, 2005. **6**(2): p. 267-72.

200. Zerbe, K., et al., *An oxidative phenol coupling reaction catalyzed by oxyB, a cytochrome P450 from the vancomycin-producing microorganism.* Angew Chem Int Ed Engl, 2004. **43**(48): p. 6709-13.
201. Woithe, K., et al., *Oxidative phenol coupling reactions catalyzed by OxyB: a cytochrome P450 from the vancomycin producing organism. implications for vancomycin biosynthesis.* J Am Chem Soc, 2007. **129**(21): p. 6887-95.
202. Hornbogen, T., et al., *Functional characterization of the recombinant N-methyltransferase domain from the multienzyme enniatin synthetase.* Chembiochem, 2007. **8**(9): p. 1048-54.
203. Billich, A. and R. Zocher, *N-Methyltransferase function of the multifunctional enzyme enniatin synthetase.* Biochemistry, 1987. **26**(25): p. 8417-8423.
204. Weckwerth, W., et al., *Biosynthesis of PF1022A and related cyclooctadepsipeptides.* J Biol Chem, 2000. **275**(23): p. 17909-15.
205. Gehring, A.M., et al., *Iron acquisition in plague: modular logic in enzymatic biogenesis of yersiniabactin by Yersinia pestis.* Chem Biol, 1998. **5**(10): p. 573-86.
206. Pospiech, A., J. Bietenhader, and T. Schupp, *Two multifunctional peptide synthetases and an O-methyltransferase are involved in the biosynthesis of the DNA-binding antibiotic and antitumour agent saframycin Mx1 from Myxococcus xanthus.* Microbiology, 1996. **142 (Pt 4)**: p. 741-6.
207. Chen, H. and C.T. Walsh, *Coumarin formation in novobiocin biosynthesis: beta-hydroxylation of the aminoacyl enzyme tyrosyl-S-NovH by a cytochrome P450 NovI.* Chem Biol, 2001. **8**(4): p. 301-12.
208. Weber, T., et al., *antiSMASH 3.0-a comprehensive resource for the genome mining of biosynthetic gene clusters.* Nucleic Acids Res, 2015.
209. Inhulsen, S., et al., *Identification of functions linking quorum sensing with biofilm formation in Burkholderia cenocepacia H111.* Microbiologyopen, 2012. **1**(2): p. 225-42.
210. Bachmann, B.O. and J. Ravel, *Chapter 8. Methods for in silico prediction of microbial polyketide and nonribosomal peptide biosynthetic pathways from DNA sequence data.* Methods Enzymol, 2009. **458**: p. 181-217.
211. Prieto, C., et al., *NRPSsp: non-ribosomal peptide synthase substrate predictor.* Bioinformatics, 2012. **28**(3): p. 426-7.
212. Rottig, M., et al., *NRPSpredictor2--a web server for predicting NRPS adenylation domain specificity.* Nucleic Acids Res, 2011. **39**(Web Server issue): p. W362-7.
213. Ziemert, N., et al., *The natural product domain seeker NaPDoS: a phylogeny based bioinformatic tool to classify secondary metabolite gene diversity.* PLoS One, 2012. **7**(3): p. e34064.
214. Platter, E., et al., *Characterization of a non-ribosomal peptide synthetase-associated diiron arylamine N-oxygenase from Pseudomonas syringae pv. phaseolicola.* Arch Biochem Biophys, 2011. **508**(1): p. 39-45.
215. He, J. and C. Hertweck, *Biosynthetic origin of the rare nitroaryl moiety of the polyketide antibiotic aureothin: involvement of an unprecedented N-oxygenase.* J Am Chem Soc, 2004. **126**(12): p. 3694-5.
216. Vallet-Gely, I., et al., *A secondary metabolite acting as a signalling molecule controls Pseudomonas entomophila virulence.* Cell Microbiol, 2010. **12**(11): p. 1666-79.
217. Carrion, V.J., et al., *Mangotoxin production of Pseudomonas syringae pv. syringae is regulated by MgoA.* BMC Microbiol, 2014. **14**: p. 46.
218. Tamura, S., A. Murayama, and K. Hata, *Isolation and Structural Elucidation of Fragin, a New Plant Growth Inhibitor Produced by Pseudomonas.* Agr. Biol. Chem., 1967. **31**(6): p. 758-59.
219. Carmi, R., et al., *(+)-(S)-dihydroaeruginoic acid, an inhibitor of Septoria tritici and other phytopathogenic fungi and bacteria, produced by Pseudomonas fluorescens.* J Nat Prod, 1994. **57**(9): p. 1200-5.
220. Talukdar, A. and P.G. Wang, *N-Nitroso Compounds*, in *Nitric Oxide Donors*. 2005, Wiley-VCH Verlag GmbH & Co. KGaA. p. 55-89.

221. Blair, L.M. and J. Sperry, *Natural products containing a nitrogen-nitrogen bond.* J Nat Prod, 2013. **76**(4): p. 794-812.
222. Tanaka, H., S. Sawairi, and T. Okuda, *Application of the random amplified polymorphic DNA using the polymerase chain reaction for efficient elimination of duplicate strains in microbial screening. III. Bacteria.* J Antibiot (Tokyo), 1994. **47**(2): p. 194-200.
223. Murthy, Y.K., et al., *Alanosine, a new antiviral and antitumour agent isolated from a Streptomyces.* Nature, 1966. **211**(5054): p. 1198-9.
224. Gale, G.R., W.E. Ostrander, and L.M. Atkins, *Effects of alanosine on purine and pyrimidine synthesis.* Biochem Pharmacol, 1968. **17**(9): p. 1823-32.
225. Fumarola, D., *Further investigations on the immunosuppressive effect of alanosine.* Pharmacology, 1970. **3**(4): p. 215-9.
226. Fumarola, D., *Preliminary studies on the immunosuppressive action of alanosine.* Pharmacology, 1970. **3**(2): p. 107-12.
227. Tyagi, A.K. and D.A. Cooney, *Biochemical pharmacology, metabolism, and mechanism of action of L-alanosine, a novel, natural antitumor agent.* Adv Pharmacol Chemother, 1984. **20**: p. 69-121.
228. Jayaram, H.N., et al., *Metabolites of alanosine, an antitumor antibiotic.* Biochem Pharmacol, 1979. **28**(24): p. 3551-66.
229. Powis, G. and J.S. Kovach, *Binding of copper and zinc by the antitumour agent L-alanosine.* Biochem Pharmacol, 1981. **30**(7): p. 771-6.
230. Heyn, A.H. and N.G. Dave, *Precipitation of metal-cupferron complexes from homogeneous solution-II: determination of titanium.* Talanta, 1966. **13**(1): p. 33-6.
231. Heyn, A.H. and N.G. Dave, *Precipitation of metal-cupferron complexes from homogeneous solution-I: determination of copper.* Talanta, 1966. **13**(1): p. 27-32.
232. Tompsett, S.L., *The use of cupferron for the estimation of large quantities of iron in faeces.* Analyst, 1946. **71**: p. 231.
233. Kolthoff, I.M. and A. Liberti, *Amperometric titration of copper and ferric iron with cupferron.* Analyst (Lond), 1949. **74**(885): p. 635-41.
234. Uiterkamp, A.J.M.S. and H.S. Mason, *Magnetic Dipole-Dipole Coupled Cu(II) Pairs in Nitric Oxide-Treated Tyrosinase: A Structural Relationship Between the Active Sites of Tyrosinase and Hemocyanin.* Proceedings of the National Academy of Sciences, 1973. **70**(4): p. 993-996.
235. Shiino, M., Y. Watanabe, and K. Umezawa, *pH-dependent inhibition of mushroom tyrosinase by N-substituted N-nitrosohydroxylamines.* J Enzyme Inhib Med Chem, 2008. **23**(1): p. 16-20.
236. Shiino, M., Y. Watanabe, and K. Umezawa, *Synthesis and tyrosinase inhibitory activity of novel N-hydroxybenzyl-N-nitrosohydroxylamines.* Bioorg Chem, 2003. **31**(2): p. 129-35.
237. Shiino, M., Y. Watanabe, and K. Umezawa, *Synthesis of N-substituted N-nitrosohydroxylamines as inhibitors of mushroom tyrosinase.* Bioorg Med Chem, 2001. **9**(5): p. 1233-40.
238. Klinman, J.P. and M. Brenner, *Role of copper and catalytic mechanism in the copper monooxygenase, dopamine beta-hydroxylase (D beta H).* Prog Clin Biol Res, 1988. **274**: p. 227-48.
239. Iimura, H., et al., *Dopastin, an inhibitor of dopamine -hydroxylase.* J Antibiot (Tokyo), 1972. **25**(8): p. 497-500.
240. Percival, M.D., *Human 5-lipoxygenase contains an essential iron.* J Biol Chem, 1991. **266**(16): p. 10058-61.
241. Nishio, M., et al., *Nitrosoxacins A, B and C, new 5-lipoxygenase inhibitors.* J Antibiot (Tokyo), 1993. **46**(1): p. 193-5.
242. Ding, C., et al., *Iron and copper as virulence modulators in human fungal pathogens.* Mol Microbiol, 2014. **93**(1): p. 10-23.
243. Kim, B.E., T. Nevitt, and D.J. Thiele, *Mechanisms for copper acquisition, distribution and regulation.* Nat Chem Biol, 2008. **4**(3): p. 176-85.

244. Askwith, C., et al., *The FET3 gene of S. cerevisiae encodes a multicopper oxidase required for ferrous iron uptake.* Cell, 1994. **76**(2): p. 403-10.
245. Patankar, A.V. and J.E. Gonzalez, *Orphan LuxR regulators of quorum sensing.* FEMS Microbiol Rev, 2009. **33**(4): p. 739-56.
246. Garst, A.D. and R.T. Batey, *A switch in time: detailing the life of a riboswitch.* Biochim Biophys Acta, 2009. **1789**(9-10): p. 584-91.
247. Kindler, H.L., et al., *A phase II multicenter study of L-alanosine, a potent inhibitor of adenine biosynthesis, in patients with MTAP-deficient cancer.* Invest New Drugs, 2009. **27**(1): p. 75-81.
248. Walsh, C.T., R.V. O'Brien, and C. Khosla, *Nonproteinogenic amino acid building blocks for nonribosomal peptide and hybrid polyketide scaffolds.* Angew Chem Int Ed Engl, 2013. **52**(28): p. 7098-124.
249. Imker, H.J., et al., *N-acylation during glidobactin biosynthesis by the tridomain nonribosomal peptide synthetase module GlbF.* Chem Biol, 2010. **17**(10): p. 1077-83.
250. Sugai, Y., Y. Katsuyama, and Y. Ohnishi, *A nitrous acid biosynthetic pathway for diazo group formation in bacteria.* Nat Chem Biol, 2016. **12**(2): p. 73-5.
251. Linne, U. and M.A. Marahiel, *Control of directionality in nonribosomal peptide synthesis: role of the condensation domain in preventing misinitiation and timing of epimerization.* Biochemistry, 2000. **39**(34): p. 10439-47.
252. Mahenthiralingam, E., et al., *Diagnostically and experimentally useful panel of strains from the Burkholderia cepacia complex.* J Clin Microbiol, 2000. **38**(2): p. 910-3.
253. Hanahan, D., *Studies on transformation of Escherichia coli with plasmids.* J Mol Biol, 1983. **166**(4): p. 557-80.
254. Flannagan, R.S., T. Linn, and M.A. Valvano, *A system for the construction of targeted unmarked gene deletions in the genus Burkholderia.* Environ Microbiol, 2008. **10**(6): p. 1652-60.
255. Stachel, S.E., et al., *A Tn3 lacZ transposon for the random generation of beta-galactosidase gene fusions: application to the analysis of gene expression in Agrobacterium.* EMBO J, 1985. **4**(4): p. 891-8.
256. Pessi, G., et al., *Response of Burkholderia cenocepacia H111 to micro-oxia.* PLoS One, 2013. **8**(9): p. e72939.
257. Anders, S. and W. Huber, *Differential expression analysis for sequence count data.* Genome Biol, 2010. **11**(10): p. R106.
258. Schwyn, B. and J.B. Neilands, *Universal chemical assay for the detection and determination of siderophores.* Anal Biochem, 1987. **160**(1): p. 47-56.
259. Mathew, A., L. Eberl, and A.L. Carlier, *A novel siderophore-independent strategy of iron uptake in the genus Burkholderia.* Mol Microbiol, 2014. **91**(4): p. 805-20.
260. Herrero, M., V. de Lorenzo, and K.N. Timmis, *Transposon vectors containing non-antibiotic resistance selection markers for cloning and stable chromosomal insertion of foreign genes in gram-negative bacteria.* J Bacteriol, 1990. **172**(11): p. 6557-67.
261. Casadaban, M.J. and S.N. Cohen, *Analysis of gene control signals by DNA fusion and cloning in Escherichia coli.* J Mol Biol, 1980. **138**(2): p. 179-207.
262. Miller, V.L. and J.J. Mekalanos, *A novel suicide vector and its use in construction of insertion mutations: osmoregulation of outer membrane proteins and virulence determinants in Vibrio cholerae requires toxR.* J Bacteriol, 1988. **170**(6): p. 2575-83.
263. Simon, R., U. Priefer, and A. Puhler, *A Broad Host Range Mobilization System for In Vivo Genetic Engineering: Transposon Mutagenesis in Gram Negative Bacteria.* Nat Biotech, 1983. **1**(9): p. 784-791.
264. Boyer, H.W. and D. Roulland-Dussoix, *A complementation analysis of the restriction and modification of DNA in Escherichia coli.* J Mol Biol, 1969. **41**(3): p. 459-72.
265. Feil, H., et al., *Comparison of the complete genome sequences of Pseudomonas syringae pv. syringae B728a and pv. tomato DC3000.* Proc Natl Acad Sci U S A, 2005. **102**(31): p. 11064-9.

266. Kovach, M.E., et al., *Four new derivatives of the broad-host-range cloning vector pBBR1MCS, carrying different antibiotic-resistance cassettes.* Gene, 1995. **166**(1): p. 175-6.
267. O'Grady, E.P., et al., *Reciprocal regulation by the CepIR and CciIR quorum sensing systems in Burkholderia cenocepacia.* BMC Genomics, 2009. **10**: p. 441.
268. Carcamo-Oyarce, G., et al., *Quorum sensing triggers the stochastic escape of individual cells from Pseudomonas putida biofilms.* Nat Commun, 2015. **6**: p. 5945.
269. Kessler, B., V. de Lorenzo, and K.N. Timmis, *A general system to integrate lacZ fusions into the chromosomes of gram-negative eubacteria: regulation of the Pm promoter of the TOL plasmid studied with all controlling elements in monocopy.* Mol Gen Genet, 1992. **233**(1-2): p. 293-301.

Chapter VI: Appendix

8 Acknowledgments

I would like to thank my PhD supervisor and „Doktorvater“ Prof. Leo Eberl. I am grateful for the opportunity to work in his lab and his guidance. I also want to thank him for the many interesting scientific discussions we had, for sharing his immense knowledge with me and for always having an open ear for me. Last but not least I would also like to thank him for letting me grow as a researcher by giving me a lot of freedom in my research and putting me back on track when it was necessary.

I want to thank my committee members, Prof. Jakob Pernthaler, Prof. Aurelien Carlier and Dr. Gabriella Pessi for their guidance and discussions.

I am very thankful to Prof. Eshwar Mahenthiralingam to act as external referee of my PhD thesis.

I would like to express my gratitude to my collaborators Prof. Karl Gademann, Dr. Simon Sieber and Christophe Daeppen for their tremendous contribution to this work and for sharing their chemistry knowledge. This project would not have been possible without them.

My special thanks go to Isabell Scholl for the countless help she provided me during my PhD work and for running the lab so smoothly. But even more importantly I would like to thank her for her friendship, for cheering me up and for sharing so many laughs with me.

I also want to thank my colleagues and friends Dr. Nejc Stopnisek and Dr. Gerardo Carcamo-Oyarce for their friendship inside and outside the lab. For many discussions, their input, ideas and help. I am also thankful to my bench neighbour Dr.

Anugraha Mathew for her thoughtful insights, positive personality and help throughout my PhD thesis.

I also want to thank all my former and current colleagues from the Eberl lab, Prof. Masanori Toyofuku, Dr. Kirsty Agnoli-Antkowiak, Dr. Gabriella Pessi, Dr. Maria Sanchez-Contreras, Dr. Elisabeth Steiner, Dr. Nejc Stopnisek, Dr. Gerardo Carcamo-Oyarce, Dr. Anugraha Mathew, Dr. Nadine Schmid, Dr. Stephan Schwager, Dr. Yilei Liu, Dr. Claudio Aguilar, Dr. Aurelien Bailly, Dr. Laure Weisskopf, Angela Suppiger, Marta Pinto, Martina Lardi, Antri Georgiou, Aspasia Mitropoulou, Gabriela Purtschert, Olga Mannweiler, Stefanie Heller, Carlotta Fabbri. Thank you all for sharing all the good and bad moments in the lab, for wonderful scientific discussions and joyful conversations.

I am grateful to Dr. Kirsty Agnoli-Antkowiak for proofreading this thesis and her guidance in the lab.

I especially want to thank Dr. Gabriella Pessi, Dr. Yilei Liu and Martina Lardi for their help with RNAseq experiments.

I want to thank my parents, Wilfried and Maria, for their love in good and bad times. For giving me the chance to pursue my personal and scientific dreams and supporting me throughout my whole life.

Last but not least I want to thank Katrin for her constant love and support. For making my life exciting and wonderful and standing by my side in good times and bad times.

9 Curriculum vitae

Personal Data

Surname	JENUL
First name	Christian Wilfried
Date of birth	4. September, 1983
Nationality	Austria

Education

2010 – 2016	PhD in Microbiology and Immunology, University of Zurich, Switzerland PhD thesis: „The Role of Nitrosohydroxylamine Secondary Metabolites in Microbial Antagonism and Cell-Cell Communication in *Burkholderia cenocepacia* H111“ Supervisor : Prof. Leo Eberl
2008 – 2010	MSc in Molecular Microbiology, University of Graz, Austria Master thesis: "Characterization of VC2058 and VC0377 regarding chemotaxis and motility in Vibrio cholerae“ Supervisors : Prof. Joachim Reidl / Prof. Stefan Schild
2004 – 2008	BSc in Molecular Biology, University of Graz, Austria Bachelor theses: "Quinolones“ and „Production of recombinant biopharmaceuticals in plants“

Publications

Mathew A., **Jenul C**., Carlier AL., Eberl L. 2016. The role of siderophores in metal homeostasis of members of the genus Burkholderia. Environ Microbiol Rep. Feb;8(1):103-9

Carlier A., Agnoli K., Pessi G., Suppiger A., **Jenul C**., Schmid N., Tümmler B., Pinot-Carbo M., Eberl L. 2014. Genome Sequence of Burkholderai cenocepacia H111, a Cystic Fibrosis Airway Isolate. Genome Announce. Apr; 10;2(2): 00298-14

Agnoli K., Frauenknecht C., Freitag R., Schwager S., **Jenul C**., Vergunst A., Carlier A., Eberl L. 2014. The third replicon of members of the Burkholderia cepacia Complex, plasmid pC3, plays a role in stress tolerance. Appl Environ Microbiol. Feb; 80(4):1340-8

Moisi M., **Jenul C**., Butler S. M., New A., Tutz S., Reidl J., Klose K. E., Camilli A., Schild S. 2009. A novel regulatory protein involved in motility of Vibrio cholerae. J Bacteriol. Nov;191(22):7027-38

Congress Presentations

2015 19th IBCWG Meeting, Vancouver, Canada (talk)

2014 72nd Annual Assembly of the Swiss Society for Microbiology (SSM), Fribourg, Switzerland (Poster)

2013 18th IBCWG Meeting, Ann Arbor, USA (talk)

2012 14th International Symposium on Microbial Ecology, Copenhagen, Denmark

(poster)

Teaching experience

2011 - 2014 Department of Plant and Microbial Biology, University of Zurich, Switzerland

Systematic Microbiology (lab course)

2011 - 2014 Department of Plant and Microbial Biology, University of Zurich, Switzerland

Microbiology (lab course)